MECHANISM AND REGULATION OF NEUTROPHIL ACTIVATION BY GOUT-CAUSING MONOSODIUM URATE CRYSTALS

by

PAYEL SIL

(Under the Direction of **Balázs Rada**)

ABSTRACT

Gout is a leading cause of joint inflammation that has been crippling mankind for centuries. Notwithstanding the tremendous progress made in the medical sciences in the recent past, the conventional treatments are suboptimal for gout to this day. So far, we know the inflammation is caused by monosodium urate (MSU) crystals aggravating immune cells, specifically neutrophils and macrophages. It is predominantly neutrophil-driven and neutrophil extracellular traps (NETs) play a major role in regulating inflammation. Our study has led to the novel finding that the P2Y6 receptor antagonist, MRS2578, inhibits MSU crystal-induced NET formation. Other neutrophil functions like superoxide production, calcium mobilization, interleukin-8 (IL-8) release and migration are also retarded. Therefore, understanding the role of P2Y6R may pave the way towards exploring the mechanism involved in regulating the NET-inducing pathway.

Additionally, we found that interleukin-1β (IL-1β), a prevalent cytokine in gout inflammation, can enhance NET formation (and hence, inflammation) in the presence of MSU crystals. Anti-IL-1β strategies are currently employed to alleviate inflammation in gout patients. Through our efforts we have progressed significantly in the mission to unveil the underlying mechanism involved in MSU crystal-triggered NETs. Our goal is to understand the relevant pathways that will advance

our knowledge and will enable the development of effective therapeutic strategies and tools that will be able to prevent gout.

INDEX WORDS: Neutrophils; Macrophages; Autoinflammation; Crystal-driven inflammation; Osteoarthritis (OA); Gout, Synovial fluid (SF); Pattern recognition receptor (PRR); Pathogen-associated Molecular Patterns (PAMPs); Damage-associated Molecular Patterns (DAMPs); Monosodium Urate crystals (MSU crystals); Neutrophil Extracellular Traps (NETs); Aggregated NETs (aggNETs); Extracellular DNA (ecDNA); Myeloperoxidase (MPO); Human neutrophil elastase (HNE); Store-Operated Calcium Entry (SOCE); Interleukin 1β (IL-1β) and Interleukin-8 (IL-8)

MECHANISM AND REGULATION OF NEUTROPHIL ACTIVATION BY GOUT-CAUSING MONOSODIUM URATE CRYSTALS

by

PAYEL SIL

B.Sc. Honors, University of Delhi, India, 2006

M.Sc., Newcastle University, U.K., 2007

MS., University of Hawaii, 2011

A Dissertation Submitted to the Graduate Faculty of The University of Georgia in Partial Fulfillment of the Requirements for the Degree

DOCTOR OF PHILOSOPHY

ATHENS, GEORGIA

2016

MECHANISM AND REGULATION OF NEUTROPHIL ACTIVATION BY GOUT-CAUSING MONOSODIUM URATE CRYSTALS

by

PAYEL SIL

Major Professor:	Balázs Rada
Committee:	David Hurley
	Donald Evans
	Pramod Giri
	Wendy Watford

Electronic Version Approved:

Suzanne Barbour
Dean of the Graduate School
The University of Georgia
December 2016

DEDICATION

I would like to dedicate my Ph.D. dissertation to honor the memory of my late father, Mr. Kailash Nath Sil (1952 – 2008). Without his guidance and empowerment during my formative years, I would not have overcome the hurdles life presented.

ACKNOWLEDGEMENTS

I am grateful for Dr. Balázs Rada's tutelage during my doctoral training. I am also thankful to my doctoral committee members, Drs. Donald Evans, David Hurley, Wendy Watford and Pramod Giri for their time, support and insightful advice throughout my PhD program.

My sincere thanks to Drs. Sherry Sanderson, Frederick Quinn, Harry Dickerson, David Peterson, Liliana Friedman, Barbara Reaves, Jamie Barber, Ms. Safiye Bakalli, Ms. Marie Goodwin, Ms. Jennifer Leyting, Ms. LaDonna Allen, Ms. Phyllis McCannon, Ms. Stephanie O'Kelley, and fellow graduate students for supporting me in many different ways as I went through this journey. I am thankful for the companionship of the undergraduate students from our laboratory, both past and present.

Most importantly, I would like to express my heartfelt gratitude to my husband, Amit K. Mukerji, without whose love and support it would have been very difficult for me to achieve my goals. Last but not the least, I would also like to thank my family-Dipali Sil, Aindrila Sil, Meeta Mukerji, Captain Ashis K. Mukerji, and Somendra Nath Banerji for providing a strong support system for me in my trying times.

TABLE OF CONTENTS

Page

LIST OF TABLES

Page

LIST OF FIGURES

Page

CHAPTER 1

INTRODUCTION AND LITERATURE REVIEW

Autoinflammatory disorders such as gout are notorious for generating an overt immune response [1-7]. Gout is characterized by joint inflammation in the synovium accompanied by frequent flares, which progressively become more aggressive over time (see Figure 1.1) [6-8]. Gout has been documented since 2000 B.C. but an effective cure has not yet been found [1, 2]. However, the diagnosis and staging of gout is well-established in the medical profession [9].

1. Gout: In 2007-2008 there were 8.3 million gout cases and each year 3 million cases are being added [10]. A frequent target for gout attack is the first metatarsophalangeal joint [1-3, 7, 11]. Currently available gout medications are only able to treat the symptoms of the disease [4, 11]. Patients manage their gout with the help of therapeutics and by making lifestyle alterations such as regular exercise and diet changes [11]. Men above the age of 40 and menopausal women are at the greatest risk to be afflicted by gout [12-14]. Gout is less common in younger women, since female hormones are known to inhibit uric acid accumulation [14].

Gout can also occur at other locations within the body, such as the knees, metatarsophalanges, proximal interphalangeal joints and distal interphalangeal joints [15-17]. Gout manifests itself as monoarthritis or bilateral asymmetric polyarthritis [11, 17, 18]. Gout has emerged as a risk factor for cardiovascular disorders [19, 20]. The hyperuricemic condition is linked to multiple comorbidities (diabetes, hypertension, and congestive heart failure), which are vital for disease

establishment [21]. When it is left untreated, the disease progresses through the following four stages, as is also shown in Figure 1.2. [22, 23]:

Stage I. Asymptomatic hyperuricemia

Stage II. Acute gout

Stage III. Intercritical gout

Stage IV. Chronic tophaceous gout

In advanced stages of gout, painful inflammation becomes chronic and leads to 'tophus' formation [23-26]. A tophus is a conglomeration of dead synovial tissue, MSU crystals and activated or dead leukocytes (like neutrophils) [23-26]. It appears chalky and gritty due to the presence of MSU crystals [16, 23-26]. Prolonged bone destruction in gout causes osteoblast retraction due to the elastase and osteoclasts resorbing cell-free areas of the matrix [22]. Tophi are very dynamic structures, which constantly undergo remodeling during gouty flares and are associated with the resolution of gouty inflammation [23-26]. This is due to the production of anti-inflammatory cytokines such as transforming growth factor β_1 (TGF-β_1), IL-10 and other nuclear receptor factors, like peroxisome proliferator activated receptor-γ (PPAR-γ), and the clearance of apoptotic cells by monocyte-macrophages [4, 7, 11, 27, 28]. Recent studies suggest that the tophus can resolve inflammation by releasing proteases that can cleave the proinflammatory cytokines [23, 25, 26, 29]. However, the jury is still out on whether tophi are beneficial or unfavorable towards the mitigation of gouty inflammation [23, 25, 26, 29].

i. Monosodium urate (MSU) crystals: MSU crystal accumulation in the joints powers the overt immune response, driven primarily by innate immune cells such as macrophages and neutrophils

[7, 26]. Primates (including humans) are unable to excrete or decompose uric acid (UA) from the body due to the evolutionary loss of the enzyme uricase [11, 23]. The uricase gene is disrupted by two mutations that introduce a premature stop codon [11]. In most cases, renal urate transporters such as uric acid transporters (URAT 1) and organic anion transporters (OAT4) malfunction, and cause accumulation of uric acid in the body [11].

Uric acid (UA) reacts with free sodium in the plasma, forming MSU crystals, which crystalizes in the synovial space [6, 30-32]. UA is a product of purine metabolism and it scavenges singlet oxygen that regulates oxidative stress in humans [11, 30]. UA is also an antioxidant [11, 30, 33]. It plays the dual role of acting as a pro-oxidant, as well as proinflammatory agent [11, 30, 33]. UA forms MSU crystals in presence of free sodium and causes reactive oxygen species (ROS)-dependent NET formation [30, 33]. In low concentrations, UA acts as an anti-oxidant and inhibits nicotinamide adenine dinucleotide phosphate (NADPH) oxidase-dependent NET formation [30, 33]. It has been shown that high concentration of non-crystalline UA (8 mg/dl) induces NADPH oxidase/ROS-independent NETosis by utilizing the nuclear factor (NF-κB) signaling pathway in neutrophils from Chronic Granulomatous Disease (CGD) patients [30]. Unlike UA, MSU crystals induce NETs in a ROS-dependent manner [30, 33]. Analyses of gout synovial fluid (SF) and tissue samples, including those in our study, have shown the presence of NETs with MSU crystals [34-36] (Sil & Rada., J.Immunol., under revision). During the resolution phase of inflammation, the crystals isolated from the SF lose IgG coating [6, 7, 28, 37]. These isolated MSU crystals are reported to bind to the lipoproteins ApoE and ApoB, which suppress MSU crystal-induced neutrophil activation [1-3, 7, 28].

ii. Risk Factors: Consumption of purine-rich foods, high fructose corn syrup, and alcohol (beer) causes the liver to produce more uric acid [11]. Human beings as a species lack uricase, and therefore, are unable to breakdown uric acid to a more soluble excretory product known as allantoin [11, 23]. Although the urate acts as an antioxidant in the human body, the evolutionary advantage gained by uricase elimination is still not apparent [11, 23].

Individuals that have a defect in uric acid transporters such as URAT1 and OAT4 tend to accumulate uric acid [11]. Asymptomatic hyperuricemic condition is an indicator for gout [11, 21, 38]. Genome-wide association study (GWAS) scans suggest that SLC2A9 and ABCG2 are the major genes responsible for the hyperuricemic condition [11, 21, 38]. SLC2A9 is involved in renal and gut excretion of uric acid [11, 21, 38]. ABCG2 gene Q141K polymorphism (A allele or AA genotype) has an increased risk of gout and is involved in only renal excretion of uric acid [11, 21, 38].

iii. Mechanism of Action: MSU crystals are damage-associated molecular pattern molecules (DAMPs), which trigger inflammasome activation in macrophages [1, 2, 7, 28, 35, 39-42]. Activated macrophages produce IL-1β and IL-18, which are strong neutrophil chemoattractants [1-3, 7, 34, 35, 40, 41, 43, 44]. Neutrophils gather at the site of inflammation and exaggerate the joint inflammation [1-3, 7, 11, 17, 28, 39]. MSU crystals are coated with immunoglobulins, which also drive the immune response [7, 28]. Gouty inflammation can self-resolve in 7-10 days in most situations [6, 11, 23, 35].

iv. Clinical Significance: To ease the pain caused by joint damage in gout, patients typically rely on pain relieving drugs, as well as on urate-lowering therapeutics [4]. The most commonly

prescribed gout drugs are colchicine and xanthine oxidase inhibitors (such as febuxostat, allopurinol) [4, 17]. Colchicine blocks microtubules, inflammasome assembly, and inducible nitric oxide (iNOS) production in neutrophils and macrophages [1-3, 28, 45, 46]. More recently, angiotensin receptor blocker drugs have been shown to increase uric acid excretion [47]. These drugs only provide temporary symptomatic relief, and are accompanied with multiple side effects [6, 7, 47].

Gout has been called the 'disease of the kings' [48, 49]. Gout is often confused with other joint-related arthritis such as pseudogout and rheumatoid arthritis (RA) [19]. Therefore, there exists a significant risk of misdiagnosis by clinicians. NETs have been implicated in both RA and pseudogout [15, 50, 51]. A hyperuricemic condition is a prerequisite for the genesis of gout and therefore, it is used as an indicator for gout diagnoses [11, 52]. However, not everyone with hyperuricemia is afflicted by gout [9, 11]. Factors such as genetic pre-disposition to hyperuricemia, obesity, diuretic medications, and kidney stones usually cause a build-up of uric acid in the body [11, 19, 53]. The autoinflammation experienced in gout is mainly driven by neutrophils [1-3, 7, 28]. Blocking the influx of neutrophils may help in coping with recurrent attacks [11, 20]. Dietary and lifestyle interventions are often incorporated into gout patients' regimens as preventive measures [9, 11, 19, 20]. However, there is a gap in the understanding of the mechanism(s) of activation in neutrophils, as well as macrophage and neutrophil interactions, which contribute towards exaggeration of the inflammation. Our study will investigate the factors contributing to neutrophil activation and will strive to shed light on the underlying mechanism(s). The ultimate goal is to effectively block this interaction and thereby, intercept the progression of gout.

2. Neutrophils in Gout: Neutrophils mature in the bone marrow and after exiting from the bone marrow they patrol tissues seeking infectious pathogens [54, 55]. They have a relatively short life span and eventually undergo apoptosis in the event that they don't encounter PAMPs or DAMPs [56]. Once the neutrophils engage with MSU crystals, they release several proinflammatory chemokines and cytokines [1, 7]. In this cytokine milieu, the neutrophils call upon more of their kind [7, 34, 35]. The summoned neutrophils follow a pathway marked by chemokines like IL-18, IL-8 and IL-1β to reach the site of inflammation [1-4, 7, 40, 57]. Once they have reached the site, the neutrophils undergo degranulation and release several antimicrobial proteins such as Myeloperoxidase (MPO), Human Neutrophil Elastase (HNE) and cathepsin G [58-60]. Some of these proteins, especially MPO and HNE, aid in NET formation, which is typical to gout [23, 36].

i. MSU crystal phagocytosis: Neutrophils recognize stimuli via PRR, and may or may not require opsonization by antibodies or the complement system for PMN recognition [7, 11, 28, 61]. Neutrophils engulf the pathogen or a particle in a phagosome and deliver it to the lysosome, forming phagolysosomes, where the acidification process occurs [34, 35, 54, 55]. There is evidence of fusion and acidification of the phagolysosome in activated neutrophils in gout [34, 35]. This implies that neutrophils attempt to phagocytose the crystals as well.

In gout, immunoglobulins (such as IgG & IgM), complement components (such as C1q, C3, C5a) or small hyaluronate may coat MSU crystals to enable phagocytosis [7, 11, 28]. As inflammation subsides, apolipoprotein B (Apo B) displaces these molecules, including IgG, by competitively coating sites on crystals [7, 11, 28]. The phagocytic process involves engagement of opsonic receptors such as Fcγ and C-type lectins [55]. FcγRIIIB on human neutrophils has been suggested

to be involved in the uptake of MSU crystals [7]. The mechanism of Fcγ with regards to MSU crystal uptake is not well understood.

In gout patients, macrophages attempt to engulf MSU crystals via Toll-like receptor (TLR2/TLR4 acting through Myd88) signaling. This, in turn, cleaves C5 and forms complement membrane attack complex (C5b-C9). C5b-C9 causes the release of proinflammatory cytokines and chemokines, thereby, initiating a massive influx of neutrophils [1-3, 11]. Additionally, it has been reported that FcγRIIIB/CD11b and CD14-TLR2-TLR4 complex may be involved in MSU crystal recognition in humans [7]. Once MSU crystals engage with TLR2 and TLR4, downstream signaling molecules such as Myd88, Rac-1, phosphatidylinositol-3 kinase (PI3K) and protein kinase B (PKB or AKT) are activated [28]. This signaling cascade activates NF-κB, which leads to the activation pro-IL-1β and pro-IL-18 [1-3, 17, 28, 40]. NLRP3 (NALP3) inflammasome assembly formation cleaves pro-caspase-1 to caspase-1[5, 40]. Caspase-1 cleaves pro-IL-1β and pro-IL-18 to form IL-1β and IL-18 [5, 40].

ii. Neutrophil migration: Cell migration is necessary for various cellular functions such as adhesion, cell growth, motility, innate immune response and wound healing [62-64]. Before migration, the neutrophils are activated and polarized [62-64]. The cell alignment is an interplay between adhesive forces and passive membrane deformations, but this process is accelerated by cytoskeleton-driven membrane motion [62-64]. Migration requires signaling and stabilization by the cytoskeleton [62-64].

Other factors, such as cytosolic neutrophil proteins like S100A8, S100A9, and leukotrienes, are chemotactic and they amplify neutrophil migration in gout [7, 11, 65]. Activation of SH2 domain-

containing tyrosine phosphatases, such as SHP-1 and SHP-2 in human neutrophils by MSU crystals increases the degranulation and synthesis of IL-8, a potent neutrophil chemoattractant [11, 28]. MSU crystals cause activation of phospholipase C to simulate intracellular calcium mobilization [7, 28].

iii. Neutrophil granular proteins: As the neutrophils mature in the bone marrow, their granules also mature and become packed with numerous proteins. Granule membranes are impermeable and the granules release proteins upon fusion [60]. The granules are classified as primary, secondary and tertiary, depending upon the stage of their development [55]. They are also categorized as secretory, azurophilic, specific or gelatinase on the basis of their content [60]. Primarily, these granules are antimicrobial in nature and they are released upon fusion with the membrane vesicles containing microorganism [60]. Below are the brief descriptions of two major azurophilic neutrophil granular proteins: MPO and HNE [33, 58, 60].

a. Myeloperoxidase (MPO): MPO is first formed in the promyelocyte stage of neutrophil development [66]. It is about 5% of the dry weight of neutrophils [60, 66, 67]. Primary azurophilic granules containing MPO catalyze the formation of hypochlorous acid (HOCL) in order to kill pathogens [58, 60]. The purified form of MPO is green in color [66]. MPO mediated neutrophil activation causes oxidation of chloride, bromide and thiocyanate by hydrogen peroxide (H_2O_2) to form HOCL, hypobromous acid and hypothiocyanous acid, respectively [33, 60].

MPO is considered vital in protein transportation across membranes and regulates neutrophil signaling [33, 60]. During the neutrophil respiratory burst, phagosomes containing microbes fuse with the azurophilic granules [66]. The MPO released from them kills the microbe by using H_2O_2

to produce HOCL [66]. Metzler *et al.,* Urban *et al.,* and Branzk *et al.* also demonstrated NET formation by yeast and hyphae forms of *Candida albicans* [60, 68, 69]. However, Metzler *et al.* specifically showed that MPO is important for NET production by the opsonized yeast form of *C. albicans* [60]. Complete MPO deficiency causes a reduction in ROS production and NET release [54]. High level of serum MPO is also found in gout patients [70]. MPO is required for the release of active NE during NETosis [60]. The NE released by the action of H_2O_2/ MPO then promotes degradation of F-actin, liberates proteases to enter the nucleus, and attacks histone H4 [58, 60]. MPO is the known culprit of several autoimmune diseases like Parkinson's disease, multiple sclerosis, and atherosclerosis. [54, 66].

b. Neutrophil Elastase (NE): NE is a serine protease that is released from azurophilic granules upon degranulation [58, 60, 71-74]. During NET formation, NE translocates across the membrane via azurosomes [60]. It has also been shown to interact with the actin cytoskeleton and chromatin [60]. Once inside the nucleus, NE attaches strongly to the DNA [60]. *In vitro* data on human gingival fibroblasts show that NE, cathepsin G, and proteinase-3 stimulate production of IL-8 and monocyte chemoattractant protein -1 (MCP-1) through protease-activated receptor (PAR)-2 [72, 74]. HNE and cathepsin G cleave the peptide at the N-terminus of PAR-2 with exposure of its tethered ligand that binds the cleaved receptor [7, 72, 74]. IL-1R-associated kinase (IRAK)-1, Myd88, and TNFR-associated factor-6 (TRAF-6) were shown to be involved in NE-induced NF-κB activation and subsequent IL-8 expression [72, 74]. Deficiency in alpha-1 antitrypsin causes NE deficit, which can result in chronic obstructive pulmonary disease (COPD), cryptogenic cirrhosis/liver disease, granulomatosis with polyangitis, bronchiectasis of unknown aetiology, panniculitis and possibly other skin disorders [75].

While HNE is required for host defense, it can also lead to tissue damage and inflammation [58, 72, 74, 76-82] . HNE can upregulate cysteinyl cathepsin B and matrix metalloproteinase-2 (MMP-2) and in doing so, it can damage the extracellular matrix [72, 74]. Serine proteases like HNE released from neutrophils cause excessive extracellular deposition, which leads to tissue damage in lungs [77]. HNE is also known to increase NF-κB signaling in macrophages, to destroy the extracellular matrix and promote inflammation [77, 78]. Sahoo *et al.* showed that NE induces tissue damage in lungs, which makes mice susceptible to *Burkholderia* species [79]. HNE is also known to amplify immune complex-mediated diseases [83]. Elevated serum NE correlates with increased lung disease severity [77]. HNE has been implicated in exacerbating disease conditions in cystic fibrosis, emphysema, chronic lung disorders, and Alzheimer's disease. [72, 74]. In RA patients, as well as in the collagen-induced arthritis (CIA) mouse model, NE causes pulmonary thromboembolism (PTE) and tissue injury [84].

3. Neutrophil extracellular traps (NETs): NETs have been implicated in many diseases such as gout, cystic fibrosis, pseudogout, or RA [50, 82, 85-87]. NETosis is a distinct process of cell death involving chromatin decondensation and loss of cell membrane integrity [59, 88-91]. NETs are a 'double-edged sword' because they come with benefits and liabilities [91, 92]. The primary function of NETs is to entangle pathogens and to destroy them [59, 88-91]. However, NETs may go awry and digress from their anti-pathogenic role. In several autoinflammatory and autoimmune diseases, NETs have proven to be a menace [15, 54, 93].

The nuclear area of a neutrophil undergoing PMA-induced NETosis ranges between 150-350 μm^2 after 4 hours [94, 95]. The cell first undergoes cytoplasmic and nuclear swelling, followed by vacuolization, membrane protrusion, enzyme binding to DNA, histone citrullination and

chromatin decondensation [55, 59, 88-90]. The NETosing nucleus loses nuclear segregation into euchromatin and heterochromatin [96]. Finally, the membrane is disrupted, releasing NETs, and the intact DNA lattice disintegrates as a result [33, 36]. Histones released by NETosis undergo proteolytic cleavage at the amino terminal [91]. NETosing DNA are studded with antimicrobial proteins (like lactoferrin, cathepsin G), proteases like NE or with enzymes producing ROS (like MPO) [68, 97]. The decondensation of DNA and histone trimming form the 'bead on string' structure containing NET-bound proteins [59, 91, 98]. HNE released from the neutrophil azurophilic granules start degrading histones such as histone H4 [34, 35, 60, 99]. Brinkmann *et al.* showed high concentration of histone H2A kills bacteria such as *S. flexneri*, *S. typhimurium* and *S. aureus* [59]. In conclusion, NET components such as DNA, histone, histone-derived components and NE are antimicrobial [59, 100]. Histone citrullination, ROS production and autophagy are features associated with NETs, and are described as follows:

i. Histone citrullination: Histone methylarginine is converted to citrulline via the action of peptidyl arginine deaminase type 4 (PAD4) and this process is known as *histone citrullination* or *demethylimination* [33, 101]. PAD4 is expressed in granulocytes and is abundant in neutrophils (PMNs) [102]. Leshner *et al.* and Rohrbach *et al.* suggested that activation of PAD4 and citrullination of histone H3 & H4 are important for NET formation [101-104]. PAD4-deficient mice are unable to release NETs and are susceptible to severe bacterial infections [101]. This process involves a promoter of the specific histone regulation required for chromatin decondensation, which is achieved by making linker DNA more accessible [105]. Deamination reprograms gene expression by post-translational modification and it reduces the positive charge on the histones, as well as relaxes the compact histone–DNA complexes [89-91]. Detection of

neutrophil nuclear citrullinated histones has become the basis for NET detection and is categorized as NET marker [106-108]. Neeli *et al.* showed that the protein kinase C ζ (PKC ζ) activates PAD4 and thereby, it increases intracellular calcium [89]. PKC ζ assists in assembling the NADPH oxidase and regulates PAD4 activity [89-91].

ii. Reactive Oxygen Species (ROS): Neutrophils kill pathogens in both ROS-independent, as well as ROS-dependent manners [33]. The ROS-independent mechanism requires release of antimicrobial peptides such as bactericidal permeability increasing proteins, defensins, and cathelicidins [33, 91].

Neutrophils undergo respiratory burst and release extracellular ROS via the NAPDH oxidase complex (see Figure 1.3) [33]. The ROS-dependent mechanism involves the formation of NADPH oxidase enzyme complex and superoxide (O_2^-) production [33]. During NET formation, ROS releases proteases, which are thought to mediate the disruption of the membranes [23, 25, 26, 29]. Calcium influx stops with activation of ROS [109, 110]. Mitochondrial ROS can also cause NETosis via NADPH oxidase-independent pathways and it is regulated by calcium activated potassium channel 3 (SK3) [33].

ROS generation causes degranulation, which may result in release of granular proteins such as NE and MPO [33]. However, there are several ROS-independent mechanisms, as well, which include β-arrestins, the Rho guanosine triphosphatase Rac2, soluble NSF attachment protein (SNAP) receptors, the *src* family of tyrosine kinases, and the tyrosine phosphatase MEG2 [111-113]. NE and MPO translocate to the nucleus, NE aids in histone degradation and MPO helps in decondensing chromatin [18, 33, 60]. Chronic granulomatous disease (CGD) patients with abnormal NADPH oxidase, as well as patients with complete MPO deficiency are unable to release

NETs and are vulnerable to *Candida albicans* infection [60]. Metzler *et al.* have shown that active MPO enzyme is required for NETosis [60]. Fibronectin and β-glucans from *Candida* together cause ROS-independent NETosis wherein they suppress ROS release and activate via an alternate pathway-MAPK/ ERK pathway (see Figure 1.3) [114]. However, in the presence of β-glucans only, neutrophils undergo ROS-dependent NETosis [114]. ROS deactivate caspases, causing the neutrophils to undertake a non-apoptotic pathway and thereby, induces autophagy (see Figure 1.3) [33, 91].

iii. Autophagy: NETosis becomes the final fate of the neutrophil upon stimulation by several stimuli [33, 95]. NETosis and autophagy share certain signaling molecules such as protein kinase B (PKB/ AKT), mammalian/ mechanistic target of rapamycin (mTOR) and mitogen activated protein kinase (MAPK) [33]. Out of these, MAPK/ERK are positive regulators of autophagy and NETosis (Figure 1.3) [33]. Hakim *et al.* showed that NET formation by phorbol-12-myristate-13-acetate (PMA) involves the Raf-MEK-ERK pathway which is located upstream of the NADPH oxidase [33, 95]. Contrary to that, Yoo D. *et al.* shows that MAP/ERK is not involved in *Pseudomonas aeruginosa* induced NET formation [82, 87]. Additionally, the MAPK/ ERK pathway has been shown to release IL-8 mRNA in CPPD and MSU crystal-triggered neutrophils [28, 50].

Two plasma membrane subunits of the NADPH oxidase are activated by the MAPK/ ERK kinase and protein phosphatase 1 and/ or 2A involving phosphatidylinositol-3 kinase (PI3K), as shown in Figure 1.3 [33]. However, the details of the mechanism are not well understood [33]. Studies have shown that PI3Ks are involved in signal transduction involving degranulation that is induced by MSU crystals (53, 67, see Figure 1.3) [7, 33]. Mitroulis *et al.* showed that NETs are formed in

gout and that MSU crystals upregulate autophagy pathway by inhibiting PI3K signaling in the neutrophils (see Figure 1.3) [15, 16, 33-35].

iv. Role of IL-1β in NET release: Neutrophil activation in gout has been shown to be associated with NET formation, autophagy and bioactive IL-1β production [34, 35, 40, 115]. Mitroulis *et al.* have shown the presence of IL-1β at the site of gout inflammation [34, 35]. IL-1β signals through IL-1R1, Myd88, TNF receptor associated factor 6 (TRAF-6) and IL-1 receptor associated kinases, resulting in NF-κB induced inflammatory genes [1-3]. In gout, resident macrophages are responsible for producing IL-1β and they bring in more leukocytes, especially neutrophils [1-3, 34, 35]. Recruited neutrophils and eosinophils also release IL-1β, thus, increasing the concentration of proinflammatory cytokines [34, 35].

IL-1β activity can be suppressed by upregulation of natural decoy receptors, IL-1R1 and IL-1 receptor type II (IL-1RII); they have a high affinities for both IL-1α and IL-1β [35, 116]. IL-1RII also interacts with IL-1RAcP and IL-1 to form a non-signaling complex [35, 116]. The soluble form of IL-1R11 (s IL-1R11) can bind to IL-1 in the extracellular space and it ablates the possibility of paracrine activation of IL-1β [35, 116]. The single Ig-IL1R belonging to the IL-1R family also inhibits IL-1 signaling [34, 35, 116, 117]. Chen *et al.,* showed that toll /IL-1R adaptor molecules like TIRAP/Mal, TRIF, TRAM and the Myd88-dependent TLR(1-11)-IL-18R axis are not involved in MSU crystal-induced IL-1β production [34, 35, 118]. IL-6 and IL-8 are also produced along with IL-1β and TNF-α. Together they increased the expression of endothelial cell adhesion molecules, such as E-selectin, intracellular adhesion molecule 1 and vascular cell adhesion molecule 1, which leads to secondary neutrophil recruitment at the site [7]. Some studies suggested that gout may have other sources of IL-1β, such as mast cells or neutrophils [44].

IL-1β plays a central role in gout inflammation [39, 44, 116, 119-121]. As a result, anti-IL-1β therapies are the most sought after gout treatments [39, 44, 116, 119-121]. Current IL-1β inhibitors in gout trials include: anakinra, rilonacept and canakinumab [119, 122] . Dumusc *et al.* mentioned that rilonacept and canakinumab are preferred over anakinra due to their longer half-lives [122]. Anakinra is an IL-1β receptor antagonist with a half-life of 4-6 hours. Rilonacept is a fusion protein that functions as the IL-1β decoy receptor and has a half-life of 7-9 days [119, 122]. Canakinumab is a human anti-IL-1β monoclonal antibody that has a half-life of 26 days [119, 122]. Schumacher *et al.*, Mitha *et al.,* and Sundy *et al.* showed that in randomized controlled clinical trials using urate lowering therapy (ULT) along with rilonacept helps in prevention of acute gout flares [123-127]. So *et al.,* and Schlesinger *et al.* showed that in clinical trials using canakinumab in their patient cohorts helped lowering pain [128-131]. For acute gout, canakinumab shows high efficacy with few safety issues and is, currently, awaiting FDA approval [122, 132].

4. NET Detection Methods

NETs are unique structures made of decondensed DNA, antimicrobial peptides, granule proteins (NE, cathepsin G, MPO, bacterial permeability increasing protein (BPI), lactoferrin, gelatinase), and histones (H1, H2A, H2B, H3, H4) [59, 88, 133, 134]. NETs are characterized by extracellular DNA studded with granular proteins (HNE and MPO) released from neutrophils [88, 133, 135]. During NET formation, the diameter of the ecDNA stretches between 15-17 nm [59, 134, 136]. The NET-associated globular proteins range between 25-50 nm when aggregated with threads of DNA [59, 134, 136]. Given the delicate nature and ‘stringiness’ of the DNA and protein complexes, it is very hard to detect NETs. Microscopy, flow cytometry and fluorescent readers (FRs) are employed for visualizing and measuring NETs [59, 82, 135, 137]. Although these

methods are able to offer distinction between necrosis (or any other ecDNA expelling process) and NETosis, they have many disadvantages such as bias by selection of the field [135]. Antibody-based detection by flow cytometer and imaging are also not ideal as NETs tend to clump together and are not specific [135]. FRs do not allow differentiation between necrosis and NETosis [59, 135, 137]. The DNA-intercalating dyes used for ecDNA detection may block catonic peptides that can interfere with the accurate measurement [59, 135, 137]. Thus, the FR detection-based methodologies are less sensitive and prone to biases [59, 135, 137]. Although cell-free DNA methodology is highly objective and quantitative, it lacks specificity [138-142]. It also does not clearly distinguish a NETosing neutrophil from a non-NETosing one [138-142]. Each of these protocols has many drawbacks [135].

Matsouka *et al.*, suggested that detection methods based on NET-associated ANCA or NET-associated neutrophil-derived proteins are more specific, objective and quantitative assays which can be easily examined [108]. Our NET-ELISA can detect NET-associated, neutrophil-derived proteins (MPO/HNE) in a complex of ecDNA has comparatively high specificity, is quantitative and has been standardized [86]. We present here a semi-quantitative assay along with FR detection, image-based detection and MPO and HNE detection [86, 143, 144]. Our NET detection assay delivers recognition of the NET-DNA with MPO and HNE protein [86]. The method requires DNase for limited NET degradation to obtain snippets of MPO-DNA and HNE-DNA, which is the basis of our detection method.

NETs can be either protective or damaging to the host [23, 59, 88, 145-147]. They can capture pathogens and destroy them, and in higher numbers they can form aggNETs and cleave proinflammatory cytokines [23, 59, 88, 135, 145-147]. NETs can cause sterile inflammation in

response to DAMPs [1, 2]. Host DNase helps in preventing NET formation in the circulation, and impaired NET degradation leads to several autoimmune and autoinflammatory diseases [135, 148]. We utilized this occurrence in our system to detect NET-DNA associated with NET marker proteins. Yoo *et al.* described this novel method [82] and Sil *et al.* demonstrated the method in a video journal [86] (Figure 5.1).

5. Purinergic signaling and MSU crystals: Along with various proteins and ecDNA, dying PMNs produce ATP, ADP, and UDP, which signal through purinergic receptors [149]. Purinergic signaling plays a vital role in maintaining tissue homeostasis and can alter their responses depending upon their cytokine milieu [150]. The activation of purinergic signaling leads to oxidative burst, degranulation and phagocytosis in neutrophils [151, 152]. It is also essential for inflammasome activation [151, 152]. Neutrophils have several P2 receptors (such as P2X1, P2X4, P2X5, P2X7, P2Y1, P2Y2, P2Y6), and adenosine receptors (such as A1, A2A, A2B & A3). [150-153]. Chen *et al.* showed that neutrophils use P2Y2 receptor to respond to extracellular stimuli like ATP [151-153]. Another neutrophil relevant purinergic receptor, P2Y6 receptor, has been shown to release IL-8 upon stimulation with human neutrophil peptides (HNPs) and MSU crystals [154, 155].

*(i) Role of the P2Y6 receptor in MSU crystal-stimulated PMN*s: P2Y6 receptor is a seven transmembrane receptor coupled to G_q protein-coupled signaling pathways [150, 155, 156]. UDP is the natural ligand for P2Y6R [156-158]. Previously, it has been shown that both P2Y2 and P2Y6 receptors can regulate human neutrophil migration and stimulate TLR2-induced IL-8 release from human monocytes [159]. Inhibition of the P2Y6 receptor using MRS2578 hinders phagocytosis in

neurons [160]. The receptor is also known to activate PKC and ERK1/2 to inhibit TNF-α-induced apoptosis in astrocytes [161]. P2Y6 receptor has a crucial role in intestinal epithelium and has high expression on T cells that causes inflammatory bowel disorder [156, 162]. A later study by Uratsuji *et al.* in 2010 showed that MSU crystals utilize the P2Y6 receptor in THP1 and keratinocytes [155]. Neutrophils exhibit low expression of the P2Y6 receptor [151]. The involvement of the P2Y6R in MSU crystal-induced NET formation has not been studied [151-153]. Activated neutrophils show increase in intracellular Ca^{2+} signaling, and this results in the production of nucleotides by them [163-166]. The involvement of ectonucleotides in MSU crystal-induced neutrophil activation and NET release remains uncharted territory.

(ii) UDP-P2Y6 interaction: P2Y6 belongs to the P2Y1 (Gq-coupled protein receptor family) group of receptors [167-169]. UDP binding to P2Y6R leads to the activation of PKC and increase in intracellular phosphate concentrations [167-169]. β-phosphate of UDP (EC_{50}=42 nM) is required to establish electrostatic interaction with the P2Y6R [170]. The pure confirmation of the ribose moiety used for ligand recognition by P2Y6 receptor favors engagement with the phosphate and nucleobase moieties of UDP [170]. Mamedova *et al.* showed that the diisothiocyanate derivative, 1,4-di-(phenylthioureido) butane or MRS2578 (IC50=37±16 nM) can ablate the P2Y6R interaction with its ligand at a concentration of 10 μM [169].

6. Aggregated NET (aggNET) formation in Gout: The presence of NETs, MPO, NE and antimicrobial peptides have been observed in the tissue sections of tophi obtained from gout patients [23, 25]. When the concentration of PMNs and MSU crystals increase, they start forming aggregated NETs or aggNETs [23, 25, 147]. As these high-density clusters of MSU crystals and

PMNs start becoming concentrated, they begin to resemble the tophi [23, 25, 26, 36, 147]. Schauer *et al.* showed that aggNETs degrade local cytokines and chemokines, which help in resolving the inflammation in the joints [23, 25, 26].

In the synovium, newly formed MSU crystals join the preexisting 'PMN and MSU crystal' clusters, and are taken up by monocytes, macrophages and neutrophils [23, 25, 26, 36, 147]. When a large amount of sodium is released from the PMNs, it disrupts the osmotic balance of the cells [25]. This causes the water to leak out of aquaporins present on the cell surface [25]. The concentration of potassium ions also decreases in the cells, which results in the activation of inflammasome in macrophages [25]. Bioactive IL-1β is released from the cells as a result [25]. IL-1β recruits more PMNs at the site where they phagocytose MSU crystals and undergo NETosis [25]. Proinflammatory mediators released from preexisting PMNs prime the newly infiltrated PMNs [25]. This results in an increase in oxidative burst, degranulation and local inflammation by the primed PMNs [25]. At low concentration of PMNs, proinflammatory mediators are produced, which further intensify the inflammation [25]. After a critical threshold of PMN concentration is reached in the joint spaces, the aggregation of NETs starts [25]. The aggNETs then disrupt the vicious cycle of PMN recruitment by cytokines, release serine proteases from NETs, and cleave proinflammatory cytokines and chemokines [23, 25, 26]. As these aggNETs become more densely packed, they wall off the MSU crystals and form a granuloma-like structure [23, 25, 26]. ATP and lactoferrin produced during NET formation also help in resolving inflammation [23, 25, 26]. When they both reach high concentrations in the synovium, they initiate the aggNET formation [23]. ATP helps in the removal of dead cells after NETosis [23]. Lactoferrin helps in inhibiting neutrophil migration [23]. The ROS produced during NET formation also helps in degrading cytokines and resolving inflammation [23]. The quiet build-up of the aggNETs can proliferate into

large tophi [23, 25]. Tophi are immunologically silent and can ward off MSU crystal and neutrophil interactions [25]. However, they are not always successful in containing newly formed MSU crystals due to the ongoing hyperuricemic conditions in the joints [25].

7. Inflammasome in Gout: Inflammasomes sense endogenous danger signals via NOD like receptors (NLRs) [40, 42, 43]. The NLRP-1 inflammasome comprises of caspase-1, caspase-5, pycard/Asc, and NALP1 (a pyrin domain-containing protein sharing structural homology with NODs) [40, 42, 43]. There are 4 inflammasomes that are involved in caspase-1 processing: NLRP1, NLRP3, IPAF and AIM2. Out of these, the NOD like receptor family (NLR), pyrin domain containing 3 (NLRP3) inflammasome is the most well studied with regards to its role in type 2 diabetes, pseudogout and gout [3, 39, 40, 149]. Dysfunction of the NLRP3 inflammasome causes cryopyrin–associated periodic syndromes (CAPs), pyogenic arthritis, pyoderma gangrenosum and acne syndrome (PAPA) [171].

The NLRP3 inflammasome is composed of NLRP3 (NALP3) protein, ASC adaptor protein, and pro-caspase-1 [3, 39-41]. The ASC protein has a PYRIN domain that interacts with the pyrin domain in NLRP3, as well as a CARD domain of pro-caspase-1 [39, 41]. Inflammasome activation requires the phagocytosis of the MSU crystals, regulation of K^+ efflux by P2X7R channel, sensing of ROS due to stress, destabilization of lysosomal membrane, and lysosomal protease cathepsin activation [3, 39, 40]. The released caspase-1 forms a dimer and cleaves pro-IL-18 and pro-IL-1β [2, 4]. Active IL-1β and IL-18 are both produced via the inflammasome pathway by macrophages that have been stimulated with MSU crystals (see Figure 1.3) [3, 33, 39, 40].

Researchers have demonstrated using the air pouch murine model that MSU crystals associate with TLR2/4 and CD14, and that MSU crystals can also launch inflammasome activation by priming

pro-IL-1β [44]. NALP3 is present in macrophages and monocytes and it forms the NALP3 inflammasome with apoptosis-associated speck like protein (ASC) [34, 35, 40, 172]. Macrophages deficient in NLRP3 components do not produce IL-1β and this has also been confirmed using a murine model [2, 3, 39, 40]. In the murine model, intra-articular injection of MSU crystals in combination with long chain free fatty acids has been known to cause acute gouty inflammation [3]. Both *in vivo* and *in vitro* experiments show that MSU crystals utilize the NLRP3 inflammasome pathway, however, the *in vivo* model also suggests an NLRP3 inflammasome-independent pathway due to the various cell types present [3].

In neutrophils, IL-1β release requires NADPH oxidase-independent ROS pathway [25, 173]. Mitochondrial and intracellular ROS activate the NLRP3/ IL-1β secretion axis [25, 174]. In the later stages of gout inflammation, neutrophils contribute to IL-1β production as well [25, 175]. Extracellular IL-1β obtained either from inflammasome-caspase-1 pathway or neutrophil serine protease-3 processing leads to arthritis [25, 34, 35, 176, 177]. Mankan *et al.* showed evidence that NLRP3/ASC/caspase-1 inflammasome pathway is active in neutrophils for intracellular IL-1β processing [175]. Thus, the above information suggests that neutrophils can also process and release IL-1β, thereby, potentially contributing to the ongoing inflammation in the joint.

IL-1β is the main culprit causing cartilage degradation and joint inflammation in gout patients [34, 35, 40, 172, 178]. Colchicine is a gout drug that inhibits the IL-1β maturation by hindering the presentation of the MSU crystal to the inflammasome [2, 3] . Colchicine can also inhibit MSU crystal-induced NLRP3 inflammasome protein complex assembly [4]. Currently practiced gout treatments include using anti-IL-1β agents (such as IL-1RA/anakinra, IL-1Trap, and anti-IL-1β monoclonal antibody /canakinumab) for resolving the attacks [34, 35, 40, 115, 178].

Conclusions: The prevalence of gout has increased over recent decades [17, 19-21]. With an increase in uric acid concentration, MSU crystals deposit in the joints and tissues [1-3, 7]. The microcrystals cause mechanical shear and tearing of the adjoining synovial tissues, synovium and other synovial cells [23, 26, 179]. The damage alerts the leukocytes that start infiltrating the site [23, 26, 179]. Excessive infiltration typically occurs in the early stages of gout that leads to accumulation of leukocytes at the damaged tissue site, resulting in tophi formation in later stages of the disease [23, 26, 179].

As mentioned before, upon PMN activation by MSU crystals, neutrophils undergo degranulation and release proteins like MPO and HNE, and form NETs [59, 88, 96, 146, 180]. These NETs, in few instances, lead to unnecessary sterile inflammation that is seen in gout. Along with ecDNA, PMNs release many ectonucleotides (such as ATP, ADP, Adenosine, UTP, UDP), which contribute to the damage response [162, 181-185]. These ectonucleotides, along with crystals, may trigger purinergic responses [151]. We specifically suspected P2Y6 receptor to play a major role in the process. This receptor is able to start many proinflammatory processes depending on its location and releases copious amounts of IL-8 [162, 184-186]. Here, we show a study to reveal the mechanism of NET formation in gout via P2Y6 receptor.

In gout pathogenesis, the activation of neutrophils is associated with proinflammatory NET-inducing autophagy and IL-1β production [34, 35]. Gout is driven largely by the interaction of MSU crystals, macrophages and neutrophils. Macrophages, when triggered by MSU crystals, activate the NLRP3 inflammasome that cleaves pro-IL-1β and pro-IL-18 to produce active cytokines, IL-1β and IL-18 [39, 40, 42, 43]. These proinflammatory cytokines summon the neutrophils at the site and thereby exacerbate the inflammation [34, 35, 39, 40, 42, 43].

The primary objective of our study was to investigate the mechanism of neutrophil activation by MSU crystals via P2Y6R and its regulation by macrophages. The central hypothesis was that NET formation by MSU crystals is caused by P2Y6 receptor activation and that macrophage-derived inflammatory mediators enhance the process. The rationale for the proposed research was to understand gout inflammation and the mechanism of macrophage-enhanced neutrophil activation in acute gout, in order to develop novel and innovative strategies to advance gout therapeutics.

Figure Legends

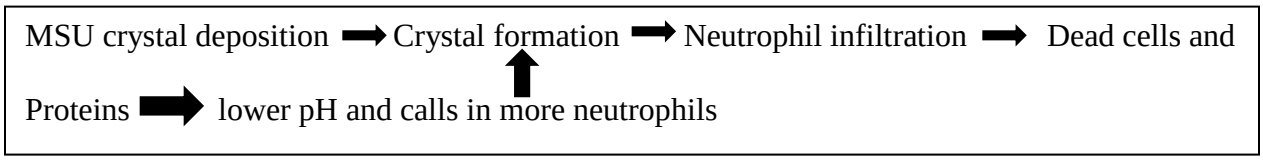

Figure 1.1. The vicious cycle of Gout progression [126]

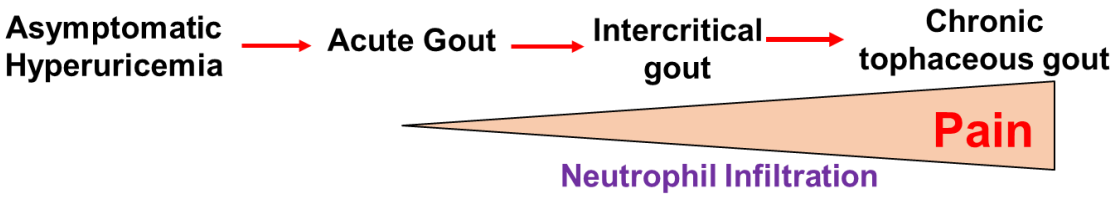

Figure 1.2. Different stages of gout and the associated symptoms [125]

.

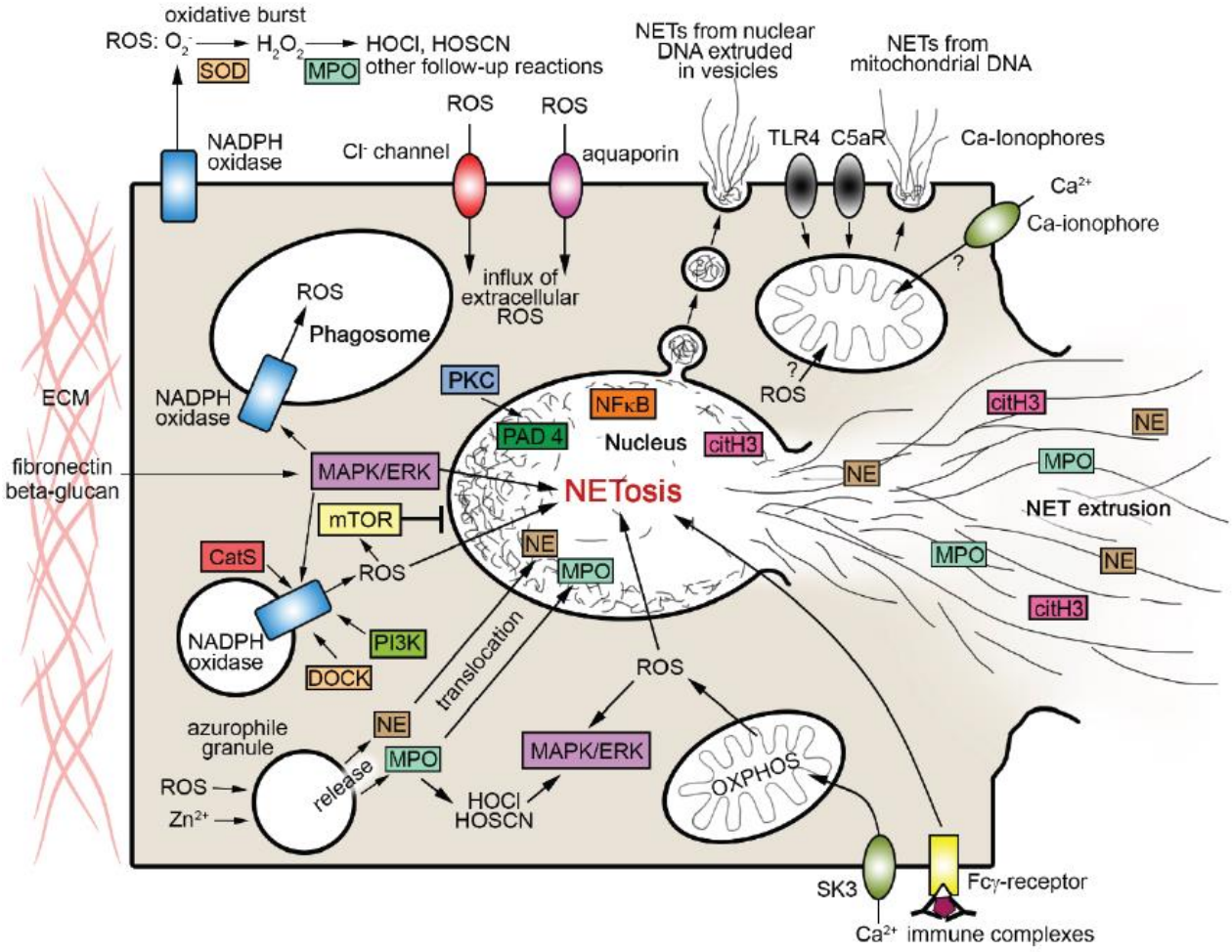

Figure 1.3. Pathways involved in NETosis [33]

(Copyrights obtained from Stoiber *et al.* [33])

CHAPTER 2

NOVEL NEUTROPHIL EXTRACELLULAR TRAP DETECTION METHODOLOGIES[1]

[1] Sil, P., Yoo, D. g., Floyd, M., Gingerich, A., Rada, B. High Throughput Measurement of Extracellular DNA Release and Quantitative NET Formation in Human Neutrophils *In Vitro*. *J. Vis. Exp.* (112), e52779, doi:10.3791/52779 (2016). Reprinted here with permission of publisher.

Short Abstract:

High throughput assays are presented that in combination provide excellent tools to quantitate NET release from human neutrophils.

Long abstract:

Neutrophil granulocytes are the most abundant leukocytes in the human blood. Neutrophils are the first to arrive at the site of infection. Neutrophils have developed several antimicrobial mechanisms including phagocytosis, degranulation, and formation of neutrophil extracellular traps (NETs). NETs consist of a DNA scaffold decorated with histones and several granule markers including myeloperoxidase (MPO) and human neutrophil elastase (HNE). NET release is an active process involving characteristic morphological changes of neutrophils leading to expulsion of their DNA into the extracellular space. NETs are essential to fight microbes, but uncontrolled release of NETs has been associated with several disorders. To learn more about the clinical relevance and the mechanism of NET formation that are reliable tools capable of NET quantitation are needed.

Here three methods are presented that can assess NET release from human neutrophils *in vitro*. The first one is a high throughput assay to measure extracellular DNA release from human neutrophils using a membrane impermeable DNA-binding dye. In addition, two other methods are described capable of quantitating NET formation by measuring levels of NET-specific MPO-DNA and HNE-DNA complexes. These microplate-based methods in combination provide great tools to efficiently study the mechanism and regulation of NET formation of human neutrophils.

Introduction

NET formation is a novel mechanism by which neutrophils fight pathogens.[59] The core of NETs is nuclear DNA.[59] This DNA network is associated with neutrophil granule proteins and histones.[59]. The main form of NET formation requires the death of neutrophils characterized by chromatin decondensation, disappearance of granular and nuclear membranes, translocation of neutrophil elastase to the nucleus, citrullination of histones and finally the spill of DNA-based NETs.[96]. NETs entrap and kill a wide variety of microbes and are an essential part of the innate immune weapon repertoire. Uncontrolled NET formation has, however, been linked to numerous autoinflammatory diseases.[188, 189] Despite their increasingly established relevance, little is known about the mechanism and regulation of NET release.

Neutrophils dying by releasing NETs are different from apoptotic or necrotic neutrophils.[82, 188]. NET-releasing neutrophils show several features that are characteristic for NET formation. Granule components are associated with DNA in NETs [59]. Myeloperoxidase (MPO) and human neutrophil elastase (HNE) are both found in primary granules in resting cells but are translocated to the nucleus to bind to DNA in NETs [59]. MPO-DNA and HNE-DNA complexes are specific for NETs, do not occur in apoptotic or necrotic neutrophils [59, 82, 188]. Chromatin decondensation is another feature typical for NETosis [96]. NET release also requires citrullination of histones by peptidyl aminidase 4 (PAD4) [105]. Citrullinated histones are hallmark of neutrophils that underwent NET release [105].

Here three methods are introduced that in combination provide excellent tools to quantitate NETs on a high throughput scale. The first assay has been used on the field with different changes and quantitates extracellular DNA release in a microplate format. The second and third assays provide confirmation of NETs by measuring NET-specific MPO-DNA and HNE-DNA complexes.

Methods:

Neutrophil Isolation: Healthy volunteers were recruited from the university health center complying to the approved guidelines of Institutional Review Board of the University of Georgia (UGA# 2012-10769-06) [50, 82, 87]. Participants signed the informed consent forms prior to the blood withdrawal. The protocol is in alignment with the ethical recommendations for medical research involving human subjects of the Declaration of Helsinki and HIPAA regulation.
Neutrophils were isolated by the 5 step percoll gradient [50, 82, 87]. Autologous serum is isolated from coagulated blood [50, 82, 87].

Extracellular DNA release measurement: The isolated neutrophil are re-suspended in assay HBSS buffer containing 10 mM Hepes, 5 mM glucose, and 1 % autologous serum. The Sytox Orange dye was used to detect ecDNA or NET release from PMNs in a microplate-based assay using fluorescent reader (varioskan). The measurement is taken for 4 hours and the kinetics is obtained to determine the amount of ecDNA release.

MPO and HNE ELISA: High binding ELISA plates immobilized our protein of interest (MPO or HNE) using capture antibody (anti-MPO and anti-HNE rabbit antibody) overnight. The plates are washed with PBS/ tween and blocked with 5% BSA. The samples or dilution of the samples were added and with the standard for overnight. The following day the plates are washed, incubated with secondary antibody for 2 hours, washed and followed up by detection antibody incubation for 45 min. The final detection done by TMB and the reaction is stopped by HCl. Once yellow coloration was saturated, microplate was read at 450 nm.

MPO-DNA ELISA and HNE-DNA ELISA: High-binding ELISA plates immobilized our protein of interest (MPO or HNE) using capture antibody (anti-MPO and anti-HNE rabbit antibody) overnight just as described with previous section. The plates were washed with PBS/ tween and blocked with 5% BSA, 1 % autologous serum and 0.1 % human serum albumin in PBS. The samples or dilution of the samples were added along with the 2 step protein standard dilution for overnight. The following day the plates were washed, incubated with anti-DNA POD antibody for 30 min. The final detection done by TMB and the reaction is stopped by HCl. Once yellow coloration was saturated, microplate was read at 450 nm.

For sample collection, 250,000 PMNs were seeded on a microplate with 100 nM PMA (for standard) or stimuli in PBS-EDTA buffer, the PMNs were incubated for 4 hours at 37 C. The NETosis process was stopped by adding 1 μg/ml DNase for 10 mins. The reaction was stopped by using 2.5 mM EDTA/PBS. The supernatant were collected, centrifuged and stored at -80C. Two-fold serial dilution of the NET Standard was developed by pooling 10% of 'PMA-NET' acquired from 5 different donors.

Data Analysis: To calculate the amount of MPO-DNA or HNE-DNA complexes compared to NET standard, the background optical density (OD) was subtracted from the OD value of the assay media. Diluted standard samples against their relative NET standard were plotted as shown in Figure 2.5 A. The average of the triplicates of the samples are presents as 'amount of MPO-DNA or HNE-DNA complexes' (% of standard) as shown in Figure 2.5 C. Amount of NETs was determined by the equation of the trend line containing OD values, dilution of samples and the slope of the line.

Results:

The Figures in this manuscript describe the method of neutrophil isolation, experimental procedures, and present representative results with explanation of data analysis. Figure 2.1 shows the sequential steps of human neutrophil preparation. This protocol represents only one possible way of neutrophil isolation. It yields large amounts of resting neutrophils capable of releasing NETs upon stimulation. Figure 2.2 shows how the fluorescence-based DNA release assay works. Using a fluorescence microplate reader kinetics of DNA release in human neutrophils were followed in 96-well microplates. Figure 2.3 explains each step of the data analysis. First, calculate maximal DNA signal in neutrophils treated with saponin (Figure 2.3A). Increase in fluorescence was always calculated as the difference between the highest fluorescence value and the background fluorescence level (Figure 2.3A). This was calculated for each well. The example shows representative data of human neutrophils left non-stimulated or activated with PMA or *P. aeruginosa* (PAO1) (Figure 2.3B). *P. aeruginosa* triggers NET formation in human PMNs [82, 85, 87]. It has been shown with several *P. aeruginosa* strains including PAO1 that bacteria alone (without neutrophils) do not bind to the used DNA-detecting dye (Sytox Orange dye) [87]. PAO1 *P. aeruginosa* was obtained from ATCC, cultured in Luria-Bertani medium overnight, harvested in late-exponential phase, washed in assay medium and used to stimulate neutrophils at a multiplicity of infection (MOI) of 10:1 (Figure 2.3B, C, 2.4B, C). Averages of increase in fluorescence of replicate wells were calculated and normalized based on maximal fluorescence (saponin) and were expressed as "DNA release (% of max)" (Figure 2.3.C.). Figure 2.3.D. shows representative fluorescence images of untreated or PMA-stimulated neutrophils.

Figure 2.4 A depicts the scheme explaining the principles of the MPO-DNA and HNE-DNA ELISA assays. Figure 2.4 B shows representative immunofluorescence images of non-stimulated, PMA-and PAO1-activated human neutrophils. Extracellular DNA shows typical NET morphology and co-localizes with MPO and citrullinated histone H4, a marker of NET formation [105]. Figure 2.4 C shows MPO-DNA and HNE-DNA release in human neutrophils under the same, previous conditions (like Figure 2.3B, 2.3C and 2.4B). The "NET" ELISA methods have been previously characterized [82]. Briefly, 2 U/mL DNase treatment (equivalent of 1 µg/mL concentration of the DNase used) for 15 min at room temperature resulted in the highest MPO-DNA and HNE-DNA signals [82]. Running samples (100 ng/lane) on an agarose gel revealed that DNA length in the lower kb range yields optimal ELISA signal.[82] DNA over digestion (DNase dose higher than 20 U/mL) or omitting either the capture or the detection antibody abolished the ELISA signals [82].

In addition, here the assays and the "NET-standard" were further characterized (Figure 2.5A). The NET-standard contains on average 19.5 µg/mL extracellular DNA (measured by using a standard with known DNA concentrations), 399 ng/mL MPO and 103.4 ng/mL HNE (commercial ELISA kits) (n=8). Based on the total molecular weights of MPO (84 kDa) and HNE (29.5 kDa) and the fact that 1 µg DNA contains $9.91x10^{14}$ nucleotides, the NET-standard contains 109 HNE molecules and 147 MPO molecules per 1000 nucleotides (kb DNA). Two-fold serial dilution experiments of the NET-standard revealed that the dynamic ranges of both the MPO-DNA and HNE-DNA ELISA assays were between 19.0-609.0 ng/mL DNA concentrations (Figure 2.5B). Dilutions of lower than 32-fold of the NET standard resulted in saturation whereas dilutions of higher than 1024-fold were not different from the background (Figure 2.5B). Treatment of the NET standard with protease inhibitors did not change its results obtained by the MPO-DNA and

HNE-DNA assays indicating that proteases do not interfere with these assays (Figure 2.5C). Thus, results obtained in the same NET-standard sample by the MPO-DNA or HNE-DNA ELISA assays strongly correlate with each other (Figure 2.5D). To show that frozen PMN supernatants could also be used in these assays without losing efficiency, some aliquots of the NET-standard were left untreated and others were exposed to one or two freeze/thaw cycles performed at -20 °C or -80 °C (1 h interval). None of the freeze/thaw treatments affected the MPO-DNA or HNE-DNA results (Figure 2.5E). In summary, the NET-standard provides a reliable reference point in these NET-quantifying assays enabling the quantitative comparison of NET results between independent experiments.

Discussion: NETs represent a fascinating novel mechanism by which neutrophils kill pathogens [59]. Although the literature on NETs has been continuously expanding over the last ten years since their discovery, several important questions related to their role in biology, mechanism and regulation remain unclear. Appropriate methodology has to be developed to measure NETs, this very unique antimicrobial mechanism. This article describes methods that can be used to quantitate NETs in a high throughput manner. The first assay follows kinetics of fluorescence of a membrane-impermeable DNA-binding dye. This assay provides large amount of information on the slope and velocity of DNA release from neutrophils. This information is crucial in investigations studying early signaling events leading to NET formation. All this information is lost in endpoint assays measuring DNA release at the end of the incubation. The extracellular DNA dye-based assay is not specific for NETs. It only measures DNA release. To confirm NETs, it is widely accepted to perform immunofluorescence on NET-forming neutrophils and show co-localization of DNA with

either granule markers (MPO, HNE) or histones. Quantitation of immunofluorescence data is though very tedious and subjective.

Here, a modification of a previously developed ELISA assay detecting MPO-DNA complexes is presented. A similar ELISA assay measuring HNE-DNA complexes that represent specific NET measures is also described [82, 188]. Both assays have been characterized in detailed [82]. The MPO-DNA and HNE-DNA ELISA assays are quantitative and NET-specific at the same time [82]. These features are not fulfilled by any other current method. The assays are easy to perform and provide reproducible data [82]. A limited DNase digestion step is included which ensures prompt and standardized handling of NETs directly on neutrophils [82]. These assays are suitable to compare several samples at the same time. In new, control measurements it is shown that freeze/thaw cycles and proteases do not affect the outcome of the MPO-DNA and HNE-DNA assays. It is unknown, however, whether proteins known to bind to DNA in NETs (including histones and LL-37 [59, 190]) would interfere with these assays.

Critical steps of the presented protocols are as follows. It is important to harvest neutrophils that are in a resting, quiescent state and do not release large amount of NETs spontaneously. Lack of a hypotonic lysis step to remove red blood cells in the presented neutrophil isolation protocol is crucial to obtain non-activated neutrophils. To inhibit neutrophil activation after the cells had been purified, it is also important to re-suspend neutrophils in a medium containing their donor's own serum. To obtain quiescent cells it is also crucial to use pyrogen-and contamination-free reagents during neutrophil preparation. Spontaneous NET release of neutrophils during the extracellular DNA release assay could also happen. Adding 1% autologous serum to the assay medium is

important to prevent it. Higher or lower doses of the autologous serum could be tested to get optimal results. It is critical during the MPO-DNA and HNE-DNA ELISA assays that released DNA should not be over-digested by the DNase because it will result in complete loss of the signal. Therefore, the optimal dose should be determined for every new DNase batch. The parameters of the DNA digestion could be slightly changed to obtain the highest ELISA signals possible. It is also important to mix the DNase and NETs thoroughly to ensure that the DNase will have clear access to the DNA. When harvesting the digested NETs, wash the well extensively to collect all the NETs.

The DNA detection limit of the MPO-DNA and HNE-DNA assays is around 10-20 ng/mL DNA (Figure 2.5 B). Serum and plasma free DNA levels of several hundred to thousand ng/mL were reported in diseases (cancer, systemic lupus erythematosus, myocardial infection) that have been associated with abnormal NET formation [191-193]. This suggests that the MPO-DNA and HNE-DNA ELISA assays also have the potential to be able to quantitate NETs in human clinical samples. This future application of the MPO-DNA and HNE-DNA ELISA assays will enable to quantitatively link NETs to disease pathogenesis.

Disclosure

The authors have nothing to disclose.

Acknowledgements

Special thanks to the personnel of the University of Georgia Health Center laboratory for their continuous support of our work on isolating human neutrophils. This work was supported by the start-up fund of Dr. Rada provided by UGA Office of Vice President for Research.

Concluding remarks:

In order to study NETs, a process of detection should be in place. The protocol presented here (as shown by Yoo *et al.* and Sil *et al.*) will help in understanding the signaling pathways mediating NET release [82, 86]. Along with the ecDNA and NET marker ELISA detection (MPO & HNE), our novel semi-quantitative NET-ELISA detects 10-20 ng/ml of DNA, which are in the physiological range [86]. The methods described here will be utilized extensively in the next two chapters. To detect NET production the presence of specific inhibitors (PPADS, Suramin, AR-C118925XX, MRS2578 or SK&F96365) or cytokines (IL-1β), we have used the same methodology. We first detected NET release by ecDNA assay which was first demonstrated before Yoo *et al.* [82, 96, 194-196] (Figure 5.1). We then confirmed NETs by follow-up analysis with MPO and HNE ELISA (Figure 5.1). For the final assurance, we performed NET-ELISA to detect MPO-DNA and HNE-DNA association (Figure 5.1). This method helps in quantitating NETs more accurately and is less prone to biases.

Although there are a few specifics to be wary off and in order to avoid over-interpreting the data, future investigation is required to ensure that the MPO and HNE are released specific for the neutrophils. In conclusion, our novel MPO-DNA and HNE–DNA 'NET' ELISA assays simplify the NET detection method and does not required specialized flair as is in the case in other NET detection methodologies.

FIGURES.

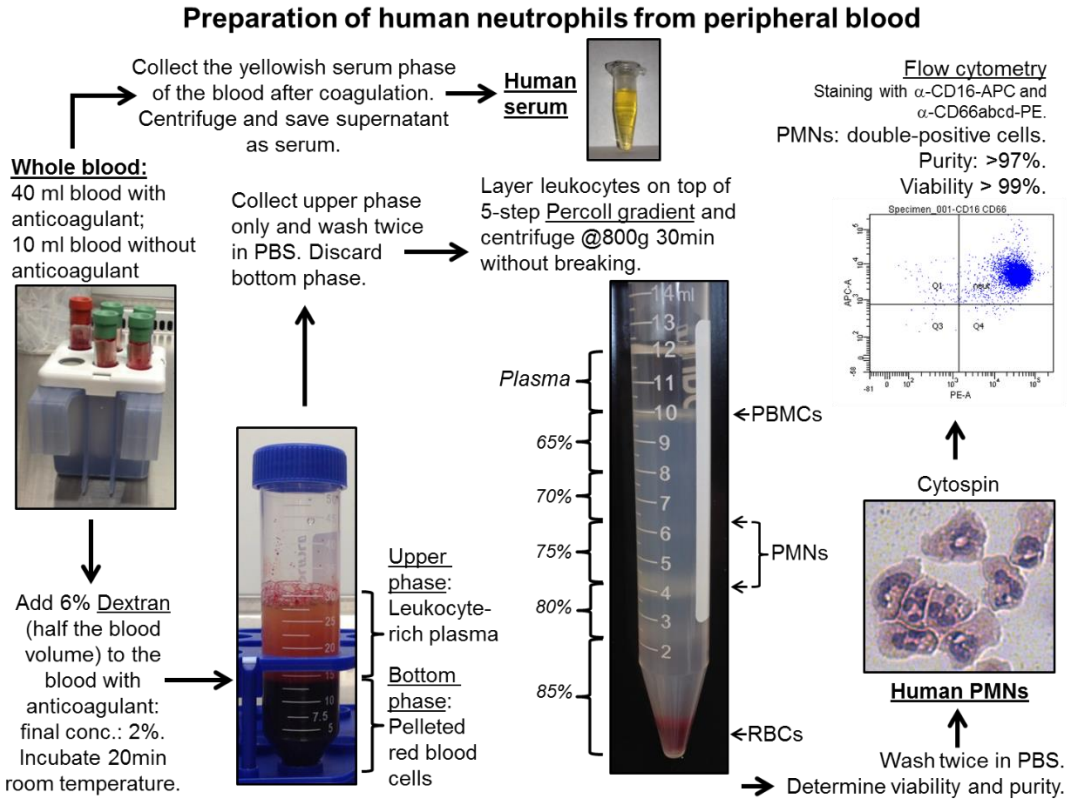

Figure2.1. Isolation of human neutrophils. Neutrophil granulocytes were isolated from peripheral blood of volunteers according to the described protocol. Blood containing anticoagulant was used to isolate neutrophils by Dextran sedimentation and gradient centrifugation. Blood without anticoagulant was used to prepare serum. Viability of the neutrophil preparations is assessed by Trypan Blue exclusion assay. Neutrophil purity is assessed by cytospin or flow cytometry (CD16, CD66abcd double-positive cells).

[copyrights obtained from the journal]

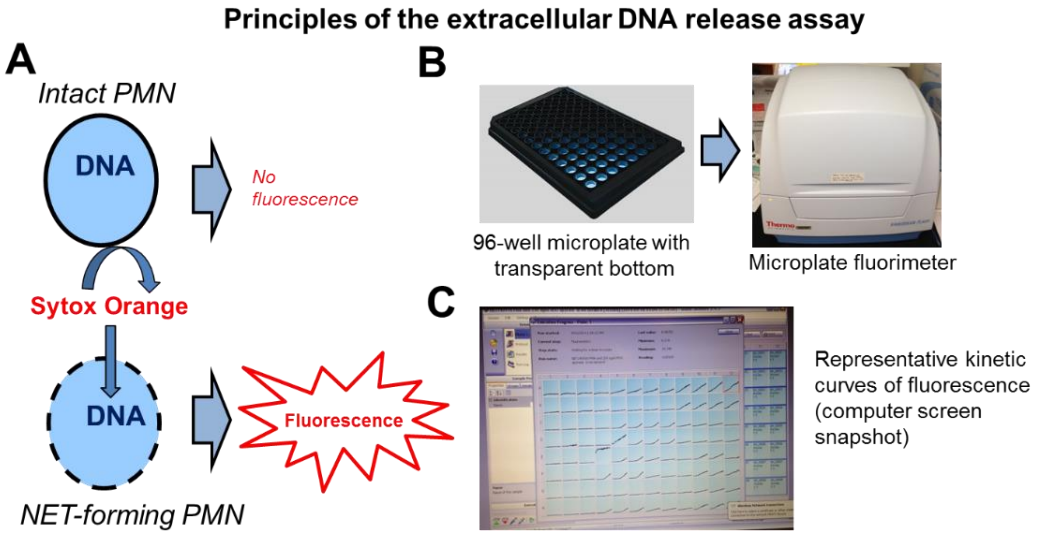

Figure 2.2. Principles of the extracellular DNA release assay. A) Fluorescence is only obtained in neutrophils whose plasma and nuclear membranes have been compromised and the membrane-impermeable DNA-binding dye can bind to their DNA. B) The assay is performed on black 96-well microplates using a microplate fluorimeter. C) The fluorimeter records real-time fluorescence curves in each well. One representative results in shown.

[copyrights obtained from the journal]

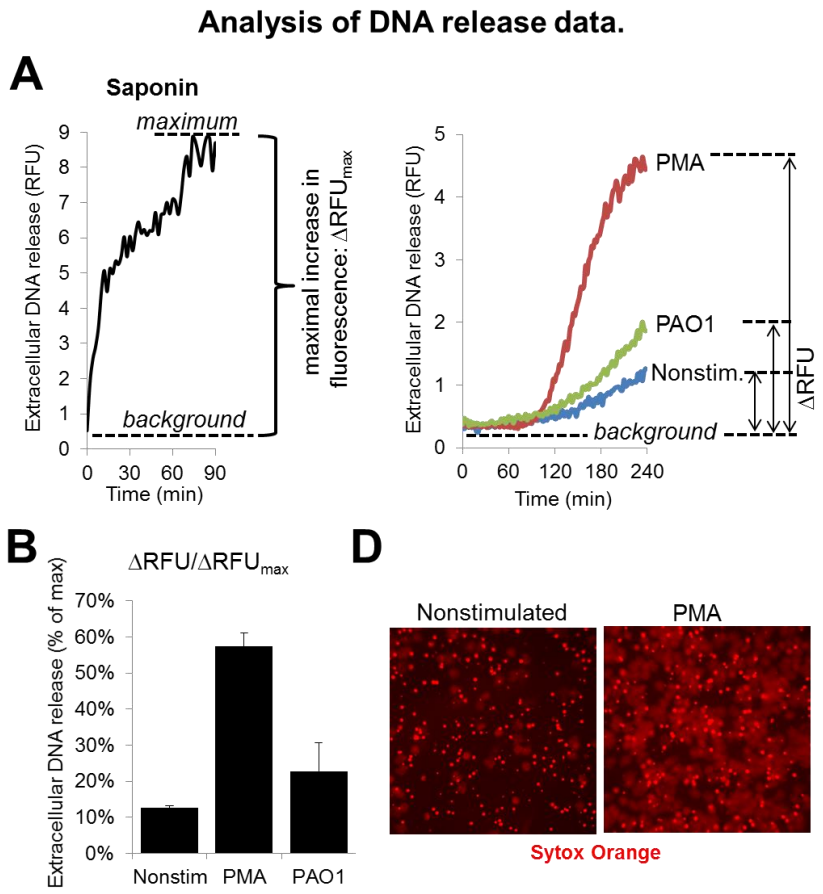

Figure 2.3. Analysis of the DNA release data. A) Saponin is used to create the maximal value since it entirely lyses neutrophils and exposes their DNA. The kinetics of saponin-induced fluorescence is shown. B) Kinetics of neutrophil DNA release induced by PMA (100 nM) and bacteria (*Pseudomonas aeruginosa* PAO1, 10 MOI). C) Normalized summarized DNA release data obtained in one experiments using quadriplicates. D) Representative fluorescence images of untreated and PMA-stimulated human neutrophils (Sytox Orange, 4 hr incubation).

[copyrights obtained from the journal]

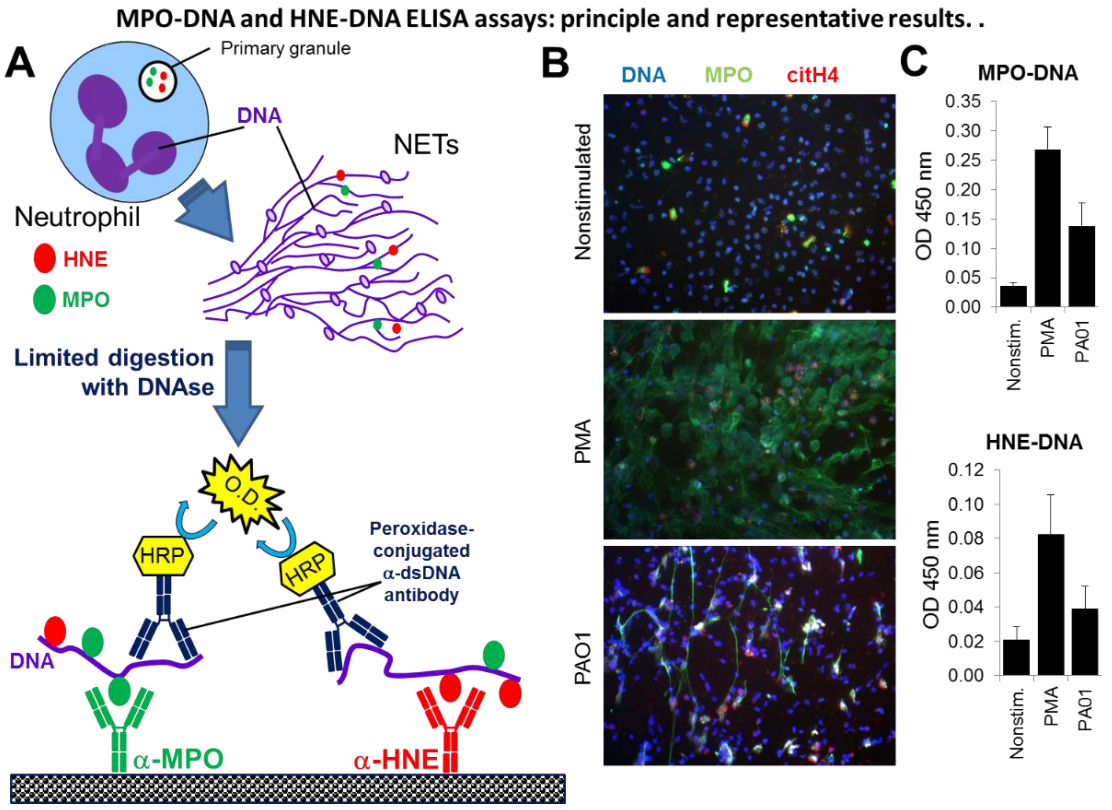

Figure 2.4. MPO-DNA and HNE-DNA ELISA assays: principle and representative results. A) Scheme explaining how the MPO-DNA and HNE-DNA ELISA assays work. B) Representative results of immunofluorescence images prepared on human neutrophils exposed to 100 nM PMA or *P. aeruginosa* PAO1 strain (10 MOI) for 4 h. Extracellular DNA (DAPI, blue) co-localizes in NETs with MPO (green) and citrullinated histone H4 (red). One representative result, n=3. C) NET release was measured in human neutrophils exposed to the same stimuli as above by the MPO-DNA and HNE-DNA ELISA assays. Mean±-S.E.M., n=3.

[copyrights obtained from the journal]

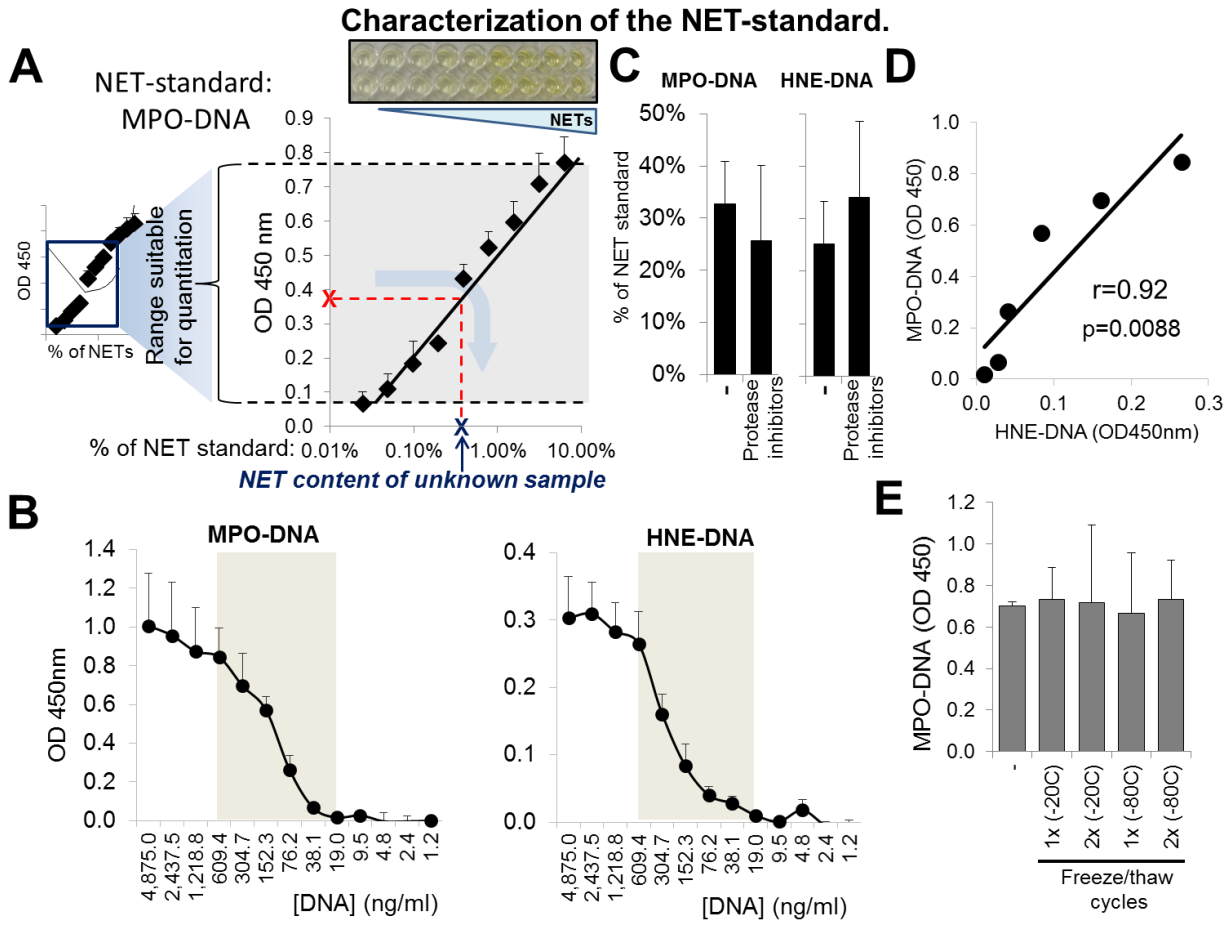

Figure 2.5. Characterization of the "NET-standard". A) Serial dilutions (1:2) of the NET standard were prepared and subjected to MPO-DNA ELISA. Measured OD values are plotted against % of NET-standard content. Red "X" indicates a measured OD value of an unknown sample. Gray arrow indicates how the "NET concentration" (blue "X") of the unknown sample is to be determined using the central range of the fitted standard curve. B) DNA concentrations in serially diluted NET-standard samples were determined and plotted against the measured OD values of the MPO-DNA or HNE-DNA ELISA assays. Gray areas indicate the dynamic ranges of the assays. C) Protease inhibitor treatment (protease inhibitor cocktail, 1%) does not affect the outcome of the MPO-DNA or HNE-DNA assays (NET-standard). Mean+/-S.E.M., n=2. D)

Correlation of MPO-DNA and HNE-DNA results (OD 450 nm) of serially diluted "NET-standard" samples in their dynamic ranges (See 5B). E) Freezing and thawing cycles (-20 °C or -80 °C; one or two) do not affect the results of MPO-DNA and HNE-DNA assays (NET-standard, mean ± S.E.M., n=2).

[copyrights obtained from the journal]

CHAPTER 3

P2Y6 RECEPTOR ANTAGONIST, MRS2578, INHIBITS NEUTROPHIL ACTIVATION AND AGGREGATED NET FORMATION INDUCED BY GOUT-ASSCOIATED MONOSODIUM URATE CRYSTALS. [2]

[2] Sil, P, Hayes C., Reaves B., Breen P., Quinn S., Sokolove J., and Rada B., Submitted to *Journal of Immunology,* September 2016 (under revision).

Abstract

Human neutrophils generate inflammatory responses within the joints of gout patients upon encountering monosodium urate (MSU) crystals. Neutrophil extracellular traps (NETs) are found abundantly in the synovial fluid of gout patients. The detailed mechanism of MSU crystal-induced NET formation remains unknown. Our goal is to shed light on possible roles of purinergic signaling and neutrophil migration in mediating NET formation induced by MSU crystals. Interactions of human neutrophils with MSU crystals were evaluated by high-throughput live-imaging using confocal microscopy. We quantitated NET levels in gout synovial fluid supernatants and detected enzymatically active neutrophil granule enzymes, myeloperoxidase (MPO) and human neutrophil elastase (HNE). Suramin and PPADS, general P2Y receptor blockers, and MRS2578, an inhibitor of the purinergic P2Y6 receptor, block all NET formation triggered by MSU crystals. Additionally, P2Y2 antagonist (AR-C1125XX) shows no inhibition with MSU crystal-induced NET formation. Live imaging of PMNs shows that MRS2578 represses neutrophil chemotaxis and blocks characteristic formation of MSU crystal-DNA aggregates following crystal exposure. Additionally, the store operated calcium entry (SOCE) channel inhibitor (SK96365) also blocks MSU crystal-induced NET release. Our results indicate that the P2Y6-SOCE-IL-8 axis is involved in MSU crystal-induced NET formation providing a novel mechanism potentially relevant to gout inflammation. The work presented here could lead to a better understanding of gouty joint inflammation and help improve the treatment and care of gout patients.

Introduction

Gout is an inflammatory disease of the joints caused by monosodium urate (MSU) crystal deposition in the synovial spaces. Gout inflammation is essentially driven by the proinflammatory cytokine, IL-1β, and accumulation of polymorphonuclear leukocytes (PMNs, neutrophils) [23, 34, 35]. Gout affects millions of patients globally [197]. The prevalence of gout and its associated co-morbidities (such as diabetes, kidney disease, cardiovascular disorders) has increased over the past decade [198-200] and is expected to rise in the future [201]. Hyperuricemia in the blood is not requisite for accumulation of MSU crystals but is one of the symptoms of gout [202]. The risk associated with high uric acid in the serum is crystallization of the excess uric acid in the joints [203, 204]. Crystal deposition triggers gouty inflammation driven by resident macrophages and PMNs. PMNs are primarily recruited by the proinflammatory cytokine, IL-1β [34, 205-208].

MSU microcrystals cause mechanical shear and tearing of the adjoining synovial tissues, [202, 205, 207] and this damage alerts leukocytes which start infiltrating the site [1]. Macrophages produce IL-1β in response to the MSU crystals by activating the NLRP3 inflammasome [34, 35]. IL-1β is a strong proinflammatory cytokine that induces neutrophil migration and can release chemoattractants from macrophage and mast cells resulting in further recruitment of leukocytes, especially PMNs [40, 57, 209]. Upon activation by MSU crystals, PMNs produce reactive oxygen species (ROS) and release granule proteins like myeloperoxidase (MPO) and human neutrophil elastase (HNE), and form neutrophil extracellular traps (NETs) [23, 34, 35]. MPO and HNE are packed in PMN primary granules and their release is imperative for the initiation of the NET pathway [2, 20-22, 64, 65]. NET formation is essentially an antimicrobial mechanism that helps PMNs to trap pathogens [59, 145, 146]. Uncontrolled NET formation has been, however, associated with several diseases, including gout [23, 35]. During NET formation, the nucleus

undergoes delobulation and chromatin decondensation [96]. The nuclear membrane disassembles, granules disintegrate and the cytoplasmic and nuclear contents fuse [210]. Citrullination of histone H3 and H4 by peptidylarginine deaminase 4 (PAD4) cause decondensation of DNA-chromatin complexes [18, 33, 59, 145, 146].

Although PMNs represent the most abundant leukocytes during gout inflammation reaching a concentration of 10^8/ml in the synovial fluid (SF) [23], their role in the complex pathogenesis of gout has been unclear. A recent study by Schauer *et al.* shed light on the dual role of PMNs in gout [23]. In addition to their proinflammatory role in initiating and mediating inflammation in gout, PMNs also play a subsequent anti-inflammatory role in limiting acute flares [23]. PMNs and MSU crystals accumulate to form high-density consolidated structures, which limit inflammation in gout and form 'aggregated NETs' (aggNETs) [23, 25]. AggNETs set the stage for gouty tophi formation, a characteristic white material that appears at the beginning of the resolution phase of acute gout flares [23, 24]. Although NET formation plays unique, dual roles in the mechanism of gout inflammation, its cellular and molecular mechanisms are not well understood.

NET formation is a cell death mechanism during which PMNs release several intracellular molecules. Uric acid is a by-product of purine metabolism, which causes gout [198]. The breakdown of purines result in the formation and accumulation of ecto-nucleotides such as ATP, UTP, UDP and nucleic acids that are recognized as danger signals by cells [151, 155, 211-213]. Immune cells like PMNs, macrophages and T cells respond to extracellular nucleotides via purinergic receptors [151, 213]. Extracellular nucleotides and purinergic receptors are involved in various PMN functions such as migration, degranulation and reactive oxygen species formation [214]. Therefore, they could potentially have a role in NET formation. Recent data shows that MSU microcrystals signal through the purinergic P2Y6R receptor in THP 1 macrophages and

human keratinocytes [155]. The P2Y6 receptor has high affinity for UDP and is involved in IL-8 mediated-chemotaxis of leukocytes [212, 213, 215, 216]. In Inflammatory bowel diseases, P2Y6 receptor activation causes stimulation of IL-8 expression in the intestinal epithelium, which leads to PMN recruitment [162]. Studies, including this investigation, show that MRS2578, a potent and specific P2Y6R antagonist, inhibits IL-8, IL-6 and CXCR1 release in PMNs stimulated by defensins [156, 182, 186, 217-220]. Thus, we hypothesized that the P2Y6 receptor is required for MSU crystal-induced NET formation in human PMNs.

We show here that P2Y6R block by its highly specific inhibitor MRS2578 hinders MSU crystal-triggered PMN activation and NET formation. Understanding the processes involved in inhibition of NET formation via P2Y6R signaling can help advance current gout therapeutics.

Methods

Materials

Inhibitors, P2Y channel Inhibitors: Stock solutions of suramin ([8,8′-(carbonylbis(imino-4,1-phenylenecarbonylimino-4,1-phenylenecarbonylimino))bis-1,3,5-naphthalenetrisulfonic acid]) (P2Y inhibitor, 300 μM, Sigma, St. Louis, MO, USA.), MRS2578 (P2Y6 inhibitor, 5-10 μM, Sigma, St. Louis, MO, USA.), PPADS(P2Y inhibitor, 200 μM, Tocris, Minneapolis, MN, USA.), AR-C118925xx (P2Y2 antagonist, 1 μM, Tocris, Minneapolis, MN, USA), HNE inhibitor (Elastase inhibitor II, Calbiochem EMD Millipore cat # 324744), PMA (100 nM, Sigma, St. Louis, MO, USA.) were prepared in DMSO. Sources and concentrations for other reagents are as follows: Saponin, cytochalasin B, ATP, ADP, adenosine, UDP were also purchased from Sigma. SK&F96365 (store-operated calcium entry (SOCE) inhibitor, 100 μM, Tocris, Minneapolis, MN, USA), lucigenin (Cayman Chemicals, 100 μg/ml) , human recombinant IL-8 (250 pg/ml, Canton

MA, USA.), human recombinant IL-1β (10 ng/ml, BioLegend, San Diego, CA, USA), MPO antibody (Millipore, Billerica, MA,USA), anti-rabbit HNE antibody (Calbiochem, Billerica, MA,USA), Sytox Orange (Life Technologies, 2.5 μM, Invitrogen, Carlsbad,CA, USA), Diogenes Superoxide Measurement Kit (National Diagnostics, Atlanta, GA, USA.), apyrase (New England Biolabs, Ipswich, MA,USA), TMB (Thermo-Scientific, Waltham, MA, USA), Monosodium Urate crystals (Invivogen, Carlsbad, CA, USA), BSA (Hyclone™, GE Healthcare Life Sciences, Logan, UT, USA), PBS (Thermo-Scientific, Fremont, CA, USA), 12-O-Tetradecanoylphorbol-13-acetate (PMA,Sigma, St. Louis, MO, USA.), IL-8 (Cell Sciences, Canton MA, USA.)

Human subjects: Healthy human volunteers were recruited anonymously at the University of Georgia to donate blood. The studies were performed according to the guidelines of the World Medical Association's Declaration of Helsinki. Enrolled blood donors signed consent forms with appropriate introduction as described previously [82, 87]. The human blood protocol (UGA# 2012-10769) and the consent form were reviewed and approved by the Institutional Review Board (IRB) of the University of Georgia.

Preparation of human neutrophils *and autologous serum:* Human PMNs were purified as described previously (19, 41). Briefly, coagulation was prevented with heparin and red blood cells were removed by Dextran sedimentation (GE Healthcare, Atlanta, GA, USA). PMNs were isolated using Percoll (Sigma, St. Louis, MO, USA) gradient centrifugation. Cell viability was determined by Trypan blue dye extrusion (>98%). PMN purity was assessed by cytospins and flow cytometry. The characterization confirmed higher than 95% purity. Autologous serum was prepared by centrifugation and sterile filtration. Calcium-and magnesium-containing HBSS (Mediatech,

Manassas, VA, USA) supplemented with 1% autologous serum of the PMN donor, 5 mM glucose and 10 mM HEPES was used as assay buffer. Autologous serum was prepared from the blood of the PMN donor by repeated centrifugations and filtration through 0.2 mm filters.

Flow cytometry: Human PMNs were identified on the basis of the scattering pattern and also staining with CD16 and CD66abce-PE antibodies (Miltenyi Biotec Inc., San Diego, CA) using LSR II flow cytometer and BD FACsDIVA V6 software. The characterization confirmed higher than 95% PMN purity (double-positive cells).

Synovial fluid samples: Synovial fluid (SF) samples were taken from patients diagnosed with gout or osteoarthritis under protocols that were approved by the Stanford University IRB and included the informed consent of the subjects. Samples of SF from actively inflamed large or medium joints were obtained by needle aspiration performed by a board certified rheumatologist (JS) at the VA Hospital (Palo Alto, CA, USA). Grossly bloody fluid was excluded from analysis. SF was centrifuged at 1,000g for 10 minutes, and supernatants were removed and frozen at -80°C until they were later used for the experiments described below. The diagnosis of gout was confirmed by identification of negatively birefringent intracellular needle-shaped crystals on microscopic examination of SF under polarizing light microscopy. The diagnosis of osteoarthritis (OA) was made as defined by the 1986 American College of Rheumatology [221].

Quantification of NETs: NETs were quantified essentially as described by Pang *et al.* [50]. PMNs were adhered to poly D-lysine coated 96-well black transparent bottom plates (Thermo Scientific, Rochester, NY) in assay buffer with 0.2% Sytox Orange (Life Technologies, Grand Island, NY,

USA). PMNs were then exposed to 250 µg/ml MSU crystals. Fluorescence (excitation: 530 nm, emission: 590 nm) was measured in a fluorescence microplate reader (Varioskan Ascent, Thermo Scientific) for 6 hours at 37 °C. Increase in fluorescence normalized on maximal value (saponin-treated PMNs) was referred to as "extracellular DNA release" and expressed as "% of max". Alternatively, results were also normalized against PMA.

Measurement of AggNET formation: 1 million PMNs suspended in assay medium were seeded in a 48 well plate with or without 1mg/ml MSU crystals at 37 °C with 10 µM MRS2578 or DMSO. Images of aggregated NETs (aggNETs) were taken after overnight incubation [23].

Quantification of enzymatic activities: To measure HNE activity, the Neutrophil Elastase Activity Assay Kit (Cayman Chemical Ann Arbor, MI, USA) was used following manufacturer's protocol. Briefly, supernatants (50 µl) were placed into 96-well black plates. Substrate (Z-Ala-Ala-Ala-Ala 2Rh110, cat no.600613) solution was added to assess elastase activity by measuring production of the highly fluorescent product (compound R110) using 485 nm excitation and 525 nm emission wavelengths in a fluorescence plate reader (Varioskan Flash, Thermo Scientific). Data are expressed either as kinetics (RFU) or end-point values normalized on maximal (PMA-stimulated) data.

Peroxidase activity was measured by hydrogen peroxide-dependent oxidation of Amplex Red. 50 µl undiluted PMN supernatants were added to 96-well non-transparent black microplates (Costar, Corning, NY) and mixed with assay solution containing 100 mM Amplex Red (Molecular Probes, Eugene, OR) and 100 µM hydrogen peroxide (Sigma, St Louis, MO). Production of the fluorescent product was measured with fluorescence plate reader (Varioskan Ascent, Thermo Scientific) after

30 min at 560-nm excitation and 590-nm emission wavelengths. Known MPO concentrations (stock: 125 ng/ml MPO; R&D Systems, Minneapolis, MN, USA) were used as the standard to determine peroxidase activities of unknown samples. Results are expressed as "equivalent ng/ml MPO activity" This data presentation was preferred (instead of showing unit enzymatic activities per time and volume) to compare MPO concentration and activity in PMN supernatants.

Live imaging of NET formation using confocal microscopy: 2 x 10^6 human PMNs in assay medium were incubated for 4 hrs at 37 °C with or without 100 nM PMA and 100 μg/ml MSU crystals in 35 mm glass bottom dishes (MatTek, Ashland, MA). The dishes were pre-coated for 1 hr with 1% human serum albumin (Sigma Aldrich, St Louis, MO, USA) in HBSS. At the end of the incubation, 0.2% Sytox Orange (Wavelength=547-570 nm) (Invitrogen, Grand Island, NY, USA) was added prior to imaging. Images were collected using a Nikon A1R confocal microscope system equipped with a Nikon Eclipse Ti-E inverted microscope, equipped with the Perfect Focus System, high-speed motorization and NIS Elements software (Nikon Instruments, Melville NY). Live cell imaging was carried out using a Tokai Hit INY-G2A-TIZ incubator (Tokai Hit CO, Ltd, Shizuoka-ken, Japan) for temperature, humidity and CO_2 control. The imaging was performed every 15 min interval for 16 hours. The Coherent Sapphire 561nm 20mW laser was used to excite Sytox Orange using a CFI Plan APO VC 60X Oil NA 1.4 WD 0.13 mm objective. Z-stacks were acquired and 3-D image reconstructions were processed using the Nikon NIS Element Version 4 software. Final image preparation was carried out using Adobe Photoshop.

High throughput live imaging and quantitation of NET formation: To perform the microplate-based NET assay, PMNs were seeded at a concentration of 250,000 cells/ well in a 96 well plate

Optical Btm Pit Polymer Base black plate (Thermoscientific, Rochester, NY). PMNs were pre-incubated with 10 μM MRS2578 for an hour prior to imaging. PMNs were then stimulated with 200 μg/ml MSU crystals for 16 hours. Nikon A1R confocal microscope system with a 10X lens was used to capture transmitted light and fluorescence images. A field of interest was chosen to perform imaging and their position was defined using the NIS elements software. The chosen field was a true representation of the entire well. Images were taken every 15 min for 12 hours using automated capture component of the NIS elements software. Mean Sytox Orange intensities of the fluorescent images were quantified using the measure region of interest (ROI) feature of the Nikon A1 Elements software. The entire image that represented the field was selected as the ROI. These measurements were used to calculate changes in Sytox Orange intensities over time (ΔMean SYTOX orange intensity). Each biological replicate represents the mean of three technical replicates.

ELISA: Levels of MPO, HNE, and IL-8 were detected by ELISA. Manufacturer's instructions were followed for sample dilutions and processing. 250,000 cells /well PMNs were seeded in 24-well plates and stimulated with 250 μg/ml MSU crystals in HBSS for up to 4 hours at 37˚C. Cell supernatants collected were either immediately processed or stored (-20˚C) for later analysis. Undiluted supernatants were used to measure IL-8 and MPO levels, whereas supernatants were diluted 1:100 to determine MPO concentrations. Concentrations of human MPO in PMN supernatants were measured by commercial ELISA kit (R&D Systems, Minneapolis, MN, USA). Serial dilutions prepared from MPO standard provided in the kit (stock: 125 ng/ml) were used to quantify MPO concentrations of unknown samples. HNE release was assessed by sandwich ELISA using an anti-HNE rabbit polyclonal antibody to capture elastase. Supernatant samples were

incubated overnight at 4˚C in 96-well high binding microlon ELISA plates (Greiner Bio-one, Frickenhausen, Germany). After blocking with 5% BSA for 2 hour (RT), anti-rabbit mouse polyclonal Ab (1:500 in PBS [Calbiochem], 481001 [EMD Millipore]) was added for 2 hours at RT. After repeated washes, samples were incubated with horseradish peroxidase–linked donkey anti-rabbit Ab (1:2000 in PBS, NA934V; GE Healthcare) for 1 h. Blue coloration developed in the presence of 3,39,5,59-tetramethylbenzidine (TMB) (Thermo Scientific, Rockford, IL) peroxidase substrate solution. Reaction was stopped by adding 1N hydrochloric acid (Sigma), and absorption was read at 450-nm wavelength with Eon microplate photometer (BioTek, Winooski, VT). Purified HNE standard (stock: 1 mg/ml; Cell Sciences, Canton, MA) was used to determine HNE concentrations in unknown samples.

MPO-DNA and HNE-DNA ELISA assays: As described by Yoo *et al.* [82, 87], the concentration of HNE-associated DNA in PMN supernatants was measured using HNE capture antibody (1:2000, rabbit, Calbiochem, EMD Millipore, Billerica, MA, USA) while MPO-associated DNA was quantitated using MPO capture antibody (rabbit, 1:2000, EMD Millipore, Billerica, MA, USA). Capture antibodies were incubated overnight at +4°C. PMNs were treated with DNAseI (1μg/ml, Roche, Basel, Switzerland) for 15min at room temperature. DNAse digestion was stopped by adding 2.5mM EGTA (Sigma, St. Louis, WA, USA). Supernatants were collected, centrifuged and diluted 10–100-fold in PBS+2.5mM EGTA. For 'NET standard', PMNs were incubated with PMA for 5 hours. After 5 hours, limited digestion of NETs was done for 10 min with 1 μg/ml DNase and the DNAse activity is stopped with 2.5mM EGTA. 2-fold serial dilution was made to generate the "NET-standard". High-binding 96-well ELISA microplates (Greiner Bio-One) were blocked with 5% BSA/0.1% human serum albumin/PBS for 1–2 h followed by overnight

incubation and three washes with Tween20 in PBS. The dilutions of PMN supernatants were incubated overnight at +4C. After 16 hours of incubation, secondary anti-DNA-POD (horse radish peroxidase conjugated anti-DNA antibody, mouse, 1:500, Roche) was added for 30–60 min at room temperature [82, 87]. After three to four washes, TMB substrate (Thermo Scientific) was added. Absorbance was either measured at this point at 650 nm (kinetics) or after the addition of 1 M HCl stop solution at 450 nm (end point) with an Eon microplate spectrophotometer (BioTek). Background absorbance values of the medium and untreated PMNs were subtracted.

NET Immunofluorescence: 200,000 PMNs were seeded on sterile 12 mm round glass cover slips (VWR International, Radnor, PA, USA) placed in 24-well plates (Thermo Scientific, Rochester, NY, USA). 100 μg/ml or 250 μg/ml MSU crystals were added to PMNs PMN and incubated for 4 hours at 37°C. After incubation, cover slips were fixed with 4% paraformaldehyde (Affymetrix, Cleveland, OH) for 15 min. Cells were permeabilized and blocked with 5% BSA (VWR, Radnor, PA, USA), 5% Normal Donkey serum (Jackson ImmunoResearch Laboratories INC, West Grove, PA, USA), 0.1% Triton-X (Sigma, St. Louis, MO, USA) in PBS (Thermo-Scientific) for 30 min. PMNs were incubated with monoclonal rabbit anti-human neutrophil elastase antibody (1:250, Calbiochem) overnight at 4°C. After incubating with Alexa Fluor 594-labelled donkey anti-rabbit secondary antibody (1:500, Invitrogen, Eugene, OR, USA) for 1 hr, cells were stained with DAPI (2 min, RT, 1:20000 of a 10 mg/ml stock solution, Molecular Probes/Invitrogen, Grand Island, NY) and washed in PBS twice. Specimens were mounted using the ProLong Antifade Kit (Life Technlogoies, Grand Island, NY, USA) following the manufacturer's instructions and analyzed with Zeiss AxioCam HRM fluorescence microscope (Axioplan2 imaging software).

Intracellular calcium signaling: To measure intracellular calcium mobilization, PMNs were loaded with 2 μM fluo4 for 30 mins (dark) with probenecid water and pluronic acid in calcium free HBSS. The PMNs are then washed 2x with calcium free HBSS. The PMNs were then incubated with 10 μM MRS2578 or DMSO. The PMNs were then stimulated with 5 ng/ml Ionomycin, 10 μM UDP and HBSS without calcium. Flow cytometer (LSR II BD, San Jose, CA, USA) was used to measure the calcium flux experiment [222]. The baseline reading was recorded for a 1 min, stimulation was added to immediately the calcium flux kinetics was recorded. The final analysis was performed using flow Jo software (version 7.6.5, FlowJo LLC, Ashland, OR, USA).

Phagocytosis Assay: The PMNs were seeded at 2 million per dish with 1 mg/ml MSU crystals with or without 10 μM MRS2578 / 0.1% DMSO. The live videos were recorded for 1 hour and the phagocytosing cells were counted at 30 min and 60 min time points.

Measurement of ROS: 100,000 PMNs/ well were seeded with or without 10 μM MRS2578 or 0.1% DMSO. The PMNs were either unstimulated or treated with 250 μg/ml MSU crystals or 100 nM PMA. The luminescence was detected using 100 μg/ml lucigenin was measured for 60 min in a Varioskan Flash microplate luminometer. Integrated luminescence units (area under the curve) indicative of intracellular ROS / superoxide production during the entire measurement were calculated and expressed as relative luminescence units (RLU).

Intrinsic Migration: Optical flow was estimated for 6 pairs of videos. Videos consisted of 1024x1024 gray scale images with 60 frames per video. The Farneback method, implemented in

OpenCV (Version 2.4.13), was used to calculate dense optical flow between consecutive pairs of video frames [321.]. Flow vectors, containing horizontal and vertical displacement components, were computed at every pixel. The flow vectors were averaged to produce an aggregate delta x and delta y for each pair of video frames. This set of frame-wise delta x and delta y pairs was visualized using a two-dimensional contour plot.

2 million PMNs and 50 μg/ml MSU crystals were imaged for 1 hour with or w/o MRS2578. Image J Fiji was used with manual tracking and MJ track plugin. The PMNs were tracked every 2 sec through 151 frames, the videos were converted into grayscale. The average distance (μm) was measured for 9-13 PMNs per video for the final analysis.

Statistical analysis: Data was statistically analyzed using GraphPad Prism software v6.01 (GraphPad Software, La Jolla, CA, USA). Differences with a *p* values, *p <0.05, **p < 0.01, ***p < 0.001 were considered statistically significant. For multiple comparisons statistical analysis, one-way ANOVA followed by a Dunnett's MCT was used to compare each group with the control group. Mann Whitney U test was performed for non-parametric statistical analysis.

Results:

NETs and neutrophil markers are present in gout SF.

Although NETs and HNE have been previously detected in the gout synovial space [23, 34, 35], NETs and enzymatic activities of HNE and MPO have not been quantitated previously. To achieve this, we used ELISA assays established previously in our laboratory to detect NET-specific MPO-DNA and HNE-DNA complexes [87]. OA is a degenerative joint disease, which causes continual cartilage degradation [223]. SF from OA patients served as a suitable negative control for our

experiment, since OA joint inflammation is not driven by MSU crystals [221]. We analyzed 8 Gout and 4 OA samples obtained from consented patients. Our analysis indicated the presence of larger quantities of MPO, MPO associated with DNA, HNE and HNE associated with DNA in gout patient samples as compared to those taken from OA patients (Figure 3.1A, C, D, F). Further, we measured the presence of active HNE and MPO enzymes and found significantly higher amounts in gout than in OA samples (Figure 3.1B and 1E): MPO (629.9 $\pm$ 166.2 ng/ml, mean $\pm$ S.E.M., n=15), HNE (318.8$\pm$ 38 ng/ml, mean $\pm$ S.E.M., n=15) .The amount of MPO and HNE in SF supernatants were significantly higher in gout SF as compared to OA (Figure 3.1A & D). Our conclusion is that NETs and enzymatically active PMN-derived enzymes are highly elevated in gout SF compared OA SF.

MSU crystal phagocytosis is required for NET formation.

In order to understand the mechanism of MSU crystals-induced NET formation, the role of phagocytosis was evaluated. A low concentration (50 μg/ml) of MSU crystals were used to enable visualization of the images and record the steps involved in NETosis. As expected, PMNs tried to phagocytose MSU crystals under these conditions (Figure 3.2.A-B). Live imaging over 12 hours with Sytox Orange showed that MSU crystals trigger NET release in PMNs (Figure 3.2 C). We performed image analysis to calculate the proportion of NET-forming PMNs among those associated with crystals. Our analysis showed that MSU crystal-associated PMNs that formed NETs were 31.9+/-2.3% (mean+/-S.E.M., n=4) of the total and the non-crystal associated PMNs were 68.1+/-2.3% (mean+/-S.E.M., n=4) (Figure 3.2.D). Figure 3.2.E shows that 88.2+/-13.7% (mean+/-S.E.M., n=4) of PMNs were interacting with MSU crystals undergo NET formation revealing that association with MSU crystals is required for NET release. The uptake of MSU

crystals by PMNs depended on the cytoskeleton [2]. In order to determine that the cytoskeleton was a critical component of MSU crystal-triggered NETosis, we used cytochalasin B, an inhibition of actin polymerization to impede phagocytosis [50, 224]. Figure 3.2 F and G shows that in presence of cytochalasin B, MSU crystal-induced NET release and aggNETs were ablated. Thus, verified that the cytoskeleton is an important aspect of MSU crystal-induced NET formation.

MSU-stimulated NETs bind HNE.

HNE is a crucial NET marker shown previously to be present in NETs stimulated with either bacteria or PMA [59]. To address whether HNE is a component of MSU crystal-triggered NETosis, we performed immunofluorescence staining. HNE staining in resting PMNs showed a typical granular pattern that did not overlap with the nuclear staining (Figure 3.2.H, insets). As expected, upon PMA stimulation the majority of PMNs form NETs and HNE co-localized with the extracellular DNA staining (Figure 3.2.H, insets). We also observed that 250 μg/ml MSU crystal-induced NET release and HNE staining co-localized with the DNA staining in PMNs stimulated with the crystals for 4 hours (Figure 3.2.H). These data confirmed that PMNs stimulated with MSU crystals release NETs under our experimental conditions.

Purinergic P2Y receptors are involved in MSU crystal-triggered NET formation.

NETosis is a form of cell death caused by various stimuli to cope with infection [59, 145, 146]. MSU crystals are perceived as DAMPs by PMNs [205]. During PMN lysis in NET formation, several molecules including ectonucleotides such as ATP, ADP, adenosine, UTP, UDP are released [151, 152]. We hypothesized that extracellular nucleotides contribute to the signaling process of MSU crystal-initiated NET formation. Purinergic P2Y receptors represent a main class

of receptors by which PMNs respond to extracellular nucleotides [151, 155, 212]. Suramin and PPADS are a widely used general inhibitor of P2Y receptors [225-229]. Kulkuski *et al.* suggested that suramin inhibits the ecto-nucleotidase NTPDase1, which is responsible for the production of extracellular adenosine via hydrolysis of ATP and ADP to AMP which can then be further degraded to adenosine by other enzymes [230].

Our data in Figure 3.3 A showed that P2Y antagonist, Suramin, inhibited the release of MPO-DNA complexes in a dose-dependent manner suggesting that P2Y receptors were involved in MSU crystal-triggered NET formation. Suramin also impeded NE formation [231] and therefore, it contradicted the notion that suramin worked solely on inhibiting crystal-induced NETs. To verify that P2Y inhibition prevented MSU crystal-induced NET formation, we needed to test other nonspecific P2Y antagonists. Figure 3.3 C. shows that an HNE inhibitor can degrade the 250 μg/ml of HNE in a cell free NE activity assay. NE activity assay was also performed with suramin, which degraded HNE in a cell-free system as is shown by Figure 3.3. B [231]. MPO–DNA ELISA showed that suramin reduced production of the MPO-DNA bound NETs (Figure 3.3. A). NE played an important role in NETosis and was crucial for chromatin decondensation [18, 33, 60]. To determine if NE was required for NET formation, we used the NE inhibitor shown in Figure 3.3 D to examine its effect on MSU crystal-induced NETs. Figure 3.3 D shows HNE inhibitor did not block MSU crystal-induced NET formation. Thus, our results showed that NETosis was not diminished in the presence of the NE inhibitor. Therefore, we verified that suramin exclusively inhibited P2Y receptor, which leads to NET inhibition.

To further confirm the role of P2Y receptors, another nonspecific P2Y antagonist, PPADS, was examined in MSU crystal-induced NET formation [232-234]. Figure 3.3.F. shows that PPADS inhibited the MSU crystal-induced NET formation. Both Suramin and PPADS blocked crystal-

induced NET formation. Our next question was to find the specific P2Y receptor involved in the process of NET formation. So, we investigated the role of the receptor in MSU crystal-induced NET formation [152, 167, 235, 236]. P2Y2 receptors are abundant on the neutrophils and regulate their migration [236]. Upon examination with ARC118925xx, a P2Y2 antagonist, we found that MSU crystal-induced NETosis was not inhibited (Figure 3.3.G).

P2Y6R inhibitor, MRS2578, inhibits MSU crystal-induced NET formation.

Several members of the P2YR family are expressed in human PMNs [155, 237]. P2Y6R has been shown to be involved in MSU crystal-initiated cytokine release in PMNs [155]. P2Y6R biology can be studied using a highly specific inhibitor, MRS2578 [169]. MRS2578 inhibits P2Y6R in the lower micromol/l concentration range [155, 156, 169, 186, 213, 238, 239]. Therefore, we assessed whether MRS2578 inhibited NET formation. As the data presented in Figure 3.4 show, 5 or 10 μM MRS2578 blocked MSU crystal-induced release of DNA, MPO, HNE and HNE-DNA complexes from human PMNs. Trypan blue staining of PMNs confirmed that MRS2578 was not toxic to PMNs (data not shown). This observation indicated the novel involvement of the purinergic P2Y6 receptor in MSU crystal-induced NET release.

Extracellular nucleotides alone fail to initiate NET formation.

The main ligand of P2Y6R is uridine-diphosphate (UDP), but it also binds uridine-triphosphate (UTP) with lower affinity [150, 237]. P2Y6R does not respond to adenine-based nucleotides [150, 237]. UDP and UTP are released from damaged cells and are reported to stimulate PMNs via P2Y6R [240]. ATP, ADP and adenosine increase migration and IL-8 release in PMNs [150, 151, 186]. Therefore, we asked whether NET formation could be initiated in human PMNs by

stimulating them with milli or micromolar concentrations of adenine- and uridine-based nucleotides. As the results in Figure 3.5 show, ATP, ADP, adenosine, UTP or UDP did not induce NET release in human PMNs when stimulated with concentrations up to the lower millimol/l concentration range. On the contrary, ATP had a slight inhibitory effect at higher concentrations (Figure 3.5A). This data indicated that P2Y6R did not directly trigger NET formation in PMNs but participated in the process rather indirectly.

P2Y6R inhibition blocks aggNET formation.

As described by Schauer *et al.* high density PMNs form aggNETs which help in resolving joint inflammation [23, 25]. In the synovium, these structures are precursors of gouty tophi as seen in gout patients [23, 25]. To test the effect of the MRS2578 inhibitor on aggNET formation, we incubated high density PMNs and MSU crystals *in vitro* with or without 10 μM MRS2578, or with 0.1% DMSO (vehicle control). AggNETs formed consolidated MSU crystal-PMN structures after overnight incubation (Figure 3.6.C). To better understand the complex mechanism of MSU crystal-induced aggNET formation, we established a high-throughput method capable of imaging NET formation over long periods of time in several samples in parallel. This high throughput live-imaging using 96-well microplates and automated confocal microscopy confirmed that human PMNs release NETs in response to MSU crystals and PMA, as well (Figure 3.6.A and B). Similarly to our previous data, MRS2578 inhibited the NET-forming ability of MSU crystals under these conditions as well (Figure 3.6 A &.B). Additionally, NET formation triggered by PMA was also delayed by MRS2578 (Figure 3.6.A & B). The recorded series of images revealed a migratory component of aggNET formation specific for MSU crystal stimulation (Figure 3.6.C). With time, PMNs migrated towards and concentrated in a few areas when exposed to MSU crystals indicating

an active migratory component of aggNET formation (Figure 3.6.C). These small early aggregates appearing in the first few hours merged later into large, macroscopic aggNETs (Figure 3.6.C). PMNs without stimulation or in the presence of PMA failed to show this phenotype (Figure 3.6). MRS2578 had a complete inhibitory effect on MSU crystal-induced migration of PMNs (Figure 3.6.A, images at 5 hrs) indicating that it prevented MSU crystal-induced NET formation by blocking PMN chemotaxis. For the first time, we are able to image MSU crystals and PMNs real time.

MRS2578 inhibits MSU crystal-induced IL-8 release, superoxide production, intracellular calcium and phagocytosis.

Since UDP also stimulates IL-8 release in PMNs [150-152, 214], we investigated the effect of MRS2578 in MSU crystal-induced release of IL-8, as our primary candidate mediating PMN migration required for aggNET formation. IL-8 signaling causes adhesion, degranulation, respiratory burst, and lipid mediator synthesis in PMNs [241]. TNF-α primed PMNs stimulated with IL-8 are able to produce NETs [242]. In Figure 3.7 A., we have shown that MSU crystal-induced IL-8 secretion is inhibited by MRS2578, which is in agreement with similar results of other groups using different stimuli [155, 156, 186].

Figure 3.7. shows that superoxide production, intracellular calcium and phagocytosis were inhibited when MRS2578 was present. Figure 3.7 C represents that P2Y6R-mediated superoxide ($O_2^{\cdot -}$) production was inhibited in the presence of MRS2578. In PMNs, NADPH oxidase is important for respiratory burst, phagocytosis, migration and NET formation [33, 50, 85, 109, 110, 243, 244]. We think that MRS2578 works in conjunction of inhibiting P2Y6 and superoxide production.

G-protein-coupled receptors like P2Y6R activate PLC and UDP causes increase in intracellular calcium concentration by release from intracellular stores [245]. In neutrophils, Calcium is required for phagolysosome fusion, chemotaxis, release of proteins from granules, and changes in cytoskeleton, just to name a few functions [156, 160, 162, 184, 246-248]. Figure 3.7.D. shows that phagocytosis with MRS2578 is impaired in PMNs stimulated with MSU crystals. Figure 3.7.D. shows that intracellular calcium signaling was reduced when PMNs treated with MRS2578 were stimulated with 10 μM UDP and 5 μg/ml ionomycin. UDP was released from dead cells and was the natural ligand for P2Y6 [249, 250]. UDP bound to P2Y6R and increased IL-8 release [182, 250]. Time-lapse images also showed the inhibition of crystal-induced NETosis, phagocytosis and intrinsic migration. Therefore, we conclude that P2Y6R in MSU crystal-stimulated PMN is needed for neutrophil activation.

Blocking the store-operated calcium entry pathway partially inhibits NET formation

IL-8 binds to two main receptors, CXCR1 and CXCR2, and stimulates a GPCR-PLCγ signaling pathway leading to calcium mobilization [251]. Calcium signaling is highly conserved in all immune cells [252]. In PMNs, calcium is an important mediator of chemotaxis, ROS production and phospholipase C-γ (PLCγ) activation [110, 246]. The main route of calcium mobilization during PMN activation is the Store-Operated Calcium Entry (SOCE) mechanism [110, 252]. The role of SOCE in NETosis had not been explored yet. Here we showed that a specific SOCE inhibitor, SK&F96365, inhibited MSU crystal-induced NET release (Figure 3.8A). Release of MPO and HNE initiated by MSU crystals were also significantly reduced by SK&F96365 (Figure 3.8B, C). PMA-induced NET formation was not affected by SK&F96365 (Figure 3.8.A-C). Interestingly, SK&F96365 also blocked MSU crystal-triggered IL-8 release (Figure 3.8.D). These

data suggest that SOCE specifically promotes MSU crystal-induced NET formation in human PMNs.

Intrinsic migration is inhibited by MRS2578 – In a chemotactic gradient, PMNs orient themselves and gravitate toward the gradient [151]. The signaling pathway(s) responsible requires extensive involvement of the cytoskeleton and its stabilization [62]. We have accumulated evidence showing that MRS2578 inhibited phagocytosis and intracellular calcium in Figure 3.7. Phagocytosis causes actin polymerization and expansion of cytoskeleton to form the phagocytic cup to engulf the foreign particle [7, 62, 110, 253]. This process needs energy and calcium mobilization [7, 62, 110, 253]. Also we know from Figure 3.2 F and G, cytoskeleton inhibition prevented NET formation. Thus, we were compelled to seek the role of MRS2578 in PMN migration as the process hugely demands the involvement of the cytoskeleton. Neutrophil migration was lost in the presence of MRS2578 as shown by Figure 3.9. Our analysis showed that the migration was more robust and intact in the absence of MRS2578 when tracked for an hour (Figure 3.9). Imaging PMNs with MRS2578 showed that the PMNs do not move as shown in Figure 3.9. MRS2578 hinders the inherit capability of PMNs to migrate and to perform chemotaxis. In defective PMNs, their intrinsic ability to migrate, produce ROS, chemotaxis and phagocytosis are hindered [254]. Over the last decade, a role of P2Y6 receptor in proinflammatory cytokine and chemokine release pathways have started to make an appearance [156, 157, 168, 184, 186, 216, 248, 255]. UDP induced migration in intestinal epithelium and phagocytosis in microglial cells was inhibited by MRS2578 [157, 168, 248]. THP1 cells and monocytes respond to chemokine CCL2 via CCR2 with co-activation of P2Y6R [216]. Thus, our data on MRS2578 and migration in PMNs corresponds to the previous data in other cell types.

Discussion

The present study demonstrates that elevated levels of NETs and NET-associated, active MPO and HNE are present in SF supernatants of gout patients. Although NETs have already been detected in the SF of gout patients [23, 34], our NET-specific ELISA assays [82] quantitate NETs for the first time in clinical bio-specimen of gout patients. Our data detects enzymatically active MPO and HNE, two primary granule markers released by PMNs. This indicates that both enzymes remain active in gout SF potentially contributing to joint damage. HNE could contribute to disease pathogenesis via several mechanisms. Once released, HNE degrades almost each component of the extracellular matrix [81, 256] [76, 78, 257]. HNE is considered the main damaging factor in the lungs of patients with cystic fibrosis, COPD and emphysema [80, 258, 259]. Free-floating HNE could potentially cause similar serious effects in the SF of gout patients and could be directly damaging synoviocytes, neutrophils and macrophages. On the other hand, HNE also degrades proinflammatory cytokines thereby, limiting the breadth of gout flares [23]. Addressing a potential, clinically very relevant correlation of gout SF or blood levels of NETs and granule enzyme activities with gout disease severity is hindered by the difficulty of adequate clinical scoring of joint inflammation in gout [138, 260, 261].

Our quantitative analysis used live imaging of crystal-PMN interactions that revealed about a third of crystal-associated PMNs released NETs under our experimental conditions but almost all PMNs releasing NETs were associated with MSU crystals. This suggests that physical interaction is required to trigger NET formation. This finding conflicts with a previous study stating that crystal phagocytosis is not a requirement for NET generation [36]. Our data on cytochalasin-B shows that an active cytoskeleton is required for NET release and aggNET formation. We also report the requirement of an intact cytoskeleton for NET formation stimulated by pseudogout-associated

CPPD crystals [50] and *P. aeruginosa* [87]. This indicates that an intact phagocytic apparatus is required to trigger NETs induced by particulate stimuli.

Mechanistic studies investigating how MSU crystals-induce NET formation has not been explored. We speculate that one possible mechanism could be that crystals form pores in the PMN plasma membrane leading to ion fluxes and initiation of NET release – similar to the activation of the NLRP3 inflammasome [262]. Recently, it has been shown that soluble uric acid triggers NET formation [263]. We do not think this mechanism plays a significant role in our system since transferring crystal-free supernatants of MSU crystal suspension containing free MSU crystal did not induce NET formation in human PMNs previously not exposed to crystals (data not shown). Alternative mechanisms suggested the involvement of specific surface receptors in MSU crystal-induced activation of PMNs [1, 2]. We identified P2Y6R in the process, but future studies are needed to determine if MRS2578 has indirect or unwanted effects that inhibit NET formation. To address this question we need to understand the machinery involved in the binding of MSU crystal to P2Y6R. Here, we showed that P2Y6 receptor may be involved in crystal phagocytosis in PMNs, which also agrees with previous finding showing that it mediates phagocytosis in microglia cells stimulated with UDP [168, 220].

Like several cell death pathways, NET formation is also likely to be accompanied by release of ample amount of ectonucleotides such as ATP, ADP, UDP, UTP and adenosine [264]. These nucleotides bind to various purinergic receptors and regulate immune signaling [237]. Purinergic signaling has been implicated as a fundamental element in several PMN functions including migration, superoxide production and various signaling pathways [152]. One of their main functions is to direct PMN chemotaxis to sites of cell damage via P2Y purinergic receptors [237]. Our data showing that suramin, PPADS and MRS2578 block the action of MSU crystals are the

first to indicate the involvement of P2Y receptors in NET formation. Whereas, ARC118925XX did not have any influence on MSU crystal-induced NETS. The involvement of P2YR signaling in the mechanism of NET formation raises several questions. Interestingly, nucleotides alone do not trigger NET formation. Suramin and PPADS are documented as general P2YR antagonists [236, 265]. MRS2578 is highly specific for P2Y6R and was confirmed in several studies using genetic (knock down or overexpression) approaches [65, 155, 237, 266]. MRS2578 does not affect P2Y2R since it impaired chemotaxis in P2Y2R KO murine PMNs in our system (data not shown) [266]. PMNs express several P2YRs including P2Y6 [237, 266]. The role of P2Y6 in PMN biology is to be understood, although it is required for IL-8 release induced by UDP [237] and by MSU crystals (our data). P2Y6R could potentially mediate aggNET formation by regulating IL-8-mediated PMN migration [237]. This is also likely since the ectonucleotidase NTPDase1 (CD39) has been shown to control IL-8 release in human PMNs [266]. P2Y6R could also play a role since IL-8 release in epithelial cells induced by neutrophil defensins is blocked by MRS2578 [154]. MRS2578 could also switch off NETosis in human PMNs, only to shorten their lifespan and accelerate apoptosis [238] .

P2Y6R is a G protein coupled receptor and signals via intracellular calcium [267]. P2Y6R activates PLCγ, produces inositol 1,4,5-triphosphate (IP_3), and activates IP3 receptors in the ER [228], resulting in an abrupt spike in cytosolic calcium levels. Depletion of ER calcium stores leads to the activation of the SOCE mechanism [268]. STIM1 works as a sensor of ER luminal calcium and redistributes to the ER luminal position to Orai1 spanning the plasma membrane [246, 269]. $STIM1^{-/-}$, $STIM2^{-/-}$, and $Orai^{-/-}$microglial cells do not perform P2Y6R mediated phagocytosis [270]. SOCE is the main mechanism of calcium signaling in PMNs during activation [268]. SOCE is mediated by STIM1 and Orai1 proteins [228]. Based on our data, we propose that P2Y6R

activates SOCE signaling that mediates IL-8-dependent migration of PMNs [216, 247, 271]. In addition, cytosolic calcium mediated by SOCE could also promote NET formation by activating protein arginine deiminase-4 (PAD4), a calcium-dependent enzyme essential for NET release [104]. PAD4 citrullinates histone H3 and H4 and promotes chromatin decompensation [251].

NETs represent a double-edged weapon since they can either drive or resolve inflammation [23]. During the acute phase of gout, PMNs encounter MSU crystals to form NETs and release proinflammatory cytokines [23, 262]. When MSU crystal-triggered NETs reach a certain threshold and start forming aggNETs, they cleave proinflammatory cytokines and create a synovial environment more conducive to healing [23, 25]. Gouty tophi are formed at this stage. In fact, aggNETs have been proposed to be the core structural unit of tophi [23]. This phenomenon is very unique to gout and so far, has not been seen in other PMN-mediated diseases.

We used high throughput confocal imaging to record real time NET formation. This novel methodology enables us to not only measure NET formation but also PMN migration. During inflammation, PMNs transmigrate from microcirculation and cross the epithelial barrier to reach the inflicted site [253] . However, dysfunction in PMNs cause excessive migration which can aggravate inflammation as seen in gout, IBD and other neutrophil driven diseases [1, 2, 35, 253]. PMNs migration is inhibited by MRS2578 that disrupts the PMN migration and surveillance of its surroundings.

The effect of MRS2578 on PMNs has some off target effects as it not only inhibits NET formation but also restricts cytoskeleton and ROS production. The NADPH oxidase apparatus is crucial for phagocytosis, degranulation, oxidative burst, intracellular ROS, NET production, and IL-8 release [33, 272] Along with that we observed that during PMA-induced NETosis, we saw inhibition of IL-8 release, intracellular calcium and ROS by PMA-stimulated PMNs. Moreover, it has been

shown that GPCR agonists like angiotensin II can activate NADPH oxidase and determine functional outcomes [273]. P2Y6 receptor has been involved in phagocytosis and intracellular calcium [248, 270, 274]. We think MRS2578 is blocking NADPH oxidase and P2Y6R together, which consequently effects mobilization of intracellular calcium, phagocytosis, migration, and NETosis in PMNs. Our data suggest that the incapacitation of PMNs caused by MRS2578 can be utilized for therapeutic purposes in diseases in which excess neutrophil function is the pathology.

AggNETs provides us the unique opportunity to understand MSU crystal-PMN and PMN-PMN interactions. NETs formed with MSU crystals prepare the synovium for resolution by forming aggNETs as the number of PMNs and MSU crystals increase. However, we are perplexed by the conglomerate of 'MSU-PMN-NET'. How they communicate to gather and form aggNETs is still unclear. Our hypothesis 'active migration of PMNs is essential to form aggNETs' suggests a novel concept of "networking amongst PMNs".

In conclusion, our work proposes that P2Y6R-mediated purinergic signaling is a crucial component of MSU crystal-induced aggNET formation and gout pathogenesis. It also suggests that targeting P2Y6R offers a breakthrough in preventing acute inflammation in gout.

Acknowledgements: We thank the personnel at the UGA University Health Center for blood collection, and the CVM Imaging Core facility for assistance with confocal microscopy and flow cytometry. We are grateful to Donald L. Evans (UGA) for his scientific input on purinergic receptors.

Disclosure: The authors have no financial conflicts of interest.

Concluding remarks:

Here we describe the novel role of P2Y6 receptor in MSU crystal-induced NET formation and production of aggNETs. To demonstrate this, we used MRS2578, a P2Y6 antagonist, to show the inhibition of NET release as detected by the methodologies described in the previous chapter, Yoo *et al.* and Sil *et al.* [82, 86]. We also validated here in that the methodologies (Figure 5.1) can be used to detect NETs in human clinical samples [82, 86]. The main crux of this paper is the mechanism required for MSU crystal-induced NETs is via P2Y6-SOCE-IL-8 axis and is NADPH oxidase-dependent, as shown in Figure 5.2 (Sil & Rada., J.Immunol., unpublished). We utilized high-throughput confocal microscopy, ELISA, NET ELISA, and ecDNA assay to determine the signaling cascades.

NET pathway is a complex series of events which triggers the responses in PMNs [59, 68, 88, 94, 135, 146]. Our hypothesis is that P2Y6R is involved in the formation of MSU crystal-induced NETs. We have shown with the use of MRS2578 that P2Y6R is a vital component of the NETosis pathway. We have also been able to reveal the downstream partners of this mechanism. Intracellular calcium, SOCE, NADPH oxidase and IL-8 signaling pathway is crucial to the outcome (Figure 5.2) (Sil & Rada, J. Immunol., unpublished). This knowledge can be innovative and groundbreaking for gout treatment.

We have also demonstrated how neutrophils interact with MSU crystals (Sil & Rada, J. Immunol., under revision). So far, we have revealed a portion of the mechanism involved in NETosis via P2Y6R-SOCE partnership (Figure 5.2). However, in the synovium there are other cell types present, which interact with the neutrophils and macrophages. In the next chapter, we present the interaction between macrophages and neutrophils in aiding NET formation.

Resident macrophages and neutrophils are the eminent cell types found in a gout-afflicted joint. It has been shown that macrophages when crossing path with the MSU crystals, produce profuse amounts of IL-1β via the inflammasome pathway [5, 49, 115, 171, 172, 178, 243, 275, 276]. From previous studies, we have evidence showing that MSU crystals, neutrophils, macrophages, NETs and aggNETs are responsible for causing gout [5, 6, 12, 16, 23, 25, 29, 31, 34, 35, 40, 45, 47, 70, 86, 115, 120, 197, 202, 205-209, 275, 277, 278]. However, macrophage-derived IL-1β is the main perpetrator of the gout flare, accompanied with pain and inflammation (Figure 5.3.) [34, 35, 39, 116, 119-121, 279, 280]. The next chapter elucidates the interaction of macrophages with MSU crystal-activated PMNs (Sil & Rada., Infl. Research., under revision).

Figure legends

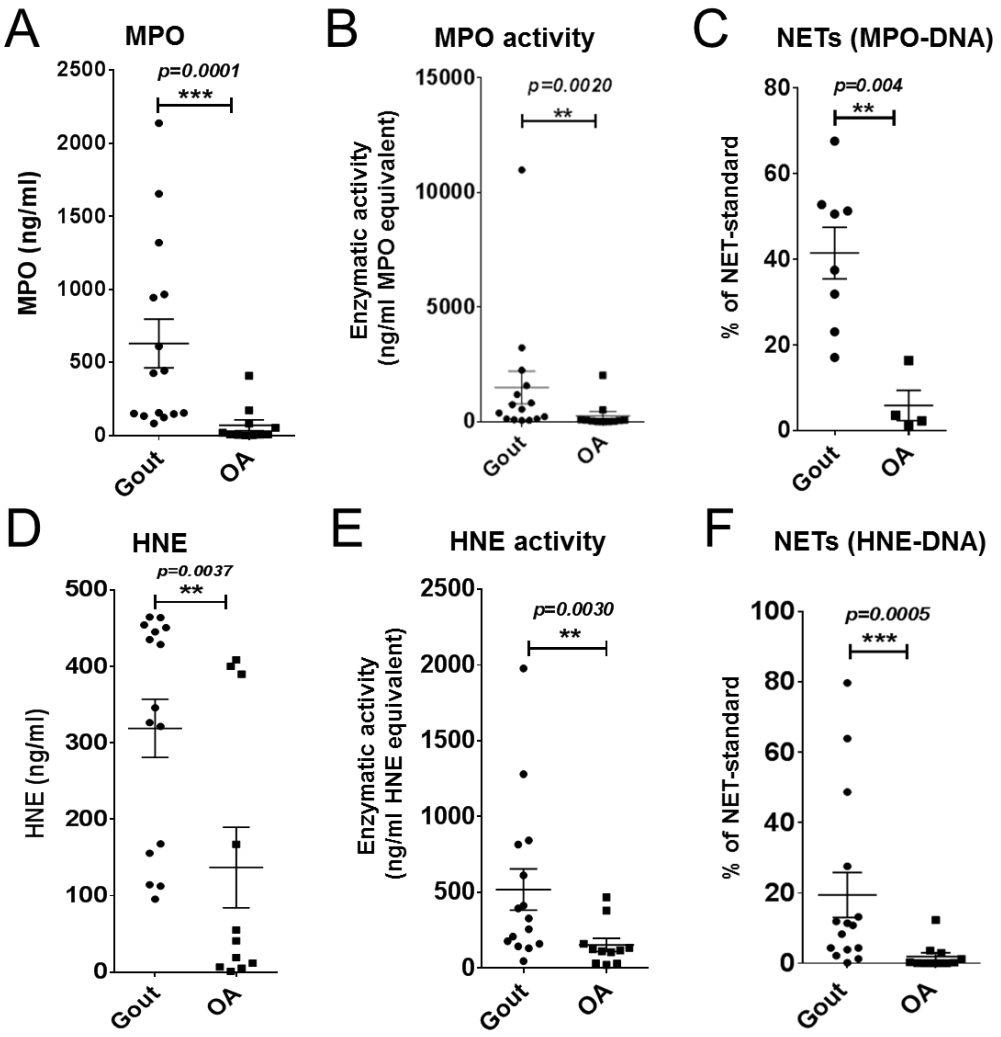

Figure 3.1. Gout synovial fluids have elevated levels of NETs and enzymatically active MPO and HNE. MPO (A) and HNE (D) protein levels, their enzymatic activities (B, E) and NETs (C, F) were quantitated in SF supernatants of gout and OA patients. Protein levels were measured by using commercial ELISA kits, enzymatic activities were assessed by fluorescent microplate assays and MPO-DNA and HNE-DNA ELISA were used to assess NET levels. (* $p<0.05$, ** $p< 0.01$,***$p<0.0001$, MSU mean+/-S.E.M., Mann-Whitney U test). MSU, monosodium urate, OA, Osteoarthritis; MPO myeloperoxidase, HNE, human neutrophil elastase, ns, not significant.

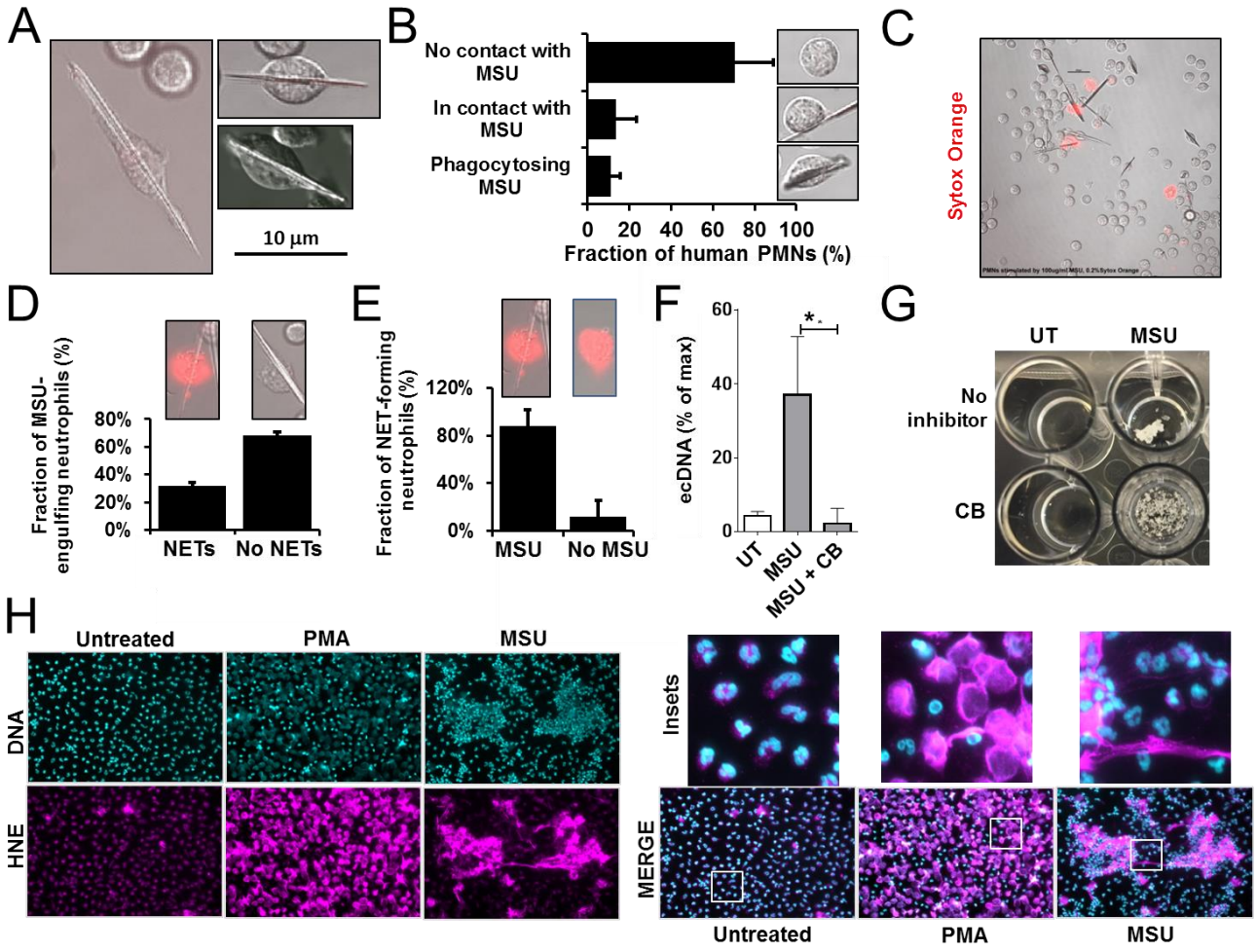

Figure 3.2. PMN cytoskeleton is requisite for MSU crystal phagocytosis.

A) Human PMNs (250,000 cells/well) suspended in assay medium were incubated with 50 µg/ml MSU crystals for three hours and DIC transmitted images of crystal-phagocytosing cells were obtained by confocal microscopy (images of one representative experiment, n=5). Scale bar, 10 µm. **B)** Quantification of PMN-crystal associations. Human PMNs incubated with MSU crystals (50 µg/ml, 3hrs) were imaged with confocal microscopy. At least 50 PMNs /donor were categorized according to their association with MSU crystals (no contact; in contact with MSU crystal; phagocytosing MSU crystal). Percent distribution of the three groups is presented as mean+/-S.E.M. of four independent PMN donors. Original magnification X1, 500. **C)** Human

PMNs were incubated with 50 μg/ml MSU crystals for three hours, and stained with the fluorescent DNA-binding dye, Sytox Orange. Images were recorded by fluorescence microscopy. One representative experiment of three similar ones. Original magnification X400. **D)** Proportions of NET-forming and resting cells (No NETs) among MSU crystal-phagocytosing PMNs were calculated. Mean+/-S.E.M., n=4. Original magnification X 1,500. **E)** Proportions of crystal-associated versus crystal-free cells amongst NET-forming PMNs were calculated. Mean+/-S.E.M., n=4. MSU, monosodium urate. Original magnification X1, 500. **F)** Inhibition of MSU crystal phagocytosis by 10 μM cytochalasin B blocks NET release (250 μg/ml MSU). NET formation was detected by Sytox Orange fluorescence. (*, $p<0.05$, MSU, n=3, mean+/-SEM, Dunnett's MCT) **G).** Inhibition of AggNET formation by 1 mg/ml MSU crystal and 2 million PMNs per well in presence of 10 μM cytochalasin B (representative of 3 independent experiment) **H)** Immunofluorescent detection of MSU crystal-stimulated human PMNs reveals co-localization of HNE with DNA in NETs. Cells were left untreated or were activated by 250 μg/ml MSU crystals or 100 nM PMA for three hours to generate NETs. PMNs were stained with primary anti-HNE antibody followed by treatment with secondary goat anti-rabbit Alexa 594 antibody. DNA was detected by DAPI. DAPI staining has been changed to light blue whereas HNE staining is shown as cyan. Original magnification X180. White boxes indicate insets shown magnified at the bottom of the Figure. Original inset magnification X 1,000. One representative result of four similar experiments received on four independent donors. MSU, monosodium urate. UT, untreated; PMA, phorbol myristate acetate.

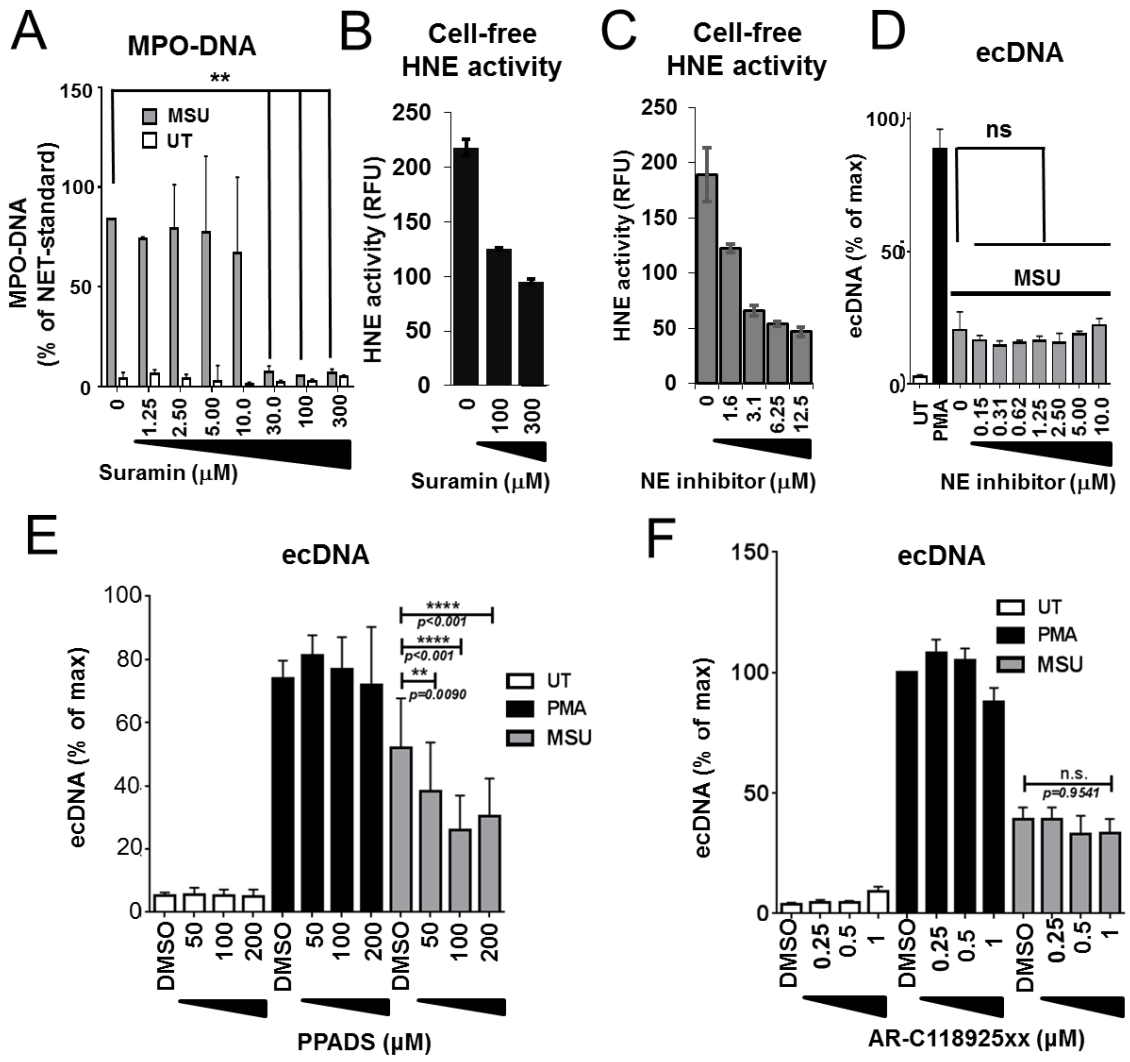

Figure 3.3. MSU crystal-initiated NET release is reduced by nonspecific P2Y antagonist. A) Human PMNs were stimulated with 250 μg/ml MSU crystals and NET formation was measured by Sytox Orange in the presence of increasing doses of the P2YR inhibitor, suramin. ** p< 0.01, MSU, n= 3, mean+/-SEM, Dunnett's MCT). B) HNE activity assay shows that suramin (300 μM and 100 μM) inhibits 250 ng/ml concentration of HNE C). shows that suramin inhibits MSU crystal-triggered NETosis. 1.6 μM of HNE inhibitor is sufficient to inhibit HNE (250 ng/ml). At 100 μM, the HNE inhibitor completely inhibits HNE D) Extracellular DNA inhibition by HNE

inhibitor and MSU crystals (n=3, mean+/-SEM, Dunnett's MCT). E) Human PMNs stimulated with 250 μg/ml MSU crystals and ecDNA formation was measured by Sytox Orange in the presence of increasing doses (0-200 μM) of the PPADS, P2Y antagonist, (****<p 0.0001, **p<0.01,n.s.= non-significant, MSU, n= 4, mean+/-SEM, Dunnett's MCT). **F).** Human PMNs stimulated with 250 μg/ml MSU crystals and ecDNA formation was measured by Sytox Orange in the presence of increasing doses (0-1 μM) of the P2Y2R inhibitor. ARC118925xx, P2Y2 antagonist (n.s. = non-significant, MSU, n= 3, mean+/-SEM, Dunnett's MCT). 0.1 % DMSO was the solvent for inhibitors and was used as the positive control.

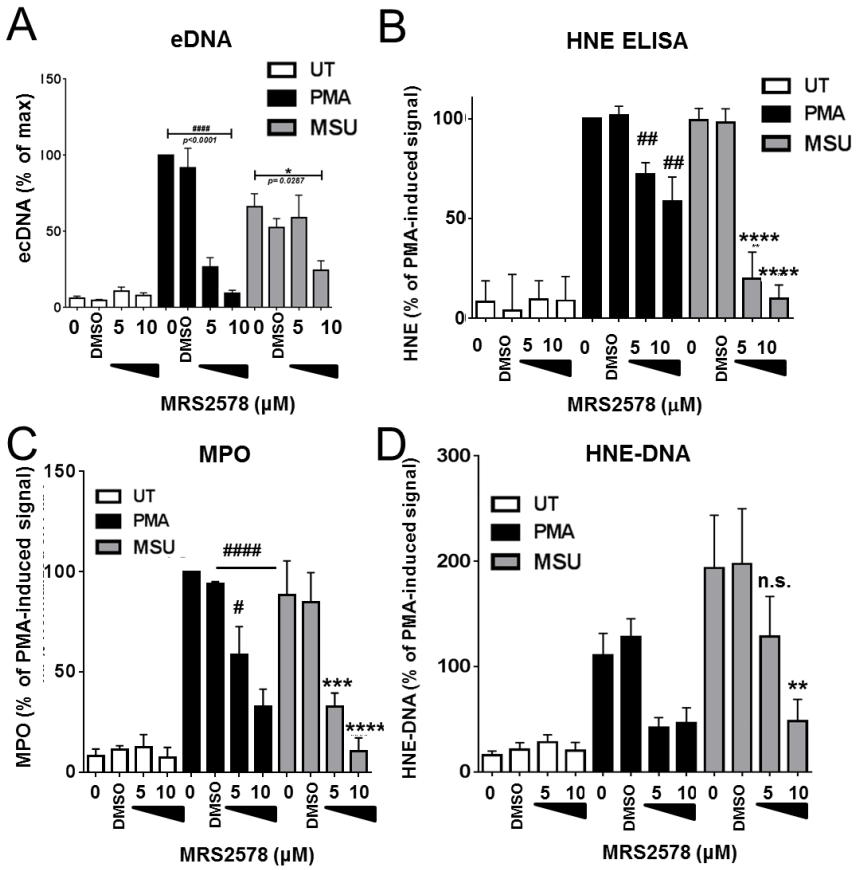

Figure 3.4. The P2Y6 receptor antagonist MRS2578 inhibits NET release induced by MSU crystals and PMA. Human PMNs were treated with 5 or 10 µM MRS2578 for 1 hour prior to stimulation with 250 µg/ml MSU crystals or 100 nM PMA to trigger NET release. Endpoint measurements (A) of ecDNA release (4 hrs, n=3, mean+/-SEM), (B) HNE release (ELISA, 4 hrs, n=3, mean+/-SEM), (C) MPO release (ELISA, 4 hrs, n=5, mean+/-SEM) and (D) NET release (HNE-DNA ELISA, 4 hrs, n=5, mean+/-SEM) were measured. Data are shown either as mean+/-S.E.M. (A-D). Non-parametric statistical analysis (Dunnett's Multi-comparison Test, MCT) was used to establish significance (A-D): ns, not significant; * $p<0.05$; ***, $p<0.001$, MSU (DMSO) ##$p<0.01$, #### $p<0.0001$, PMA (DMSO). 0.1 % DMSO was the solvent for inhibitors and was used as the positive control.

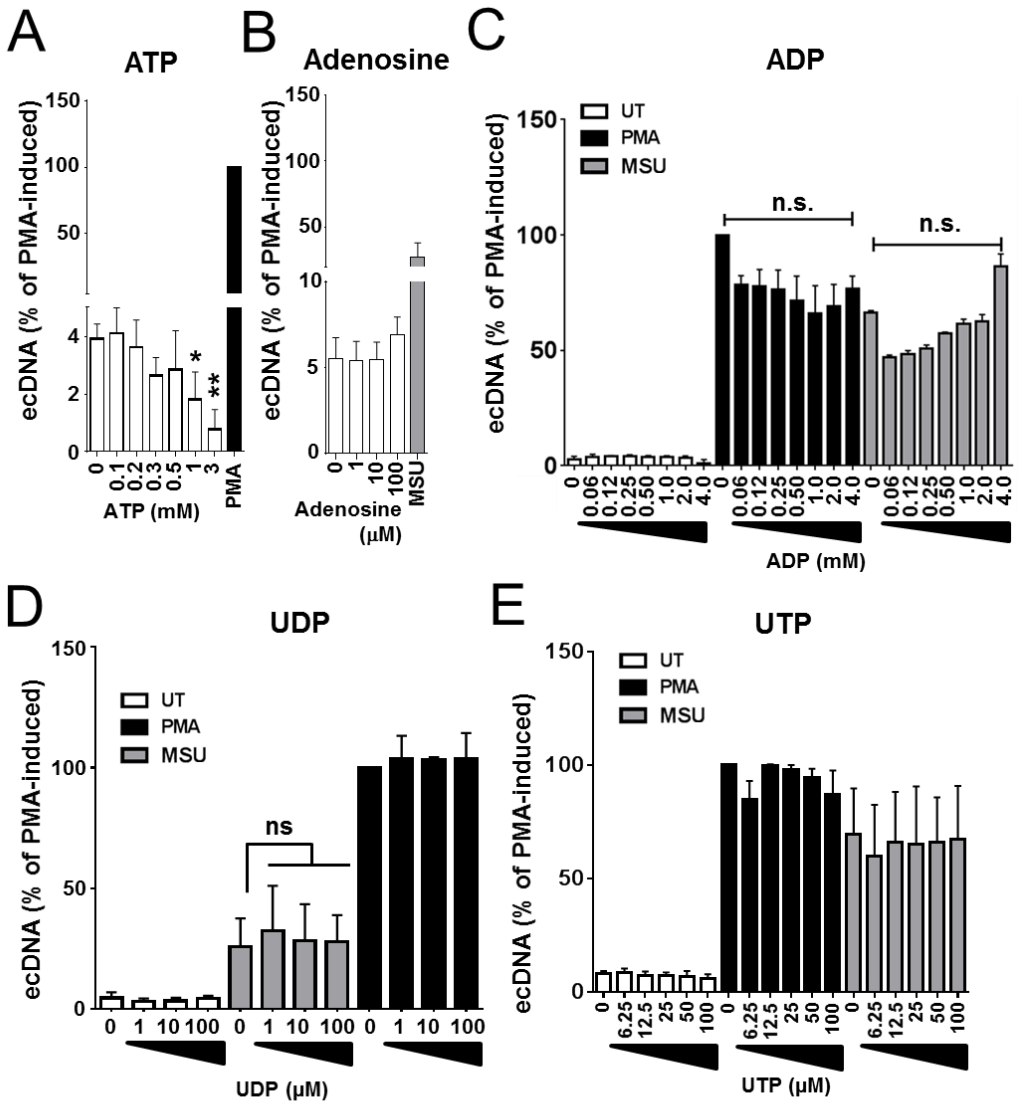

Figure 3.5. Ectonucleotides do not trigger NET release. Human PMNs were left unstimulated or stimulated with 100 nM PMA or 250 mg/ml MSU crystal in the presence of different doses of ATP (n=4) **(A)**, adenosine **(B)** (n=3), ADP (n=4) **(C)**, UDP (n=3) **(D)** and UTP (n=3) **(E)**. ecDNA release was measured by Sytox Orange-based fluorescence assay and normalized to the signal obtained by PMA without exo-nucleotides. Statistical significance was established by Dunnett's Multi-comparison Test (MCT), Mean+/-S.E.M. n.s., not significant; *, $p<0.05$; ***, $p<0.001$.

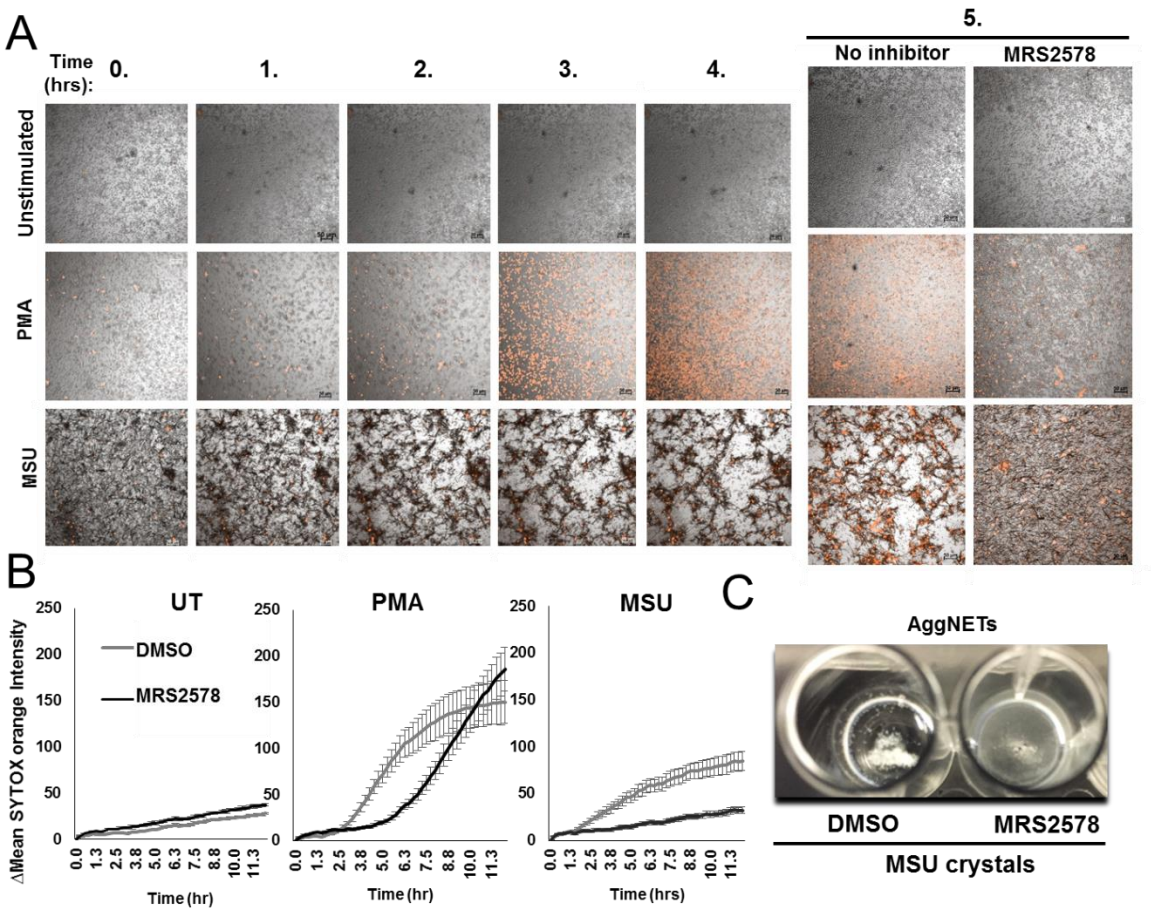

Figure 3.6. MRS2578 blocks MSU crystal-induced aggregated NET formation by blocking PMN migration. A) 250,000 PMNs were incubated in wells of a 96-well microplate with MRS2578 (10 μM) 1 hour prior to stimulation with 250 μg/ml MSU crystals or 100 nM PMA for 5 hours in presence of the extracellular DNA-binding dye, Sytox Orange. Interactions of PMNs and MSU crystals were followed using confocal microscopy every 15 minutes. Representative kinetics are shown (n=3). **B)** Representative images of the same experiments are shown taken at every hour (n=3, 100X, images at 5hrs: 120x). **C).** 1,000,000 PMNs were stimulated with1mg/ml MSU in 24-well plates in presence or absence of 10 μM MRS2578 or 0.1% DMSO (vehicle control) and formed aggregated NETs were recorded after overnight incubation. (One representative image, overnight incubation, n=3).

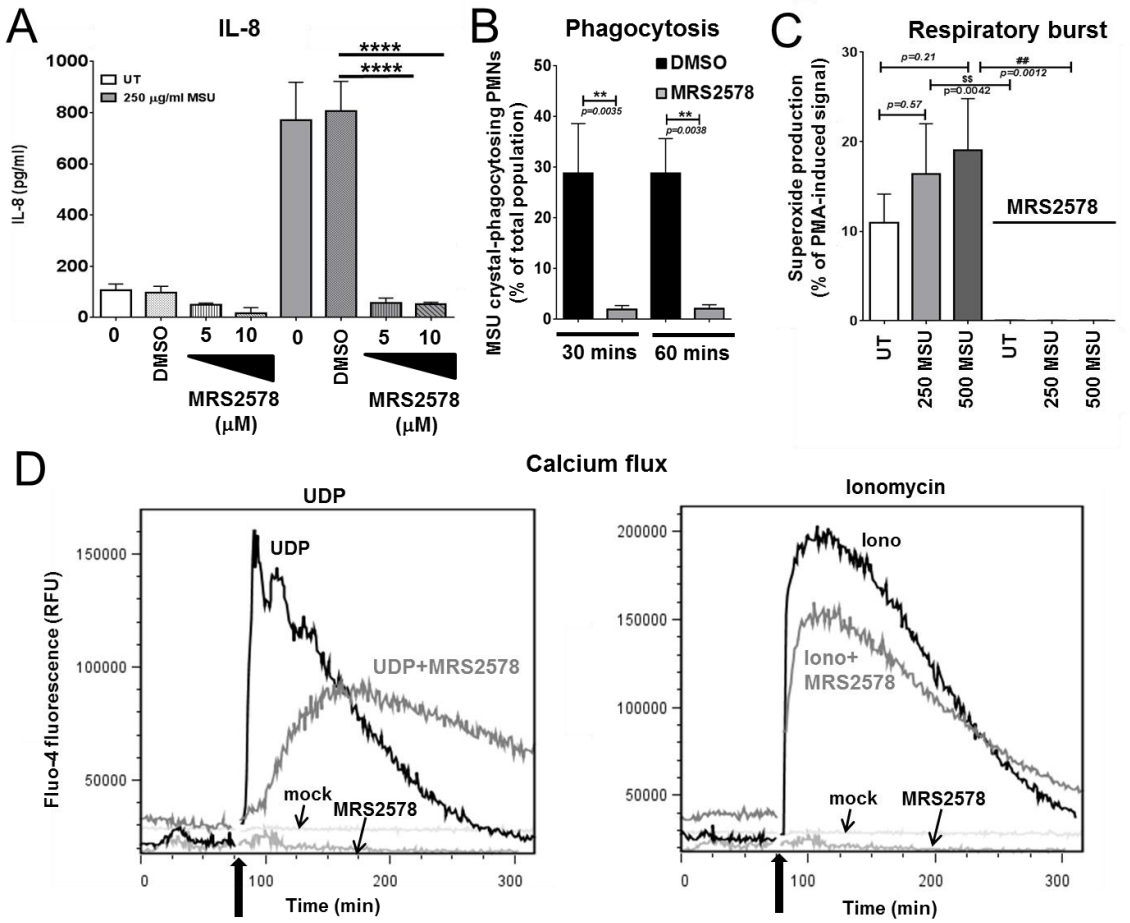

Figure 3.7. MRS2578 inhibits MSU crystal-stimulated IL-8 release, phagocytosis, superoxide release and intracellular calcium release in human PMNs. A) PMNs were treated with the indicated concentrations of MRS2578 for 1 hour prior to stimulation with 250 μg/ml MSU for 4 hours. IL-8 levels were quantified in the supernatants using ELISA (****p<0.0001, MSU, n=5, SEM, Dunnett's Multi-comparison Test). **B)** PMNs were treated with 10 μM of MRS2578 of 0.1% DMSO and imaged for an hour. Percentage of phagocytosis by PMNs were counted at 30 mins and 60 mins. **C)** Respiratory burst by PMNs were calculated by normalizing on PMA-induced superoxide production. The luminescence was detect by the lucigenin assay in PMNs treated with 10 μM of MRS2578 of 0.1% DMSO (n=3, SEM, Dunnett's MCT). **D).** Calcium flux was measured

in calcium free media to detect the intracellular calcium release with 10 μM of MRS2578 of 0.1% DMSO. Stimulants (HBSS ca free,5 μg/ml Ionomycin or 10 μM UDP) were added after 1 min (shown by arrow). (Representative of 4 independent experiment).

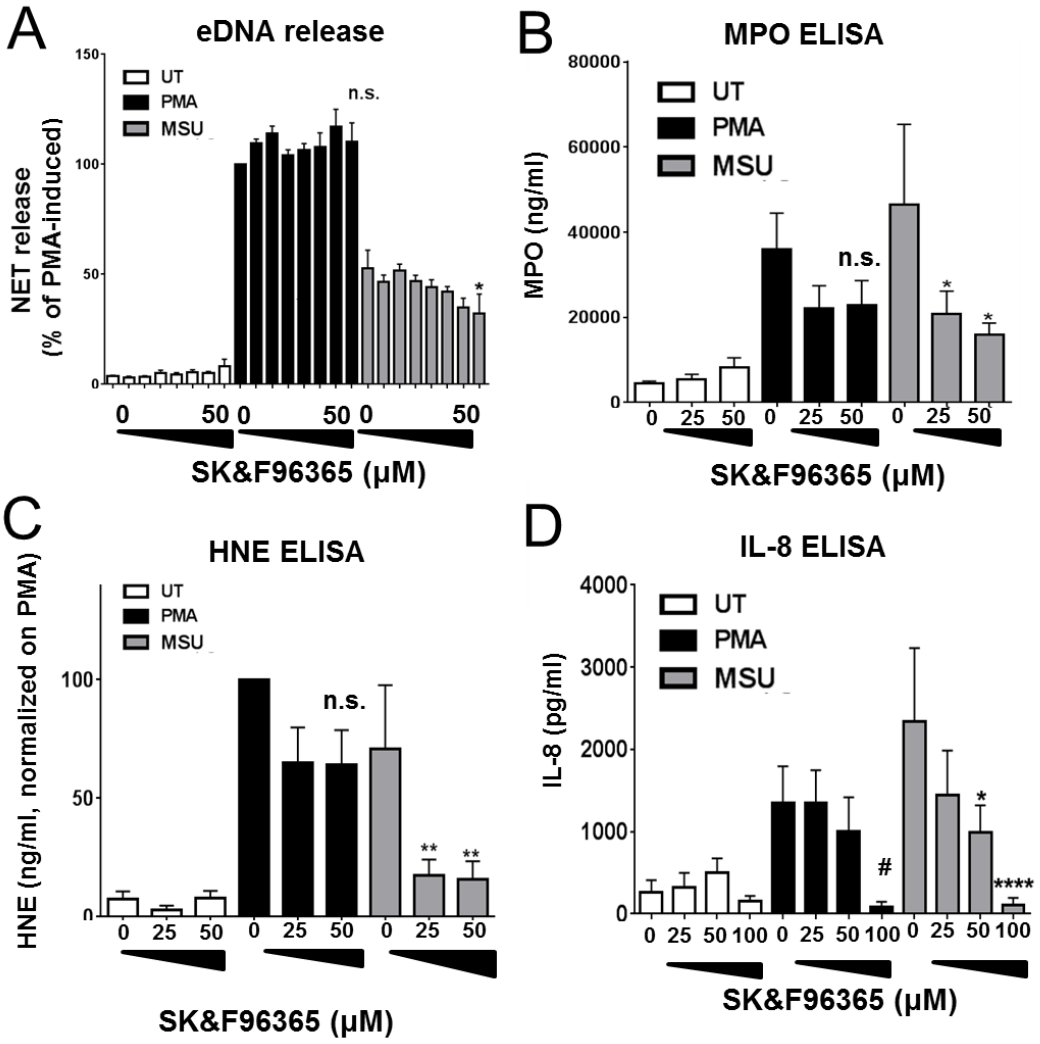

Figure 3.8. The store-operated calcium entry pathway contributes to PMN activation by MSU crystals. Human PMNs were treated with the store-operated calcium entry inhibitor, SK&F96365, for 45 mins prior to stimulation with 250 μg/ml MSU crystals or 100 nM PMA for 3 hours. SK&F96365 has significantly reduced ecDNA release (n=5, Mean+/-.S.E.M.) (A), MPO release (n=6, Mean+/-.S.E.M.) (B), HNE release (n=5, Mean+/-.S.E.M.) (C) and IL-8 secretion (n=4, Mean+/-.S.E.M.) (D) induced by MSU crystals but not by PMA. MSU, *$p<0.05$, **$p<0.01$,****$p<0.0001$, Dunnett's Multi-comparison Test. PMA, #$p<0.05$, n=4, Mean+/-.S.E.M., Dunnett's Multi-comparison Test.

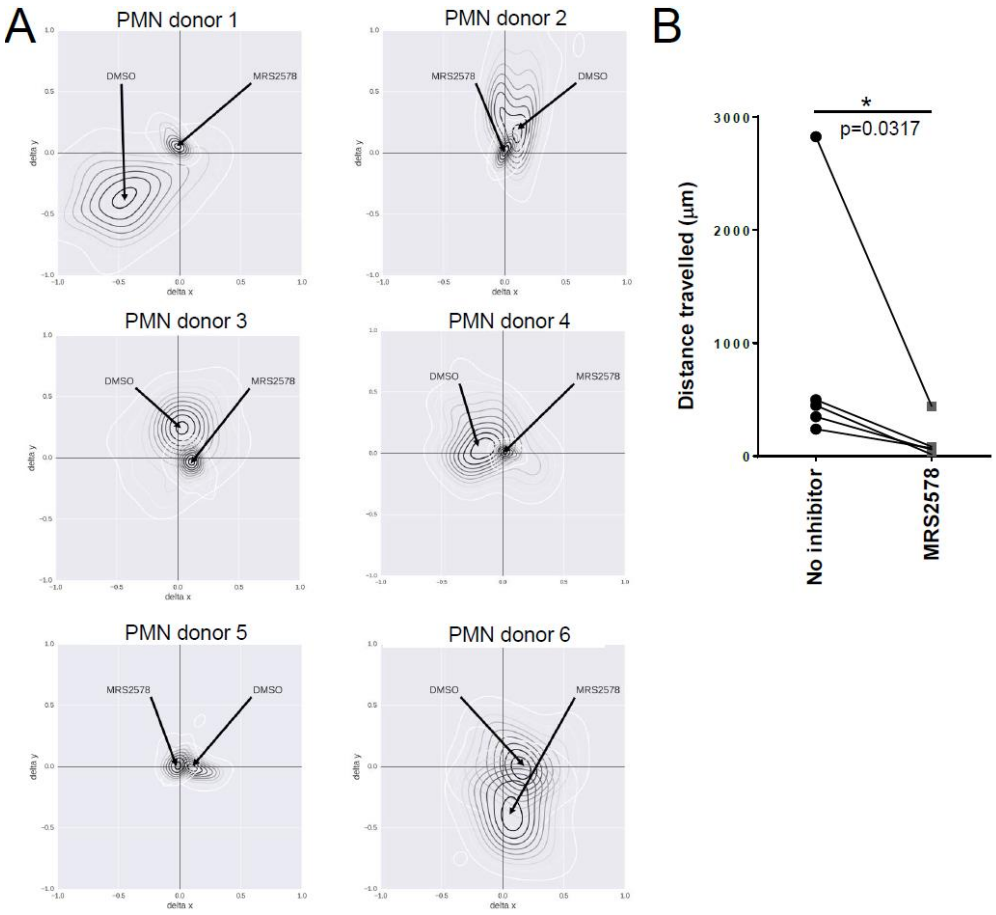

Figure 3.9. MRS2578 inhibits intrinsic migration in human PMNs.

Human PMNs were pretreated with 10 µM MRS2578 or 0.1% DMSO for 1 hour and their migration was recorded using a confocal microscope. PMNs obtained from six independent healthy donors were used. At least 10 individual PMNs per video were tracked. A) The directionality of PMN migration was characterized by determining the optical flow based on calculation of aggregate delta x and delta y values for each pair of videos as described in the Methods. Results are visualized as two-dimensional contour plots. B) Total distances of migration per cell were calculated using Image J software. The average distance was calculated on the basis of no. of PMNs tracked with 0.21µm/ pixel setting.(* $p<0.05$, Student's t test, n=3, mean +/- S.E.M)

CHAPTER 4

MACROPHAGE-DERIVED IL-1β ENHANCES MSU CRYSTAL-TRIGGERED NET FORMATION [3]

[3] Sil, P, Surrell C., Wicklum H., and Rada B., Submitted to *Inflammation Research* July 2016, (under revision).

Abstract:

Objective and design: Arthritic gout is caused by joint inflammation triggered by the damaging effects of monosodium uric acid (MSU) crystal accumulation in the synovial space. Neutrophils play a major role in mediating joint inflammation in gout. Along with neutrophils, other immune cells such as macrophages are present in inflamed joints and contribute to gout pathogenesis. Neutrophils form neutrophil extracellular traps (NETs) in response to MSU crystals. In the presence of MSU crystals, macrophages release IL-1β, a cytokine crucial to initiate gout pathogenesis and neutrophil recruitment. Our research investigated interactions between human macrophages and neutrophils in an *in vitro* model system and asked how macrophages affect NET formation stimulated by MSU crystals.

Materials or subjects: Human neutrophils and PBMCs were isolated from peripheral blood of healthy volunteers. PBMCs were differentiated into macrophages *in vitro* using human M-CSF.

Treatment: Human neutrophils were pretreated with macrophage-conditioned media, neutrophil-conditioned media or recombinant human IL-1β prior to stimulation by MSU crystals.

Method: Interaction of neutrophils with MSU crystal was evaluated by live imaging using confocal microscopy. The presence of myeloperoxidase (MPO) and Human neutrophil elastase (HNE) were measured by ELISA. NET formation was quantitated by Sytox Orange-based extracellular DNA release assay and NE-DNA ELISA. AggNET formation was assessed by macroscopic evaluation.

Results: We found that crystal- and cell-free supernatants of macrophages stimulated with MSU crystals promote MSU crystal-stimulated NET formation in human neutrophils. This observation was confirmed by additional assays measuring the release of MPO, NE and the enzymatic activity of NE. MSU crystal-induced NET formation remained unchanged when neutrophil supernatants

were tested. IL-1 β is a crucial cytokine orchestrating the onset of inflammation in gout and is known to be released in large amounts from macrophages following MSU crystal stimulation. We found that IL-1β strongly promoted MSU crystal-induced NET formation in human neutrophils. However, IL-1 β alone did not induce any NET release.

Conclusions: Macrophage-derived IL-1β enhances MSU crystal-induced NET release in neutrophils. We identified a new mechanism by which macrophages and IL-1β affect neutrophil functions and could contribute to the inflammatory conditions present in gout.

Introduction:

Gout is a sterile inflammation of the joints mediated mainly by infiltrated macrophages and polymorphonuclear neutrophilic granulocytes (PMN) driven by Monosodium Urate (MSU) crystal deposition [3]. These innate immune cells mistakenly recognize MSU crystals as danger and undergo unnecessary activation resulting in painful, tissue-damaging inflammation [278]. While macrophages are the initiators of the inflammatory cascade, PMN infiltration and activation play a major role in bringing inflammation to its full expansion in gout [35, 39, 147, 281].

Macrophages in the synovium initiate the acute inflammatory phase in gout. Macrophages stimulated with MSU crystals activate the Erk1/2 MAPK pathway leading to activator protein and nuclear factor κβ activations which trigger the production of proinflammatory mediators such as IL-1β, TNF-α, IL-6, IL-8 and cyclooxygenase-2 [282].

IL-1β is a crucial and potent proinflammatory cytokine that also orchestrates gouty inflammation [57, 121, 283]. IL-1β is abundant in the synovial fluid of gout patients [35]. Its central role in gout inflammation and successful administration of IL-1β-inhibitory therapies to mitigate gout inflammation is a testament of that [121, 284, 285]. Anakinra, a recombinant IL-1Ra protein, rilonacept, an IL-1 receptor fusion protein and canakinumab, an anti-IL-1β antibody have all been shown to successfully treat acute gout attacks [121]. The primary role of IL-1β in mediating the inflammatory cascade in gout is thought to be its potent effect to recruit PMNs to the synovial space [121, 178]. The NLRP3 inflammasome mediates the formation of bioactive IL-1 β via caspase-1 activation in macrophages. Macrophages deficient in NLRP3 components do not produce IL-1β [2, 3, 39, 40, 209, 277]. MSU crystals activate the NLRP3 inflammasome and induce release of IL-1β in macrophages [3, 39, 40]. The NLRP3 inflammasome is composed of NLRP3 protein, ASC adaptor protein, and pro-caspase-1 [3, 39, 40, 42]. NLRP3 inflammasome

activation requires the phagocytosis of MSU crystals, regulation of K^+ efflux by P2X7R channel, the sensing of reactive oxygen species (ROS) due to stress, destabilization of lysosomal membrane and activation of the lysosomal protease cathepsin [3, 39, 40]. We and others have shown that MSU crystal-induced NLRP3 inflammasome activation requires calcium and NADPH oxidase-independent ROS [50, 286, 287]. Caspase-1 activated by the inflammasome cleaves pro-IL-18 and pro-IL-1β forming bioactive cytokines [2, 4]. IL-1β signals through IL-1R1, Myd88, TNFR associated factor 6 and IL-1R associated kinases, resulting in NF-κB-induced inflammatory genes in target cells [1-3].

PMNs are the most abundant leukocytes during gout inflammation and reach very high concentrations in the synovial fluid [7, 23, 34, 35]. PMNs are known to engulf MSU crystals triggering ROS production, cytokine release and neutrophil extracellular trap (NET) formation [7, 23, 34, 147, 288]. In a previous study, we described robust NET release of human PMNs in response to CPPD microcrystals, the causative agents of pseudogout, a condition similar to gout [50]. NETs are composed of extracellular DNA network associated with histones and PMN granule proteins including myeloperoxidase (MPO) and human neutrophil elastase (HNE) [59, 88, 133]. NET formation in gout is misguided which leads to the spewing of dangerous PMN molecules or peptides into the synovium. In gout, the primary antimicrobial function of NETs (trapping extracellular microbes) manifests in MSU crystal immobilization [22, 23, 36, 147]. MSU crystal-induced NET release requires autophagy, NADPH oxidase-dependent ROS production and RIP3K-MLKL signaling pathway [23, 34, 35, 289]. A recent study shed light on a potential anti-inflammatory role of NETs in gout [261]. At high PMN densities, NETosed PMNs and MSU crystals form ‘aggregated NETs’ (aggNETs), the proposed basis of gouty tophi, a characteristic white material that appears at the beginning of the resolution phase of acute gout flares [23, 24,

290, 291]. Although our view on the role of NETs in gout pathogenesis is improving, less is known about how the two most important cell types initiating and mediating inflammation in gout, macrophages and PMNs, interact. M1 inflammatory macrophages were shown to remain immunologically silent while engulfing NETs [292, 293], whereas M2 macrophages displayed a proinflammatory signature [292]. It is unknown how macrophages affect NET formation in PMNs. Our study addressed the question, "how do macrophages influence NET formation stimulated by gout-causing MSU crystals?" Our data show that proinflammatory macrophages, stimulated with MSU crystals, released mediators that cause neutrophils to have over-exaggerated release of NETs induced by the crystals. We also show that IL-1β is a potent enhancer of NET formation. We propose that both macrophages-and IL-1β -enhance NET formation acting as a 'double whammy' in magnifying gout inflammation.

Materials and Methods:

2.1. Human subjects.

De-identified of the healthy human volunteers were recruited at the University of Georgia to donate blood. The studies were performed according to the guidelines of the World Medical Association's Declaration of Helsinki. Enrolled blood donors signed consent forms as described previously [50, 82, 86, 87]. The human blood protocol (UGA# 2012-10769) and the associated consent form were reviewed and approved by the Institutional Review Board (IRB) of the University of Georgia.

2.2. Human neutrophils and autologous serum.

Human neutrophils were isolated as described previously [50, 82, 86]. Briefly, coagulation was prevented with heparin and red blood cells were removed by Dextran sedimentation (GE

Healthcare, Fairfield, CT, USA). Neutrophils were isolated using 5-step Percoll gradient centrifugation. Cell viability was >98% (Trypan Blue) and neutrophil purity was > 95% (cytospin and flow cytometry). Autologous serum was prepared by centrifugation and sterile filtration. Calcium-and magnesium-containing HBSS (Mediatech, Manassas, VA, USA) supplemented with 1% autologous serum, 5 mM glucose and 10 mM HEPES was used as assay buffer.

2.3. PBMC isolation and in vitro macrophage differentiation.

PBMCs were isolated from 65% Percoll gradient interphase, washed twice with PBS and seeded at 2-3 million cells/well concentration in RPMI media with Glutamax (Gibco Thermo Fischer, Waltham, MA, USA). The next day the media was supplemented with 50 ng/ml m-CSF and 1% autologous serum or FBS and macrophages were differentiated for 5-7 days into M1 phenotype as described previously [243].

2.4. Macrophage supernatant collection.

Differentiated macrophage cultures were primed with 10 μg/ml LPS for 30 mins to mimic proinflammatory conditions found in the gout synovium. Macrophages were then washed 4X HBSS to remove LPS and were subsequently incubated with or without 250 μg/ml MSU crystals for 5 hours. Supernatants were collected and then spun at 10,000g for 5 mins. The pellet was discarded, cell-, crystal-and debris-free supernatants were frozen at -80 °C and called the 'macrophage-conditioned medium'.

2.5. Extracellular DNA release assay.

NETs were quantified essentially as described previously [50, 187]. Briefly, neutrophils were allowed to adhere to poly D-lysine coated 96-well black transparent bottom plates (Thermo Scientific, Rochester, NY, USA) in assay buffer with 0.2% Sytox Orange (Life Technologies, Grand Island, NY, USA). Fluorescence (excitation: 530 nm, emission: 590 nm) was measured in a fluorescence microplate reader (Varioskan Ascent, Thermo Scientific, Rochester, NY, USA) for 6 hours at 37 °C. Increase in fluorescence normalized on maximal value (saponin-treated PMNs) was referred to as "extracellular DNA release" and expressed as "% of max". The obtained relative fluorescence units (RFU) were sometimes also normalized against PMA.

2.6. Confocal microscopy of NETs.

As previously detailed [50], 2 x 10^6 human neutrophils in assay medium were incubated for 4 hrs at 37 °C with or without 100 nM PMA and 100 μg/ml MSU crystals in 35 mm glass bottom dishes (MatTek, Ashland, MA, USA) pre-coated for 1 hr with 1% human serum albumin (Sigma Aldrich, St Louis, MO, USA). 2.5 μM Sytox Orange (Invitrogen, Grand Island, NY, USA) was added prior to fluorescence imaging (exc/em: 547/570 nm). Images were collected using a Nikon A1R confocal microscope system equipped with a Nikon Eclipse Ti-E inverted microscope, built in perfect focus, high-speed motorization and NIS Elements software (Nikon Instruments, Melville NY, USA). Live cell imaging was carried out using a Tokai Hit INY-G2A-TIZ incubator (Tokai Hit CO, Ltd, Shizuoka-kenwith Japan) for temperature, humidity and CO_2 control. The Coherent Sapphire 561nm 20mW laser was used to excite Sytox Orange using a CFI Plan APO VC 60X Oil NA 1.4 WD 0.13 mm objective. Optical sections of neutrophils were analyzed, Z-stacks spanning 1 μm were acquired and 3-D image reconstructions were processed using the Nikon NIS Element

Version 4 software (Nikon Instruments, Melville NY, USA). Final image preparation was carried out using Adobe Photoshop (Version cc 2014, San Jose, CA, USA).

2.7. High-throughput live imaging of NET formation.

A microplate-based NET imaging assay was established using a motorized stage support of a confocal microscope. PMNs were seeded at a concentration of 250,000 cells/ well in a 96 well plate Optical Btm Pit Polymer Base black plate (Thermoscientific, Rochester, NY, USA). PMNs were pre-incubated with 10 ng/ml IL-1β prior to imaging. PMNs were then stimulated with 200 μg/ml MSU crystals for 16 hours. Nikon A1R confocal microscope system with a 10X lens was used to capture transmitted light and fluorescence images. A field of interest was chosen to perform imaging and their position was defined using the NIS elements software. The chosen field was a true representation of the entire well. Images were taken every 15 min for 12 hours using automated capture component of the NIS elements software. Mean Sytox Orange intensities of the fluorescent images were quantified using the measure region of interest (ROI) feature of the Nikon A1 Elements software. The entire image which represented the field was selected as the ROI. These measurements were used to calculate changes in Sytox Orange intensities over time (ΔMean SYTOX orange intensity). Samples were always run as three biological replicates.

2.8. Measurement of AggNET formation.

Visualization of aggregated NET formation was modified after adaptation [23, 25, 29, 147]. 1,000,000 PMNs in assay medium were added in a 48-well plate with or without 1mg/ml MSU crystals at 37 °C with or without 10 ng/ml IL-1β. Images of aggNETs were taken after 5 hr incubation using an inverted light microscope [23, 25, 29, 147].

2.9. ELISA.

Myeloperoxidase (MPO), IL-1β or IL-8 levels were quantitated using commercial ELISA kits from R&D systems (Minneapolis, MN, USA), Millipore and BioLegends (San Diego, CA, USA), respectively. Manufacturer's instructions were followed for sample dilutions and processing. 250,000 PMNs/well were seeded in 24-well plates and stimulated with 250 μg/ml MSU crystals in HBSS for up to 4 hours at 37˚C. Cell supernatants collected were either immediately processed or stored (-80˚C) for later analysis. Undiluted supernatants were used to measure IL-8 and IL-1β, whereas supernatants were diluted 1:100 to determine MPO and HNE concentrations. HNE release was assessed as described [82, 87] by ELISA using anti-HNE rabbit polyclonal antibody (Merck Millipore, Billerica, MA, USA). Supernatant samples diluted with coating buffer (25 mM carbonate, 25 mM bicarbonate, pH 9.6) were incubated overnight at 4˚C in 96-well high-binding microlon ELISA plates (Greiner bio-one, Fricken-hausen, Germany). After blocking with 1% BSA for 1 hour, anti-rabbit mouse polyclonal Ab (1:500 in PBS [Calbiochem, EMD Millipore, Billerica, MA, USA], 481001 [Merck Millipore, Billerica, MA, USA]) was added for 2 hours at RT. After repeated washes, samples were incubated with horseradish peroxidase–linked donkey anti-rabbit Ab (1:2000 in PBS, NA934V; GE Healthcare, Little Chalfont, U.K.) for 1 h. Yellow coloration of the TMB substrate (Thermo Scientific, Rockford, IL, USA) after the addition of 1N hydrochloric acid (Sigma, St. Louis, MO, USA) was read at 450-nm wavelength with Eon microplate photometer (BioTek, Winooski, VT, USA). Commercially available HNE (stock: 1 mg/ml; Cell Sciences, Canton, MA, USA) was used as standard.

2.10. HNE-DNA ELISA.

NETs were quantitated as described previously [82, 86]. Briefly, PMN supernatants were exposed to DNAse1 digestion for 15 min that was stopped by adding 2.5 mM EGTA. Diluted supernatants and "NET standard samples" were added to 96-well high binding microlon ELISA plates (Greiner bio-one, Fricken-hausen, Germany) coated anti-HNE rabbit antibody. Horse radish peroxidase-labelled anti-DNA secondary antibody (1:500 in PBS) was added for 2 hours followed by repeated washes. Absorbance of the TMB substrate was read after addition of 1N hydrochloric acid (Sigma, St. Louis, MO, USA) at 450 nm with Eon microplate photometer (BioTek, Winooski, VT, USA). NET's were quantitated as percentage of the NET-standard in the undiluted supernatants.

2.11. Quantification of enzymatic activity.

To measure HNE activity, the Neutrophil Elastase Activity Assay Kit (Cayman Chemical Ann Arbor, MI, USA) was used following manufacturer's protocol. Briefly, supernatants (50 µl) were placed into 96-well black plates. Substrate (Z-Ala-Ala-Ala-Ala 2Rh110, cat no.600613, Cayman Chemical, Ann Arbor, MI, USA.) solution was added to assess elastase activity by measuring production of the highly fluorescent product (compound R110) using 485 nm excitation and 525 nm emission wavelengths in microplate fluorimeter (Varioskan Flash, Thermo Scientific, Waltham, MA, USA). Data are expressed either as kinetics (RFU) or end-point values normalized on maximal (PMA-stimulated) data.

2.12. Statistical analysis: Data are represented as mean +/− S.E.M. P value was calculated with ANOVA and Dunnett's post-hoc test and was marked as * when $p < 0.05$, ** when $p < 0.01$ and *** when $p < 0.001$.

Results

3.1. Secreted neutrophil products do not affect MSU crystal-induced NET release.

PMNs release large amounts of NETs in response to gout-causing MSU crystals [23, 34-36, 147, 171]. While MSU crystal-induced NET formation seen at lower PMN densities has been implicated in the proinflammatory phase of gout pathogenesis, aggNET formation observed at high PMN densities has been shown to be anti-inflammatory [23]. Despite the increase in the amount of information about the complex role and mechanism of MSU crystal-induced NET release, little is known about its regulation.

To assess whether PMNs themselves would promote NET formation, we first stimulated human PMNs with MSU crystals and collected supernatants after 5 hours. Cells, debris and crystals were removed by centrifugation resulting in a clean supernatant referred to as "PMN-conditioned medium". This conditioned medium was then added to the same donor's, unchallenged PMNs in presence or absence of MSU crystals and detection of DNA release was measured. As shown in Figure 2.4.1A, the PMN-conditioned medium did not affect NET formation indicating that PMNs do not intrinsically accelerate MSU crystal-induced NETs in a positive feedback manner.

3.2. Macrophages release NET-enhancing mediators upon MSU crystal stimulation.

Since macrophages are represented in the gout synovium in large numbers and are responsible for initiating inflammation [278], we repeated the same experiment as before using macrophages, not PMNs, as the source of conditioned medium. When this "macrophage-conditioned medium" was added to human PMNs, MSU crystal-induced DNA release was significantly enhanced (Figure 4.1.B). Spontaneous NET formation remained unaffected (Figure 4.1.B). These data were also confirmed by confocal microscopy showing the larger amount of three-dimensional extracellular

DNA release in the presence of macrophage-conditioned medium than in its absence (Figure 4.1.C). These results indicate that MSU crystal-exposed macrophages release secretory products that strongly accelerate NET formation of PMNs stimulated by MSU crystals.

3.3. Macrophage-conditioned media increases the release of primary granule markers and NETs from MSU crystal-stimulated PMNs.

NETs are composed of an extracellular DNA meshwork associated with histones and PMN granule components, such as MPO and HNE [59]. The definition of NETs requires the detection of DNA-protein complexes characteristic for NETs. First, we confirmed that we could detect MPO and HNE by ELISA in the supernatants of human PMNs after MSU crystal stimulation (Figure 4.2.A-B). Second, we observed that addition of macrophage-conditioned medium significantly enhanced MSU crystal-induced MPO and HNE release (Figure 4.2.A-B). To prove that released MPO and DNA were part of the NETs complex, we utilized an ELISA developed in our laboratory capable of quantitating NET-specific MPO-DNA complexes [82, 86]. MSU crystals initiated NET release that was further enhanced by mediators secreted by macrophages (Figure 4.2C). Overall, our results presented so far describe a novel mechanism that enhanced the formation of NETs in PMNs.

3.4. IL-1β potentiates MSU crystal-induced DNA release from PMNs.

Macrophages have been described to release several cytokines and other inflammatory mediators upon MSU crystal exposure [278]. IL-1β was our prime suspect responsible for the NET-promoting effect of macrophages because IL-1β is a central cytokine orchestrating gout inflammation, and it is released in copious amounts from MSU crystal-stimulated macrophages [40, 49, 120, 121, 278]. We confirmed that differentiated macrophages also produced IL-1β upon

MSU crystal activation in our hands, as well (data not shown). We stimulated human PMNs with MSU crystals in presence of recombinant human IL-1β and measured extracellular DNA release. IL-1β did not show any effect, when used with 100 μg/ml MSU crystals. However, it strongly amplified the NET formation in a dose-dependent manner (over the range of 0-10 ng/ml) when 250 μg/ml crystal concentration was applied (Figure 4.3A-B). The highest dose of IL-1β enhanced NET formation to the extent observed with the positive control, PMA (Figure 4.3.A-B). Interestingly, IL-1β alone (without MSU crystals) did not induce NET release (Figure 4.3.A-B). These results demonstrate a novel effect of IL-1β, a central cytokine in gout inflammation, on PMN activation by MSU crystals.

3.5. IL-1β enhances MPO, HNE and NET release following MSU crystal stimulation.

To confirm that the DNA release-promoting effect of IL-1β is also accompanied by increased release of granule markers and NETs, we quantitated MPO, HNE, HNE-DNA and HNE enzymatic activity levels in supernatants of MSU crystal-induced PMN in the absence or presence of IL-1β. We found that IL-1β significantly promoted the release of MPO and DNA-associated complex, active HNE from human PMNs after MSU crystal stimulation (Figure 4.4.A-D). These data are in accordance with those presented in Figure 4.3 indicating that IL-1β alone does not induce NET formation but it significantly promotes NET release triggered by MSU microcrystals.

3.6. Imaging the NET-promoting effect of IL-1β by high-throughput confocal live microscopy.

Next, we performed high throughput imaging in order to visualize NET formation real-time using confocal microscopy. This method developed in our laboratory enables simultaneous imaging of

NET-forming live PMNs on a 96-well-based format in presence of Sytox Orange. Recorded videos allow spatiotemporal resolution of the NET-forming processes while kinetic data enables concomitant quantitative comparisons.

The recorded videos confirmed previous data. IL-1β alone did not induce DNA release while MSU crystals triggered NET formation (Figure 4.5A-B). Addition of IL-1β to MSU crystals resulted in more robust NET release in the same time frame when compared to MSU crystals alone (Figure 4.5A-B). In addition, video recordings show that PMNs start to aggregate soon after MSU crystal exposure (Figure 4.5A).

3.7. IL-1β enhances aggregated NET formation.

Since MSU crystals form aggregated NETs (aggNET) at higher PMN densities [23], we wanted to study how IL-1β affects this process also. Human PMNs at higher cell density were exposed to higher MSU crystal concentration (1mg/ml) modeling peak phases of gout inflammation for 5 hours [158]. As shown in Figure 4.5C, MSU crystals initiated aggNET formation that was further enhanced by IL-1β, as assessed by light microscopy.

Discussion:

The interaction between PMNs and macrophages is an essential component of gout inflammation in joints [1, 2]. Resident macrophages at the synovium represent the first cell type to come in contact with MSU microcrystals [1, 2] that leads to inflammasome activation and production of the proinflammatory cytokine IL-1β [1, 2, 40, 49]. IL-1β initiates PMN chemotaxis that is thought to be the main mediator of PMN influx to the synovium in gout [40]. In this paper we present novel data showing that macrophages and IL-1β enhances MSU crystal-induced NET formation. These

results corroborate the previously published data showing that gout synovial fluid supernatants promote spontaneous NET release in human PMNs that is partially inhibited by anakinra [34]. Recent data suggest a more complex mechanism by which macrophages interact with PMNs in gout indicating that macrophage-derived IL-1β not only attracts PMNs to the site of inflammation but it also accelerates the release of PMN-derived inflammatory mediators including NETs. Not only macrophages, but PMNs, as well as mast cells are also, sources of IL-1β in gout that promote NET release, in addition to those secreted by macrophages [35, 44, 57]. The role of caspase-1 in cleaving pro-IL-1β producing bioactive IL-1β is taken up by neutrophil elastase in PMNs [35, 294]. This mechanism is thought to accelerate inflammation since IL-1β would enhance its own activation by activating PMNs to release NET-related proteases. Targeting IL-1β in gout *in vivo* could fulfill its beneficiary effects not only by diminishing PMN recruitment but also via attenuating PMN activation by MSU crystals.

IL-1β alone does not induce NETs in our system, but it enhances NET release induced by MSU crystals. Whether this observation is unique for MSU crystals or has similar effects on other NET-triggering stimuli such as bacteria, fungi or other microcrystals, remains to be investigated.

Several potential mechanisms could underlie the NET-enhancing effect of IL-1β. IL-1β may increase NET formation by its known beneficiary effect on the activation of the NADPH oxidase [295, 296]. The NADPH oxidase is required for MSU crystal-induced NET formation [23]. IL-1β could enhance the phosphorylation of the oxidase subunits or their expression. This mechanism is likely because human PMNs of IRAK4-or NEMO-deficient patients with impaired TLR/IL-1R signaling have reduced NADPH oxidase priming and activation [297]. IL-1β is a known chemoattractant for PMNs [298]. Although it remains to be studied, a migratory component of MSU crystal-induced NET/ aggNET formation is likely that could be promoted by this cytokine.

At the same time, IL-1β also promotes aggNET formation, a novel mechanism proposed to shut down acute inflammation in gout [23]. The highly concentrated protease activity of aggNETs degrades several proinflammatory cytokines including IL-1β putting a break on the inflammatory process [23]. Therefore, our results implicate that promoting the aggNET-enhancing mechanism of IL-1β offers a novel anti-inflammatory strategy and could have therapeutic benefits.

Although IL-1β is the major proinflammatory molecule released by macrophages promoting gout inflammation, other secretory products could also have a role in NET formation. IL-8, C5a, G-CSF, IFN-γ, and TNFα have all been reported to stimulate NET formation (Table 3) [23, 50, 55, 91, 145]. G-CSF is indispensable for neutrophil functions [299] and assists in the NETosis process [2, 36, 280] (Table 3). TNF-α is released during the acute phase of gout and can trigger a NET response (Table 3) [2, 36, 50, 91, 280].

In summary, our data presented here provide a new link between macrophages and PMNs, two important innate immune cell types mediating the general and pathological inflammatory pathways. Thus, the study upholds the fact that IL-1β is a major player in gout [34, 35, 171] and also unveils a unique role of IL-1β in exaggerating the MSU crystal-triggered NET formation, and therefore, contributing to gouty inflammation.

Abbreviations:

NETs – Neutrophil Extracellular Traps

AggNET -Aggregated Neutrophil Extracellular Traps

PMN -Polymorphonuclear neutrophils

IL-1β – Interleukin-1 beta

PBMC -Peripheral Blood Mononuclear cells

NLRP3 – NACHT, LRR and PYD domains-containing protein 3

ROS – Reactive oxygen species

SF – Synovial fluid

MSU – Monosodium urate

MPO – Myeloperoxidase

NE – Neutrophil elastase

HNE – human neutrophil elastase

M-CSF – macrophage colony stimulating factor

Acknowledgements: We thank the personnel at the UGA University Health Center for blood collection and the College of Veterinary Medicine Imaging Core for technical assistance with confocal microscopy and flow cytometry. We are also grateful to Dr. Pramod Giri (UGA) for his help with optimizing macrophage differentiation.

Disclosure: The authors have no financial conflicts of interest.

Concluding Remarks:

Gout has prevailed for centuries and continues to plague mankind due to a lack of a cure [2, 48]. Neutrophils, IL-1β and very recently NETs have been shown to be responsible for debilitating joints in gout [1, 2, 6, 11, 17, 23-25, 34-36, 39, 147, 199, 202, 203, 206-208, 291]. In 2004, Brinkmann *et al.* coined the term NETs and showed its role in immunity [59, 88, 133] . Association between NETs and MSU crystals was made more recently in the past decade [1-3, 23, 36, 147, 263, 289]. Schauer *et al.* and Schorn *et al.* revealed the occurrence of aggregated MSU crystal-NETs conglomerations separately and Schauer *et al.* 2012 showed the anti-inflammatory role in the resolution of gout [23, 36, 147]. Although astounding leaps have been in the gout research, there still is an absence of treatment.

To understand the disease and the mechanism of inflammation, we need to study the signaling pathways of NETs and aggNETs. For that purpose, firstly, we need a scheme to detect them accurately. Figure 5.2 and chapter 2 summarizes a novel method used to detect NETs *in vitro* [82, 86]. Secondly, we need to understand the interaction between PMNs and MSU crystals as shown in Figure 5.2 and chapter 3 (Sil & Rada, J. Immunol., under revision). Thirdly, we must seek the possible interaction of PMNs and MSU crystals with other cell types such as macrophages that may aggravate NETosis process as shown in this chapter and Figure 5.3 (Sil & Rada, Infl. Research., under revision).

Although further research is warranted to advance the field of gout and arthritis research, it is essential to locate potential associates of MSU crystal-triggered NETs that will reveal the key players in the pathway. Finding all the ‘parts of the puzzle’ forming this signaling cascade will help formulate a potential treatment to heal the joints, and override the current fleeting treatment regimen. The method described in chapter 2, will embark an educational journey leading to a better

understanding of the PMN –MSU crystal interaction, macrophage-PMN interaction and potential molecular players in modulating NET pathway. Thus, these efforts can potentially help make therapeutic advancement and strides in other NET-driven diseases.

Figures

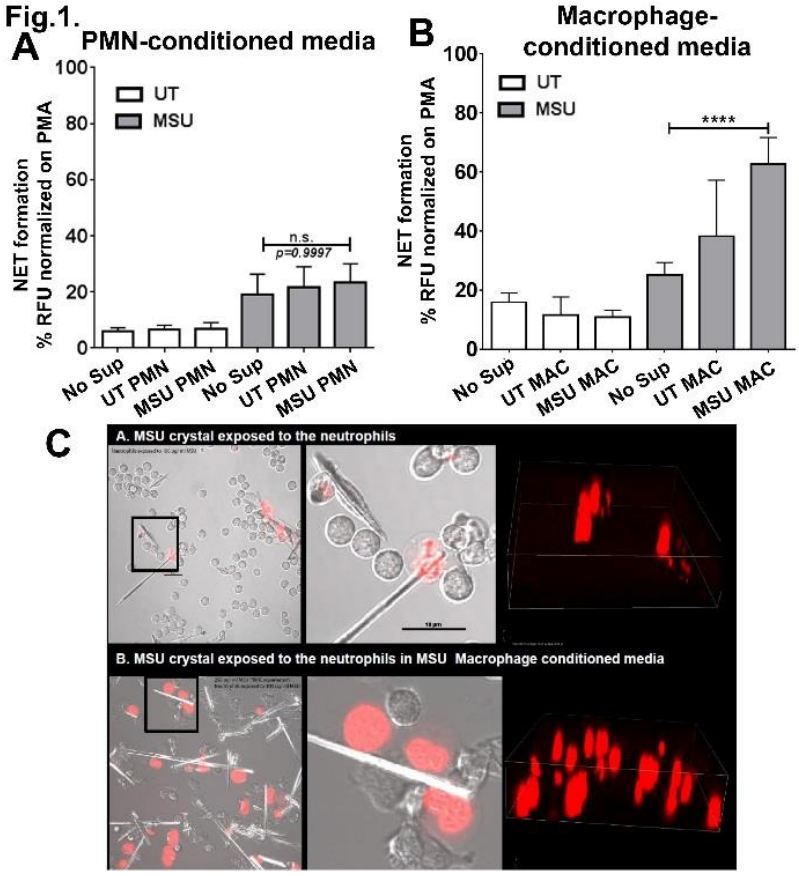

Figure 4.1. Supernatants of macrophages, but not neutrophils, enhance extracellular DNA release from MSU crystal-stimulated human neutrophils. Human macrophages differentiated with M-CSF for 5-7 days or neutrophils were exposed to 250 μg/ml MSU crystals for 5 hours. Collected supernatants were centrifuged to remove cells, crystals and debris and referred to as "PMN-conditioned medium" or "macrophage-conditioned medium", respectively. The effects of conditioned media on NET formation were subsequently tested on human neutrophils stimulated in the absence (UT, untreated) or presence (MSU) of 250 μg/ml MSU crystals by Sytox Orange-based fluorescence. Fluorescence data were normalized against the 100 nM PMA-triggered signal, used as the positive control for NET formation. **A)** "PMN-conditioned media" of neither MSU crystal-stimulated (MSU PMN) nor untreated neutrophils (UT PMN) had any significant effect on

NET release (No Sup). Mean+/-S.E.M., n=4, Dunnett's test. **B)** "Macrophage-conditioned media" of MSU crystal-stimulated macrophages (MSU MAC) significantly increased NET formation in comparison to that seen in absence of conditioned media (No Sup). Conditioned media of macrophages without crystal stimulation (UT MAC, untreated) had no significant effect. Mean+/-S.E.M., n=11, Dunnett's test. **C)** Representative confocal microscopy images of MSU crystal-stimulated human neutrophils show enhanced DNA release (Sytox Orange) by the MSU crystal-stimulated macrophage conditioned media compared (lower panels) to that without addition of conditioned media (upper panels) (n=3). RFU, relative fluorescence unit; PMA, phorbol myristate acetate; MAC, macrophage; PMN, neutrophil; MSU, monosodium urate; n.s., not significant; ****, $p<0.0001$.

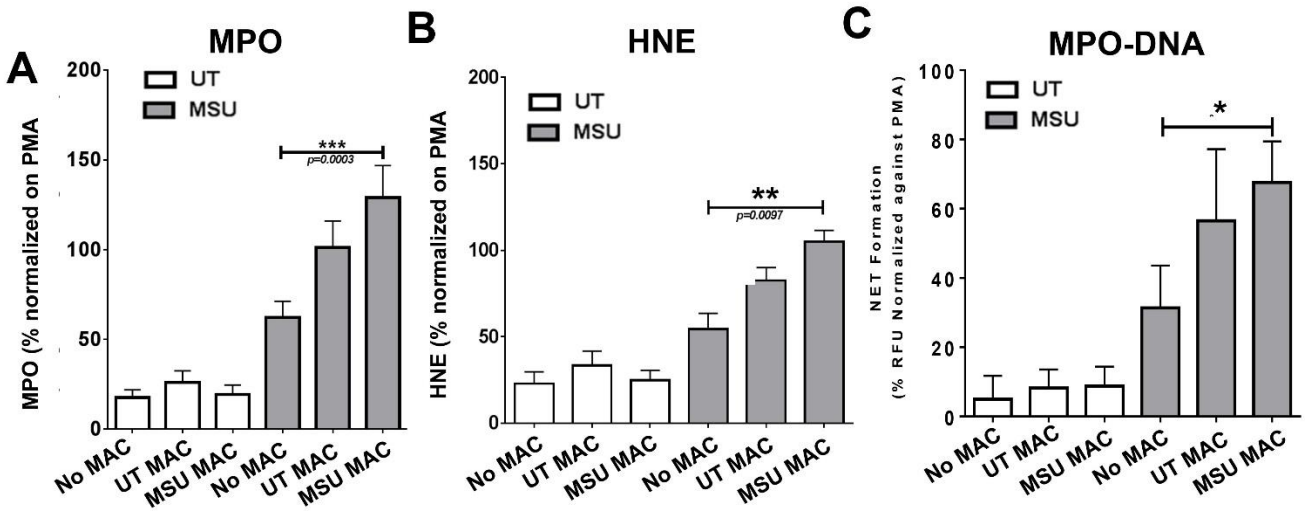

Figure 4.2. Macrophage supernatants increase MPO, HNE and NET release from human neutrophils following MSU crystal stimulation.

Differentiated human macrophages were exposed to 250 μg/ml MSU crystals for 5 hours to collect and centrifuge their supernatants. This "macrophage-conditioned medium" (MSU MAC) was added to MSU crystal-stimulated human neutrophils and releases of **A)** MPO (n=9), **B)** HNE (n=9) and **C)** NETs (MPO-DNA, n=6) were quantitated by ELISA assays (mean+/-S.E.M., Dunnett's test). As comparisons, PMNs were also treated with mock only (No MAC) or supernatants of macrophages without crystal stimulation (UT MAC, untreated). MPO, myeloperoxidase; HNE, human neutrophil elastase; MAC, macrophage. *, $p<0.05$; **, $p<0.01$; ***, $p<0.001$.

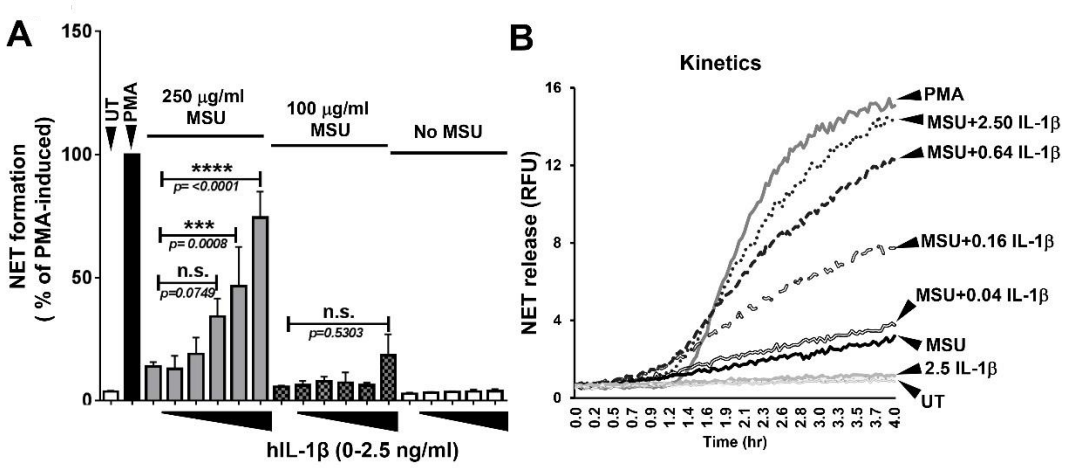

Figure 4.3 IL-1β promotes DNA release from human neutrophils stimulated with MSU crystals. Following treatment with increasing doses of recombinant human IL-1β, human neutrophils were left unstimulated or were stimulated with 100 or 250 μg/ml MSU crystals and DNA release was measured in presence of the membrane-impermeable DNA-binding dye, Sytox Orange. DNA release over 4 hours was presented as either **A)** endpoint values (mean+/-S.E.M., n=3) or **B)** kinetic data (one representative). Fluorescence data were normalized on the maximal signal obtained by stimulation with 100 nM PMA. RFU, relative fluorescence unit; MSU, monosodium urate; UT, untreated; PMA, phorbol myristate acetate; n.s., not significant; ***, $p<0.001$; ****, $p<0.0001$.

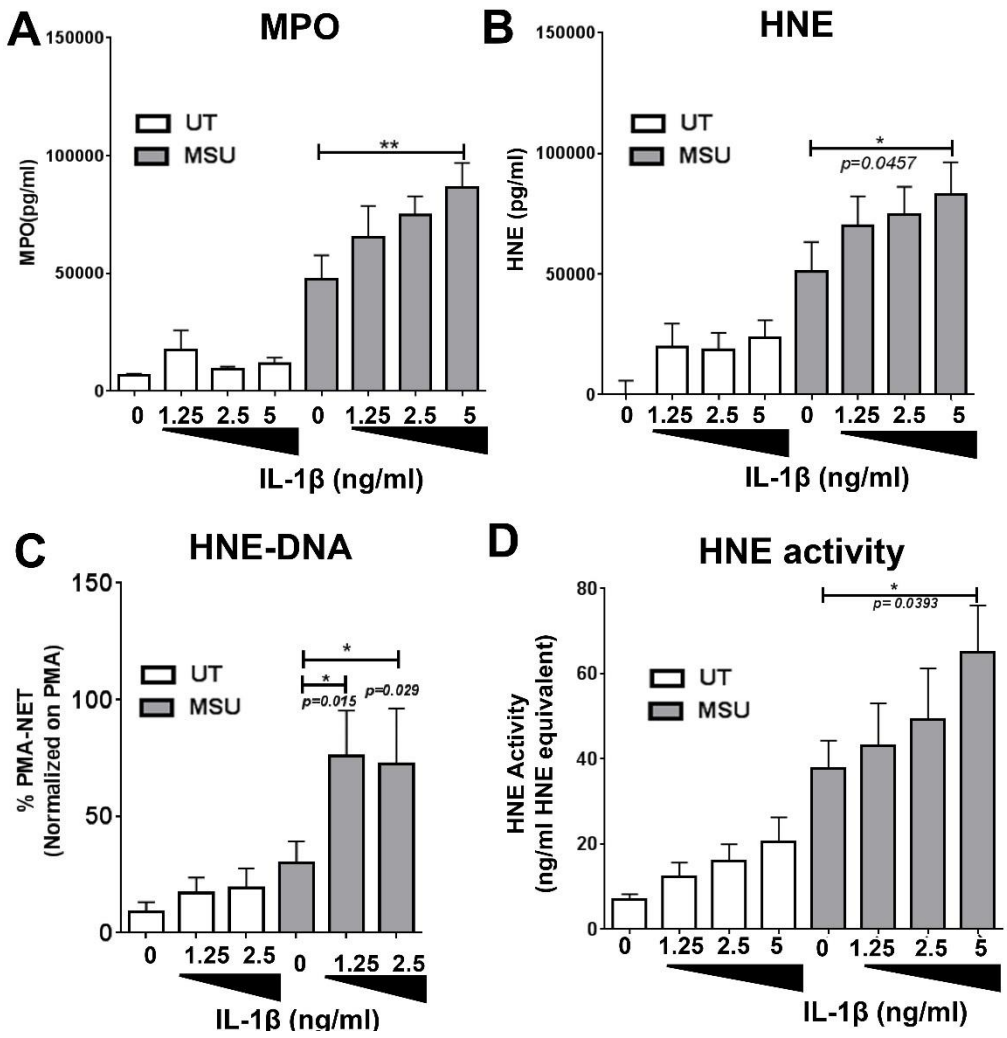

Figure 4.4. IL-1β enhances MSU crystal-stimulated releases of MPO, HNE and NETs from human neutrophils. Human neutrophils were treated with recombinant human IL-1β (0-5 ng/ml) prior to addition of 250 μg/ml MSU crystals. Neutrophils were also left unstimulated (UT, no crystals). Five hours later the following parameters were quantitated in the supernatants: **A)** MPO by commercial ELISA (n=5), **B)** HNE by ELISA (n=9), **C)** NETs (HNE-DNA ELISA, n=7) and **D)** HNE activity by commercial kit (n=7). NET release values were normalized on PMA (100%). Data are shown as mean+/-S.E.M. Significance was calculated using Dunnett's test. *, $p<0.05$; **, $p<0.01$. MPO, myeloperoxidase; HNE, human neutrophil elastase; PMA, phorbol myristate acetate.

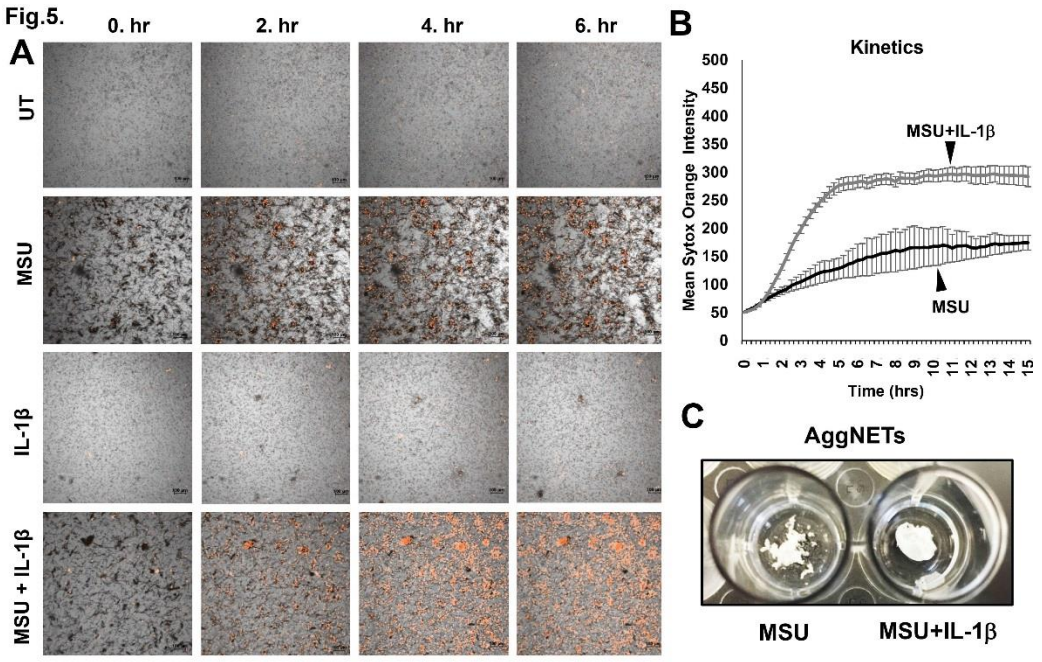

Figure 4.5. IL-1β increases MSU crystal-induced aggregated NET formation. 250,000 human PMNs/well were incubated in wells of a 96-well microplate with IL-1β (10 ng/ml) and stimulated with 100 μg/ml MSU crystals or 100nM PMA for 15 hours in presence of the extracellular DNA-binding dye, Sytox Orange. Interactions of PMNs and crystals were followed using confocal microscopy every 15 minutes. **A)** Representative images taken at t=0, 2, 4, 6. hrs are shown (n=3, 10X). **B)** Representative kinetics of Sytox Orange fluorescence followed for 15 hours (n=3, mean+/-S.D. at each time point) **C)** AggNET formation was evaluated by light microscopy after a 5-hour incubation of human PMNs with 1 mg/ml MSU crystal in presence or absence of 10 ng/ml human IL-1β (One representative image, n=3). MSU, monosodium urate; aggNET, aggregated NETs.

CHAPTER 5

CONCLUSIONS

NET formation has gained a lot of attention in the last 12 years [59] and rightfully so, as NETs are pertinent to several diseases like cystic fibrosis, systematic lupus erythematous, rheumatoid arthritis and gout [50, 59, 82, 85, 87, 88, 96, 105, 188-190, 192, 193, 209]. In order to study NETs and explore the NET formation mechanism further, a precise, quantitative laboratory-based detection technique with high specificity is required. An accurate as well as a high throughput NET detection technique had been missing until we devised a scheme to quantitate NETs and to perform follow up semi-quantitative assays to evaluate NET formation [86]. The mere detection of NET-associated granule proteins such as HNE and MPO in supernatants/ samples is not sufficient to assign ecDNA an identity as NETs. It is the association of ecDNA with HNE or MPO that confirms the presence of NETs [86]. Previously, this association has been demonstrated by co-localization of ecDNA with MPO or HNE by microscopy [60, 133]. In light of this information, we tried to fulfill this gap in detection by our NET-ELISA assays [86]. Yoo *et al.*, and Sil *et al.* have validated the application of this approach *in vitro* in PMN supernatants [50, 82] and clinical samples (Sil & Rada, J. Immunol., under revision) as well.

Once a standard method for NET detection had been established [86], we started with NET detection in SF of gout and Osteoarthritis (OA) patients (Sil P. and Rada B., J.Immunol., under revision). Gout results from an auto-inflammation, caused by the deposition of MSU crystals in SF, which consequently triggers NETs [7, 23, 39, 40, 277]. OA serves as a good control as it is a non-crystal driven joint inflammation [221]. The dynamics of the gout attack and resolution is not

very well studied and the role of NETs in the process is unclear [1-3]. So far the literature advocates that NETs are responsible for the unnecessary inflammation in the sterile joints [23]. Our data introduces a new mechanism that requires the P2Y6 pathway in MSU crystal-induced NETosis (data unpublished). Using MRS2578, a specific inhibitor for P2Y6, we showed that the MSU crystal-induced neutrophil activation is inhibited by obliterating NET formation, MPO and HNE release, ROS release, migration and intracellular calcium (Sil and Rada, J.Immunol., under revision).

Additionally, we uncovered the underlying roles of macrophages and IL-1β in exaggerating MSU crystal-induced NET formation. Macrophages are the other cell types found in the synovium that interact with MSU crystals and releases IL-1β [49]. IL-1β stimulates the influx of neutrophils at the site of inflammation and it is the hallmark of the acute gout phase [11, 25, 282]. Schauer *et al.* showed that the accumulation of IL-1β along with serine proteases, ROS, ATP and lactoferrin set the stage for anti-inflammatory processes to form aggNETs, which are in turn indicative of the beginning of the resolution phase in gout [23, 29]. A combination of both IL-1β and other macrophage mediators present in the synovium (as listed in Table 3) can potentially enable a more aggressive MSU crystal-induced formation of NETs (Sil & Rada., Infl. Research., under revision) [2, 3, 6, 5, 24, 38, 83, 51, 56, 269]. The onset of the resolution phase is marked by an increase in serine proteases, ROS and ATP, resulting in the emergence of aggNETs and M2 anti-inflammatory macrophages in the synovium [6, 25, 29, 35, 39, 120, 202, 205-208].

Below is a summary of our novel NET detection procedure and the two pathways that augment MSU crystal-induced NET pathways:

1. Characterization of NETs

NETs are a unique mechanism to entrap and disarm foreign particles. Until now, there has been a lack of methodologies that can effectively validate NET formation. Previously used methods included immunofluorescence assays, microscopic evaluation and measurement of the diameter of the NETosing PMNs using image J [133, 143, 144, 300-303]. Kraaji *et al.* also recently showed a 3-D imaging-based NET detection, HNE detection and histone citrullination technique using confocal microscopy [137]. Here we are describing a non-imaging-based detection method that is not only more economical, but also less tedious, time consuming and less susceptible to human errors. Figure 5.1 shows a summary of our high throughput NET quantitation with Sytox Orange assay, NET marker detection, and semi-quantitative NET ELISA. Together they validate NET formation by various stimuli, such as bacteria, fungi and MSU crystals [187]. Our first goal was to determine the amount of ecDNA released by PMNs, which is represented by the fluorescence of the Sytox Orange [187]. Our next approach was to determine the amount of HNE and MPO in the neutrophil supernatants [50, 82, 87]. To ensure that the ecDNA release was indeed resulting from NET formation, we modified our NET marker detection ELISA (MPO and HNE ELISA) to detect MPO-DNA or HNE-DNA complexes [187]. The supernatants subjected to limited digestion in a controlled manner ensured the formation of NET-DNA complexes, which was the central to the detection [82]. Limited ecDNA digestion by DNase helps in obtaining fragments of MPO-DNA or HNE-DNA complexes and also ensured standardized handling of NETs [187]. MPO or HNE-associated with ecDNA is the hallmark of NET formation, since MPO or HNE alone is not enough to verify the presence of NETs [58, 60, 70, 82]. To remedy this, HNE or MPO co-localization with ecDNA was detected by microscope-based immunofluorescence (IF) techniques. This method detects about 10-20 ng/ml of NET-DNA in PMN supernatant samples. However, it

requires fixation of the samples, which is prone to artifacts and requires finesse while performing the protocol. NETs are extremely delicate and fragile structures that must be carefully handled to ensure they remain intact while performing immunofluorescence. The DNA detection range for NET ELISA is around 10-20 ng/ml DNA as shown in Figure 2.5 B that allows us to accurately detect NETs not only in PMN supernatants but also in clinical samples. Our method has provided a new dimension to quantify NETs and also a substantially less cumbersome process to evaluate precious clinical samples, which is not possible with an image-based detection method [86].

2. Role of P2Y6R–SOCE-IL-8 axis in MSU crystal-induced NET formation

Dying of PMNs by NETosis causes release of many nucleotides such as ATP, ADP, UDP and UTP [91, 151, 210]. These nucleotides start a cascade of various inflammatory pathways, including purinergic signaling pathways [151-153, 264]. PMN migration, superoxide production, inflammasome activation have been associated with purinergic signaling pathways [236, 264, 304-306]. Uratsuji *et al.* showed that the MSU crystals use P2Y6 receptor to induce an inflammatory pathway in THP1 cells and keratinocytes [155]. This inspired us to investigate the role of P2Y6R in MSU crystal-induced NET formation. We found that MRS2578, a specific antagonist for P2Y6R, not only inhibited NET formation, but also other neutrophil functions such as primary granule proteins (MPO and HNE) release, NADPH oxidase-dependent ROS release, intracellular calcium signaling, migration, and IL-8 release (Sil & Rada, J. Immunol., under revision) (Figure 5.2) [184, 186]. These functions are not limited to NET formation, they are also required for regular neutrophil homeostasis [55].

Calcium signaling and mobilization are crucial for PMN migration and IL-8 release [110]. P2Y6R is a G-protein-coupled receptor (GPCR), which uses SOCE for signaling and is linked to IL-8

signaling [155-157, 169, 181-186, 216, 218, 220, 255, 307, 308]. Thus, it becomes imperative to study the P2Y6 receptor in conjunction with SOCE and intracellular calcium signaling pathways [157, 218]. Future studies must be performed with the MRS2578 and SK&F9678 (SOCE inhibitor), with regards to IL-8 signaling and NETosis to understand its mechanism of action. Sil and Rada (J. Immunol., under revision) demonstrated the principal association between SOCE and P2Y6R in MSU crystal-induced NETosis in their study, showing that SOCE and intracellular calcium are indispensable in the mentioned pathway. Pharmacological agents can modulate calcineurin and NFAT 2 in PMNs. There are several studies suggesting that mTOR pathway is not utilized in the PMA, IL-8 and ionomycin-induced NETosis process [251]. PMA-induced NET formation is independent on calcium and calcineurin, and is not affected by SK&F96365 [251]. In the present study, we suggest that Orai1 and STIM1 are both required for MSU crystal-induced NET formation in PMNs. SK&F96365 (inhibits STIM1 and TRP channels required for the SOC entry) reduces release of ecDNA, IL-8, MPO, HNE and HNE-DNA from human PMNs. Our data suggests that both the pharmacological agents may work upstream of the 'NADPH oxidase and superoxide production' factory.

Bearing in mind that MRS2578 inhibited PMA-induced NETosis, ROS production, and IL-8 release, it should probably be considered that MRS2578 is a universal anti-NETosis agent and disrupts NADPH oxidase activity (Sil & Rada, J. Immunol., under revision). We have shown in chapter 3 that MRS2578 at 10 μM is not toxic to PMNs (Sil & Rada, J. Immunol., under revision). Exploring MRS2578, or other analogous NET suppressive agents, will present multiple utilities in treating not only gout but also rheumatoid arthritis, lupus and cystic fibrosis. Allopurinol, colchicine and anti-IL-1β therapies are the most regularly prescribed medications in the field of gout [309]. However, these medications are suboptimal and have several side effects [4, 45, 46].

Inflammation in gout is driven mainly by PMNs [11, 24, 25, 34, 35]. NETs are abundant in the synovial environment and our data show that the NET formation can be completely ablated by using the P2Y6 antagonist, MRS2578. PMN activity can be retarded by MRS2578, thus, it can be a potential therapeutic strategy for gout.

Studying the extent and potential of this receptor is essential to understanding the mechanism of neutrophil activation [155]. Diseases abetted by neutrophil invasion could be avoided by using this P2Y6 receptor antagonist. Future studies investigating the untapped therapeutic advantage of this receptor may be beneficial in treating neutrophil driven diseases.

3. Role of IL-1β in exaggerating the MSU crystal-induced NET formation

Activation of inflammasome pathways and IL-1β by MSU crystals in macrophages has been studied extensively [40, 275, 279, 310, 311]. Resident macrophages in the synovium are the first cell type to come in contact with MSU microcrystals [1, 2, 292]. These microcrystals then activate the inflammasome pathway in the macrophages, which results in production of proinflammatory cytokines such as IL-1β and IL-18 [3, 40]. Release of IL-1β and IL-18 coerces neutrophils to meander to the synovium following the chemotactic gradient, where the neutrophils encounter crystals and undergo NETosis [1-3, 7, 29]. In gout, IL-1β is the main culprit causing joint inflammation [1, 2, 11, 17, 24, 25, 179].

We present our novel observation that NETosis, as well as NET markers in PMNs (stimulated with MSU crystals), are both enhanced in macrophage conditioned media (Sil & Rada., Infl. Research., under revision). Our data reflects that macrophages that have been stimulated with MSU crystals secrete mediators, which exaggerate NET response in neutrophils (Sil & Rada., Infl. Research.,

under revision). IL-1β, being our prime suspect, lead us to investigate its influence on MSU crystal-induced NET formation. In acute gouty synovium, macrophages produce inflammatory mediators including IL-1β due to the presence of MSU crystals [40, 49]. These mediators, mentioned in Table 2 and 3, then evoke a proinflammatory response by summoning more neutrophils to the site [40, 49]. Our *in vitro* model (Figure 5.3) shows the interactions exclusively between PMNs and macrophages, and it also provides an insight into modulating the system to our advantage. Further investigating the role of IL-1β in the MSU crystal-induced NET response, we show that IL-1β is responsible for the exaggerated NET formation observed in these situations [23, 25]. As the proinflammatory cytokines including IL-1β increase in the synovium, more neutrophils are attracted and they start infiltrating the site [34, 35]. The increasing numbers of these neutrophils along with preexisting MSU crystals start amassing to form aggNETs [23, 25]. The major component of aggNETs is migration of the PMNs towards the nearest conglomeration of PMN-MSU crystals [23, 25]. High concentration of IL-1β and PMNs kick-starts the accumulation of serine proteases, ATP and lactoferrin [23, 25]. As a result, this fosters aggNET formation, commences the resolution phase by initiating the steps to form tophi and arrests the ongoing inflammation [23, 25].

Reber *et al.* showed that mast cell-derived IL-1β contributed to acute inflammation caused by MSU crystals in mice [44]. Thus, other IL-1β releasing cell types (such as mast cells, dendritic cells and neutrophils) present in the synovium potentially play a role in driving inflammation along with macrophage-derived IL-1β [44]. Sil & Rada, (Infl. Research., under revision) show that NET and aggNET formation stimulated with MSU crystals are expedited in the presence of IL-1β. IL-1β increases ecDNA release, NET marker release (MPO and HNE protein) and HNE-DNA association. AggNETs are formed in a matter of 4-5 hours. Our data indicates that IL-1β is altering

the NET induction pathway and it shows a possible means by which macrophage-derived IL-1β further contributes to inflammation in the synovium in early gout stages. IL-1β induces ROS production, mediates PMN motility and increases PMN infiltration in the synovium [312-314]. However, Yan *et al.* showed that IL-1 β-MYD88 axis and NADPH oxidase-mediated ROS pathways can regulate neutrophil migration independently in zebrafish injury-induced inflammation model [296, 315]. IL-1β upregulates the NADPH oxidase 2/ ROS signaling, which activates MAPKs, NF-κB and AP-1 [312, 316]. This causes induction of metalloproteinase -9 (MMP-9) expression, which can sway the cells to migrate [312, 316]. Bradley *et al.* showed that MMP-9 increases neutrophil migration in airways infected by influenza virus [317]. MMP-9 is also abundant in the NETosing DNA of RA and lupus patients [318, 319]. The macrophage-derived IL-1β can potentially upregulate MMP-9 expression, causing enhanced NET induction by MSU crystals in PMNs. To verify this, future experiments are needed to investigate the involvement of MMP-9 in exaggerated NET induction and accelerated migration in the presence of IL-1β. Additionally, macrophage-derived IL-1β mediates inflammatory processes and migration by upregulating NF-κB activation in gout [34, 35].

Our finding confirms that there is a distinct association between MSU crystal-induced NETosis and IL-1β [34, 35]. Therefore, we are able to provide additional evidence as to why IL-1β inhibition strategies are effective in mitigating gouty inflammation [2-4, 116]. IL-1β and NETs have been implicated in various other diseases like rheumatoid arthritis, atherosclerosis, systemic inflammatory response syndrome (SIRS) [241] . Understanding the mechanism of how IL-1β is able to influence the NET pathway could help to advance therapeutic strategies to counter other IL-1β-mediated disorders.

Implications

The work shown here is a step-up from the previous image-based detection methodologies [86, 133, 137, 144]. Our high-throughput NET detection technique will improve diagnosis of NETs in *in vitro* PMN supernatants and clinical samples [86]. Yoo *et al.* established a simpler method to detect NET formation [82]. This approach will not only be valuable to understand the mechanism of NET formation, but it will also prove beneficial to explore the role of various players in the pathway.

Our novel finding demonstrates that the P2Y6-SOCE-IL-8 axis has a role to play in the MSU crystal-induced NET pathway (Sil & Rada., J. Immunol., under revision). We also show that macrophage-derived IL-1β enhances NET formation (Sil & Rada., Infl. Research., under revision). Combined therapeutic strategies with anti-IL-1β treatment and P2Y6 blockage could show promise for improving the current state of gout care. Allopurinol and colchicine are favored treatments for gout, however, they come with severe side effects and do not provide long term relief [1, 2, 179, 203]. IL-1β neutralizing antibody (canakinumab), IL-1R (rilonacept) antagonist and anti-IL-1β receptor targeting strategies (anakinra) are commonly used for gout treatment and are being tested in clinical trials to improve efficacy [4, 34, 35, 45, 47, 119, 282]. We envision a double-pronged approach, involving both neutrophil inactivation, as well as IL-1β neutralization, which will likely help in more effectively resolving the chronic inflammation, with fewer side effects.

Appendices:

TABLE 1.–List of the reagents used for NET ELISA

Materials

Name	Company	Catalog Number	Comments
Anti-Human Neutrophil Elastase Rabbit Ab	Calbiochem	481001	1:2,000x coated
Anti-Myeloperoxidase Ab (Rabbit)	Millipore	07-496	1:2,000x coated
DNase-1	Roche	10-104-159-001	1 µg/ml used for digestion
20 mM EGTA/ PBS	Sigma-Aldrich	E3889-25G	
2.5 mM EGTA/PBS	Sigma-Aldrich	E3889-25G	
Cell death detection ELISA Anti-DNA POD	Roche	11544675001	1:500x
Eon Microplate Spectrophotometer	Biotek		
Gen5 All-in-One microplate software	Biotek		analytical tool (ELISA)
Sytox orange	Life Technology	S11368	0.2% final concentration/volume
1 M Hepes	Cellgro	25-060-CI	Use 10 mM final concentration.
1 M glucose	Sigma		Use 5 mM final concentration.
HBSS	Corning	21-023-CM	
Varioskan Flash Ver.2.4.3	Thermoscientific		
PMA	Sigma	P 8139	100 nM final used
ELISA Plate	Greiner bio-one	655061	
Conical tubes 15 ml	Thermoscientific	339650	
Conical tubes 50 ml	Thermoscientific	339652	
Percoll (pH 8.5 - 9.5)	Sigma	P 1644	Sodium Chloride, Sigma, S7653-250G
Dextran	Spectrum	D1004	
RPMI 1640 media	Corning Cellgro	17-105-CV	
96 well assay plate black plate clear bottom	Costar	3603	

Table 2. Cytokines and Chemokines released by macrophages stimulated by MSU crystals

Cytokines or Chemokines	**Role in gout**	**Source**	**Reference**
IL-18	Inflammation, neutrophil activation and chemotaxis	Macrophages	[40]
TNFα	Cellular activation, neutrophil apoptosis, endothelial adhesion (E selectin), phagocytosis	Macrophage, monocytes	[2, 35, 50, 280]
IL-6	Role N/R in gout , proinflammatory cytokine	Macrophage, monocytes	[2, 11, 280]
G-CSF	Neutrophil survival and proliferation	Macrophages	[10, 11]
IL-8	Potent chemoattractant	Macrophages	[11, 12]
CXCL1 / KC	Neutrophil chemotaxis	Macrophages	[2, 280]
CCL2	Monocyte chemotaxis	monocyte	[2, 280]
CCL3/ MIP	Neutrophil chemotaxis	Monocyte, macrophage	[2, 280]
TGFβ	Inflammation Resolution-ingestion of apoptotic neutrophils, secretes IL-1RA[6]	Macrophage	[1, 35]
IL-10	Inflammation Resolution	Macrophage	[1, 35]
Other Mediators	**Actions contributing to gouty inflammation**	**Produced by**	**Reference**
C5a	Neutrophil recruitment	Macrophages	[35]
MIP 1α (mouse)	Activates neutrophils	Macrophages	[280]
Triggering receptor expressed on myeloid cells 1 (TREM-1)	TREM-1 amplifies inflammatory responses initiated by TLRs	Macrophages, Neutrophils	[320]
Leukotrienes (LTB4)	ROS production via MSU driven NLRP3 pathway	Macrophage	[35, 178]
Peroxisome proliferator-activated receptor (PPAR-γ)	Reduces the expression of TNFα, IL-6, IL-8, iNOS, gelatinase B, scavenger receptor A & COX-2	Monocytes, Macrophages	[7, 11, 28, 320]
Liver X receptor (LXR) α	Works with PPARγ to resolve inflammation in joint	Macrophages	[320]

Myeloid related proteins (MRP-8/S100A8, MRP10-S100A9)	Calcium binding protein upregulate inflammation	Monocytes, Neutrophil	[28]
Lipid mediators (resolvins, protectins, lipoxins, maresins, prostaglandins – PGD2/ PGJ2)	Resolves inflammation, limits neutrophil trafficking, enhances apoptosis by macrophages	Macrophages	[6]

Table 3. Mediators enhancing NET formation

Macrophage Mediator	Release by MSU crystal triggered macrophage	Promotes NETs	Species/ cells	Concentration	Elevate level in Gout synovial fluid (SF)	Elevate level in Gout Serum
IL-1RA	Yes [3, 6], neutrophils also produce them [5, 29]	N/R, present in AggNETs [24]	Human [29]		IL-1RA is high in the synovial fluid [6]	-
TNFα	Yes [2, 38, 269]	Yes [51, 83]	HUVEC cell line and Large white pigs [308] , murine air pouch model [309], Human monocytes in-vitro [41] Murine crystal-induced ankle arthritis model [269]	Approx. 350 pg/ml in-vitro Human monocytes [41], 6.0 pg/ml mice ankle [269]	Present in joint fluid [2, 4], Soluble TNFR1 and II inhibits TNFα [5, 26], In-vivo presence of TNF-α in Pig monoarthritis model [37, 308].	-
IFN-γ	No	Yes [83]				
IL-6	Yes [2, 38, 269]		Murine air pouch model [309],Human monocytes in-vitro [41], Murine crystal-induced ankle arthritis model [269]	Approx. 225 pg/ml in-vitro Human monocytes [41] , Mice ankle -150.1 pg/ml [269], Mice serum -33.2 pg/ml [269]		Soluble proinflammatory IL-6R is high in serum of Gout patients. sIL-6R/IL-6 complex are formed. [6]
G-CSF	Yes [2, 38, 269]	Yes [56]	Murine crystal-induced ankle arthritis model [269]	Mice ankle – 261.7 pg/ml [269], Mice serum – 334.2 pg/ml [269]		
IL-8	Yes [2, 38, 269]	Yes[51, 83, 310], present in AggNETs [24]	Rabbit [37], Mouse [269]and Human		Rabbit synovial fluid [37] CXCR2/ IL-8 R in mice synovium [37]	
CXCL1 / KC	Yes [2, 269]		Murine crystal-induced ankle arthritis model [269]	Mice ankle – 608.8 pg/ml [269], Mice serum – 80.1 pg/ml [269]		
CCL2	Yes [2, 269]		Murine crystal-induced ankle arthritis model [269]	Mice ankle –638.3 pg/ml [269]		
CCL3/ MIP	Yes [2, 269]		Murine crystal-induced ankle arthritis model [269]	Mice ankle – 494.4 pg/ml [269]		
TGFβ	Yes [2, 3, 38, 269, 307]	N/R				
IL-10	Yes [2, 36, 38, 269]	N/R	Murine Air pouch model [12]		Inhibits MSU crystal produced TNFα [6]	
C5a	Yes [1]	Yes, once neutrophils are primed with Type I and II IFN [83]			High levels of complement split product found in the synovium [37]	Complement proteins like C1,C2, C3, C4, C5 and factor 8 is high in patient sera [37]
TREM-1	Yes [307]		Murine air pouch model [307, 309]			
LTB4	Yes [162]		Murine Gout model [162]		Mice synovium [162]	
MRP-8/S100A8, MRP10-S100A9 & S100A8/A9	Yes [29]		Mice and Human [29]		Patient Synovial fluid [29]	
MIP 1α	Yes [2]					
Nuclear hormone receptors (PPAR-γ and LXR-α)	Yes [12, 307]		Murine air pouch model [307]			
Lipid mediators (resolvins, protectins, lipoxins, maresins, prostaglandins –PGD2/ PGJ2)	Yes -lipoxin[12]				-	-

Figure 5.1. Methods involving NET detection.

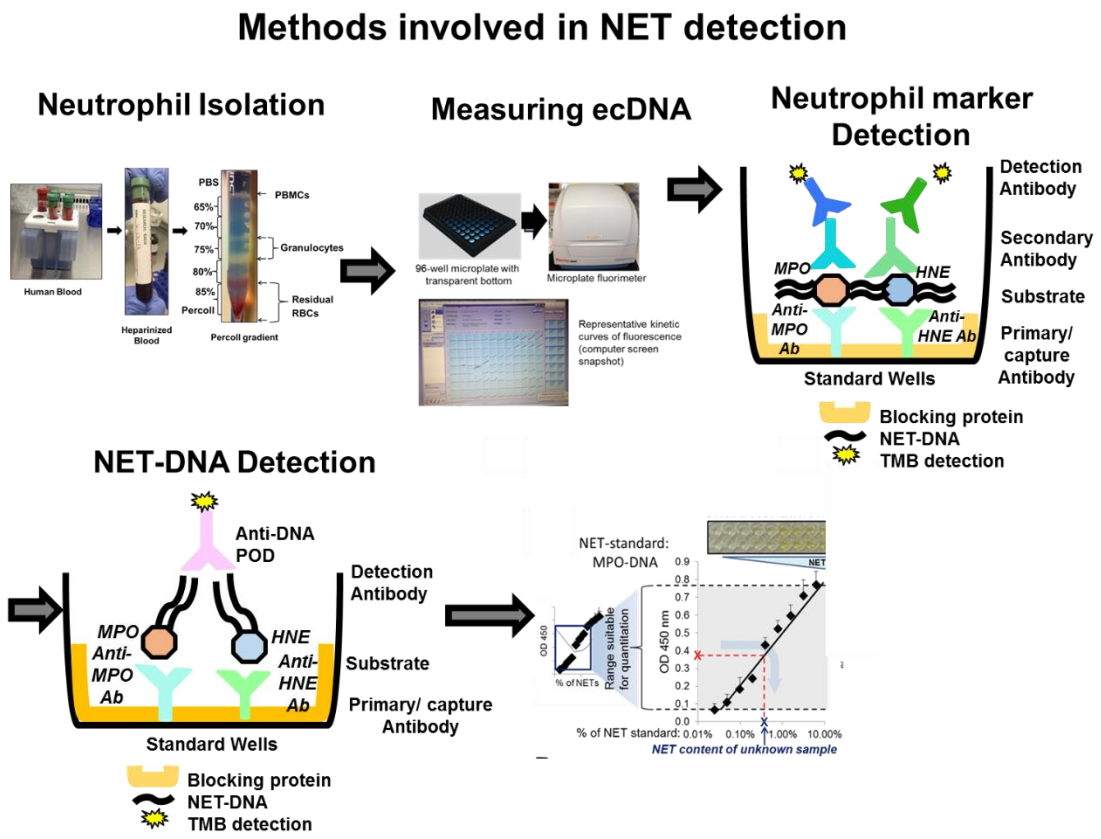

Figure 5.1. : The neutrophils are isolated by 5-step percoll gradient. Isolated neutrophils are then stimulated with NET inducers and in presence of Sytox Orange dye ecDNA is measured (Chapter 2). To confirm the presence of NETs, we then use MPO and HNE ELISA to detect the production of NET markers-HNE and MPO. Finally, we use our NET-ELISA to confirm the presence of MPO-DNA and HNE-DNA complexes. Data analysis was performed by obtaining the optical density at 450 nm.

Figure 5.2. MSU crystal-stimulated PMNs utilizes the P2Y6R-SOCE-IL-8 axis to form NETs.

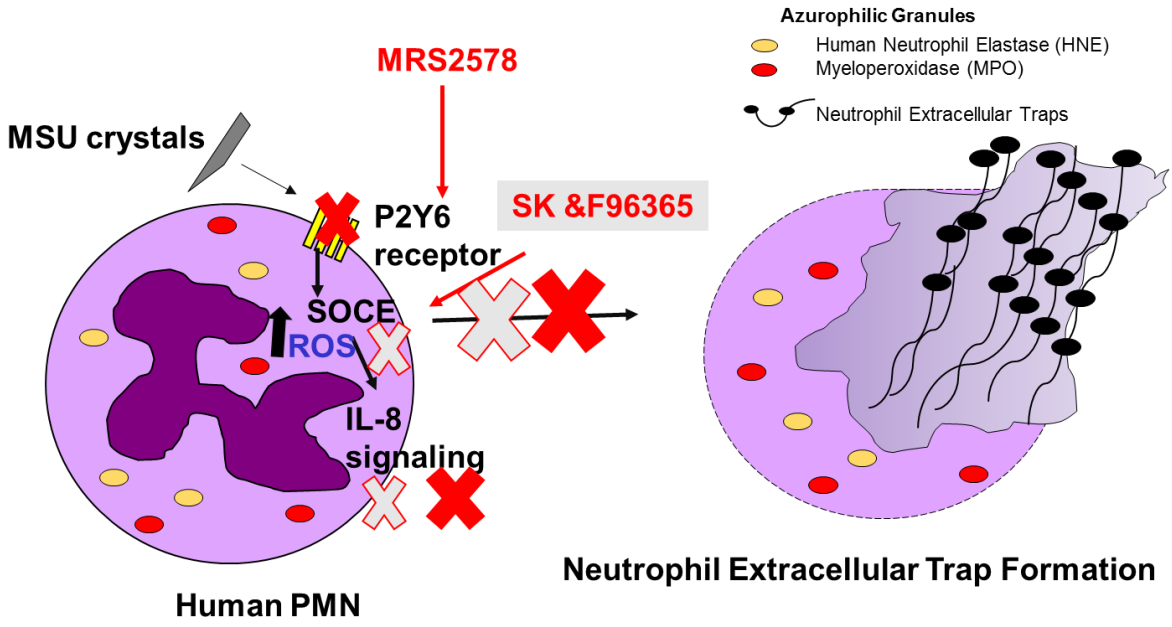

Figure 5.2.: Sil and Rada, J. Immunol., under revision shows that PMNs when stimulated with MSU crystals produced NETs (Chapter 3). NET production is obliterated by MRS2578. MRS2578 simultaneously also inhibits ROS production, SOCE, intracellular calcium, HNE and MPO release, and IL-8 signaling. Thus, we conclude that MSU crystal-induced NETs uses the P2Y6-SOCE-IL-8 axis and is NADPH-oxidase-dependent.

Figure 5.3. IL-1β derived from macrophages increases NET formation in MSU crystal-stimulated neutrophils.

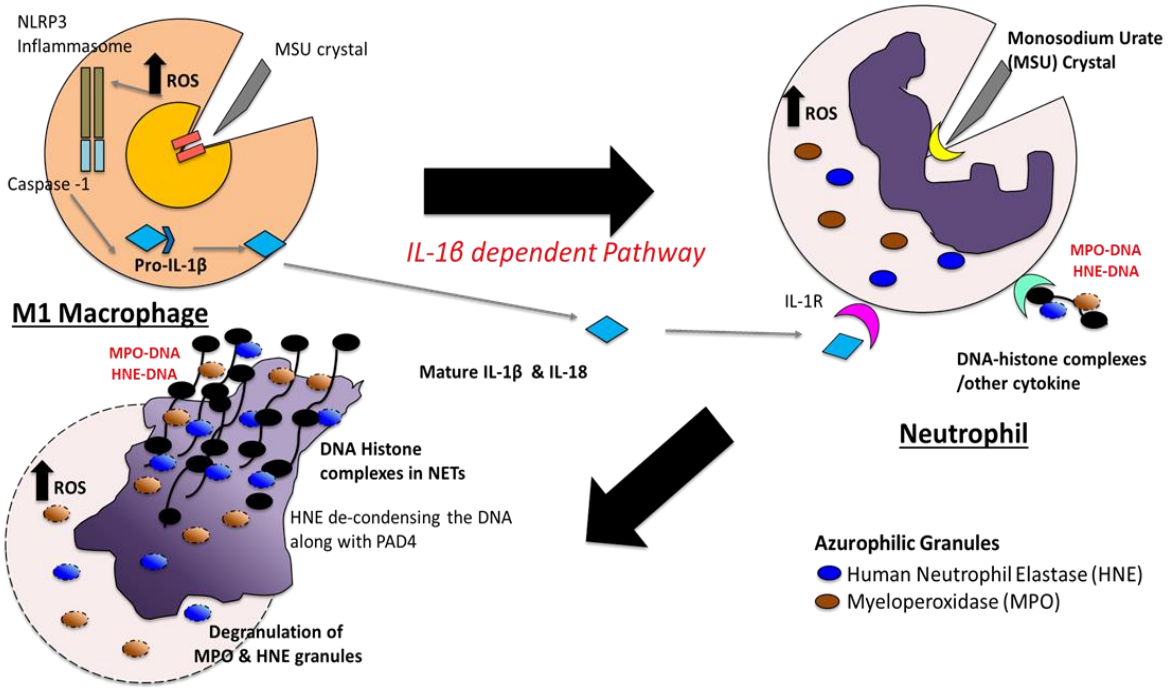

Figure 5.3. PMNs show enhanced NET production in presence of macrophages as shown in chapter 4 (Sil & Rada, Infl. Research., under revision). One of the macrophage mediators released by MSU crystals is IL-1β that also enhances MSU crystal-triggered NET formation.

REFERENCES:

1. Busso, N. and H.K. Ea, *The mechanisms of inflammation in gout and pseudogout (CPP-induced arthritis).* Reumatismo, 2011. **63**(4): p. 230-7.
2. Busso, N. and A. So, *Mechanisms of inflammation in gout.* Arthritis Res Ther, 2010. **12**(2): p. 206.
3. Busso, N. and A. So, *Microcrystals as DAMPs and their role in joint inflammation.* Rheumatology (Oxford), 2012. **51**(7): p. 1154-60.
4. Cronstein, B.N. and R. Terkeltaub, *The inflammatory process of gout and its treatment.* Arthritis Res Ther, 2006. **8 Suppl 1**: p. S3.
5. Martin, W.J., et al., *Monosodium urate monohydrate crystal-recruited noninflammatory monocytes differentiate into M1-like proinflammatory macrophages in a peritoneal murine model of gout.* Arthritis Rheum, 2011. **63**(5): p. 1322-32.
6. Steiger, S. and J.L. Harper, *Mechanisms of spontaneous resolution of acute gouty inflammation.* Curr Rheumatol Rep, 2014. **16**(1): p. 392.
7. Popa-Nita, O. and P.H. Naccache, *Crystal-induced neutrophil activation.* Immunol Cell Biol, 2010. **88**(1): p. 32-40.
8. Zumelzu, C., et al., *Black patients of African descent and HLA-DRB1*15:03 frequency overrepresented in epidermolysis bullosa acquisita.* J Invest Dermatol, 2011. **131**(12): p. 2386-93.
9. Rees, F., M. Hui, and M. Doherty, *Optimizing current treatment of gout.* Nat Rev Rheumatol, 2014. **10**(5): p. 271-83.

10. Zhu, Y., B.J. Pandya, and H.K. Choi, *Prevalence of gout and hyperuricemia in the US general population: the National Health and Nutrition Examination Survey 2007-2008.* Arthritis Rheum, 2011. **63**(10): p. 3136-41.

11. Choi, H.K., et al., *Pathogenesis of gout.* Ann Intern Med, 2005. **143**(7): p. 499-516.

12. Jelley, M.J. and R. Wortmann, *Practical steps in the diagnosis and management of gout.* BioDrugs, 2000. **14**(2): p. 99-107.

13. Shi, Y., A.D. Mucsi, and G. Ng, *Monosodium urate crystals in inflammation and immunity.* Immunol Rev, 2010. **233**(1): p. 203-17.

14. Hak, A.E., et al., *Menopause, postmenopausal hormone use and risk of incident gout.* Ann Rheum Dis, 2010. **69**(7): p. 1305-9.

15. Khandpur, R., et al., *NETs are a source of citrullinated autoantigens and stimulate inflammatory responses in rheumatoid arthritis.* Sci Transl Med, 2013. **5**(178): p. 178ra40.

16. Khandpur, S., A.K. Minz, and V.K. Sharma, *Chronic tophaceous gout with severe deforming arthritis.* Indian J Dermatol Venereol Leprol, 2010. **76**(1): p. 69-71.

17. Burns, C.M. and R.L. Wortmann, *Latest evidence on gout management: what the clinician needs to know.* Ther Adv Chronic Dis, 2012. **3**(6): p. 271-86.

18. Wang, J. and H. Arase, *Regulation of immune responses by neutrophils.* Ann N Y Acad Sci, 2014. **1319**: p. 66-81.

19. Singh, J.A., S.G. Reddy, and J. Kundukulam, *Risk factors for gout and prevention: a systematic review of the literature.* Curr Opin Rheumatol, 2011. **23**(2): p. 192-202.

20. Sivera, F., et al., *Multinational evidence-based recommendations for the diagnosis and management of gout: integrating systematic literature review and expert opinion of a*

broad panel of rheumatologists in the 3e initiative. Ann Rheum Dis, 2014. **73**(2): p. 328-35.

21. Merriman, T.R., *An update on the genetic architecture of hyperuricemia and gout.* Arthritis Res Ther, 2015. **17**(1): p. 98.
22. Allaeys, I., et al., *Osteoblast retraction induced by adherent neutrophils promotes osteoclast bone resorption: implication for altered bone remodeling in chronic gout.* Lab Invest, 2011. **91**(6): p. 905-20.
23. Schauer, C., et al., *Aggregated neutrophil extracellular traps limit inflammation by degrading cytokines and chemokines.* Nat Med, 2014. **20**(5): p. 511-7.
24. Chhana, A. and N. Dalbeth, *The gouty tophus: a review.* Curr Rheumatol Rep, 2015. **17**(3): p. 19.
25. Christine Czegley, M.B., Daniela Weidner, Markus Hoffmann, Martin Herrmann, and C. Schauer, *Monocytes and granulocytes orchestrate induction and resolution of inflammation in gout.* Gout and Hyperuricemia, 2014. **1**(3): p. 88-93.
26. Maueroder, C., et al., *How neutrophil extracellular traps orchestrate the local immune response in gout.* J Mol Med (Berl), 2015. **93**(7): p. 727-34.
27. Riva, M., et al., *Human S100A9 protein is stabilized by inflammatory stimuli via the formation of proteolytically-resistant homodimers.* PLoS One, 2013. **8**(4): p. e61832.
28. Liu-Bryan, R. and F. Liote, *Monosodium urate and calcium pyrophosphate dihydrate (CPPD) crystals, inflammation, and cellular signaling.* Joint Bone Spine, 2005. **72**(4): p. 295-302.
29. Pisetsky, D.S., *Gout, tophi and the wonders of NETs.* Arthritis Res Ther, 2014. **16**(5): p. 431.

30. Arai, Y., et al., *Uric acid induces NADPH oxidase-independent neutrophil extracellular trap formation.* Biochem Biophys Res Commun, 2014. **443**(2): p. 556-61.

31. Perez-Ruiz, F. and A.M. Herrero-Beites, *Crystal arthritis: Environment and genetics in gout: a maze for clinicians?* Nat Rev Rheumatol, 2014. **10**(1): p. 8-9.

32. Mohamed, A.A. and E. Matijevic, *Preparation and characterization of uniform particles of uric acid and its salts.* J Colloid Interface Sci, 2013. **392**: p. 129-36.

33. Stoiber, W., et al., *The Role of Reactive Oxygen Species (ROS) in the Formation of Extracellular Traps (ETs) in Humans.* Biomolecules, 2015. **5**(2): p. 702-723.

34. Mitroulis, I., et al., *Neutrophil extracellular trap formation is associated with IL-1beta and autophagy-related signaling in gout.* PLoS One, 2011. **6**(12): p. e29318.

35. Mitroulis, I., K. Kambas, and K. Ritis, *Neutrophils, IL-1beta, and gout: is there a link?* Semin Immunopathol, 2013. **35**(4): p. 501-12.

36. Schorn, C., et al., *Monosodium urate crystals induce extracellular DNA traps in neutrophils, eosinophils, and basophils but not in mononuclear cells.* Front Immunol, 2012. **3**: p. 277.

37. Aleyd, E., et al., *IgA enhances NETosis and release of neutrophil extracellular traps by polymorphonuclear cells via Fcalpha receptor I.* J Immunol, 2014. **192**(5): p. 2374-83.

38. Qiu, Y., et al., *The ABCG2 gene Q141K polymorphism contributes to an increased risk of gout: a meta-analysis of 2185 cases.* Mod Rheumatol, 2014. **24**(5): p. 829-34.

39. Pope, R.M. and J. Tschopp, *The role of interleukin-1 and the inflammasome in gout: implications for therapy.* Arthritis Rheum, 2007. **56**(10): p. 3183-8.

40. Martinon, F., et al., *Gout-associated uric acid crystals activate the NALP3 inflammasome.* Nature, 2006. **440**(7081): p. 237-41.

41. Schroder, K. and J. Tschopp, *The inflammasomes.* Cell, 2010. **140**(6): p. 821-32.

42. Tschopp, J. and K. Schroder, *NLRP3 inflammasome activation: The convergence of multiple signalling pathways on ROS production?* Nat Rev Immunol, 2010. **10**(3): p. 210-5.

43. Petrilli, V., S. Papin, and J. Tschopp, *The inflammasome.* Curr Biol, 2005. **15**(15): p. R581.

44. Reber, L.L., et al., *Contribution of mast cell-derived interleukin-1beta to uric acid crystal-induced acute arthritis in mice.* Arthritis Rheumatol, 2014. **66**(10): p. 2881-91.

45. Dalbeth, N., T.J. Lauterio, and H.R. Wolfe, *Mechanism of action of colchicine in the treatment of gout.* Clin Ther, 2014. **36**(10): p. 1465-79.

46. Paschke, S., et al., *Technical advance: Inhibition of neutrophil chemotaxis by colchicine is modulated through viscoelastic properties of subcellular compartments.* J Leukoc Biol, 2013. **94**(5): p. 1091-6.

47. Hainer, B.L., E. Matheson, and R.T. Wilkes, *Diagnosis, treatment, and prevention of gout.* Am Fam Physician, 2014. **90**(12): p. 831-6.

48. R., M., *GOUT: THE KING OF DISEASES AND THE DISEASE OF KINGS.* JOURNAL OF THE SIENA ACADEMY OF SCIENCES, 2012. **4**.

49. Martinon, F., *Mechanisms of uric acid crystal-mediated autoinflammation.* Immunol Rev, 2010. **233**(1): p. 218-32.

50. Pang, L., et al., *Pseudogout-associated inflammatory calcium pyrophosphate dihydrate microcrystals induce formation of neutrophil extracellular traps.* J Immunol, 2013. **190**(12): p. 6488-500.

51. Shelef, M.A., et al., *Peptidylarginine deiminase 4 contributes to tumor necrosis factor alpha-induced inflammatory arthritis.* Arthritis Rheumatol, 2014. **66**(6): p. 1482-91.

52. Zychowicz, M.E., R.S. Pope, and E. Graser, *The current state of care in gout: Addressing the need for better understanding of an ancient disease.* J Am Acad Nurse Pract, 2010. **22 Suppl 1**: p. 623-36.

53. Huffman, J.E., et al., *Modulation of genetic associations with serum urate levels by body-mass-index in humans.* PLoS One, 2015. **10**(3): p. e0119752.

54. Bardoel, B.W., et al., *The balancing act of neutrophils.* Cell Host Microbe, 2014. **15**(5): p. 526-36.

55. Mayadas, T.N., X. Cullere, and C.A. Lowell, *The multifaceted functions of neutrophils.* Annu Rev Pathol, 2014. **9**: p. 181-218.

56. Mullen, L.M., G. Chamberlain, and S. Sacre, *Pattern recognition receptors as potential therapeutic targets in inflammatory rheumatic disease.* Arthritis Res Ther, 2015. **17**(1): p. 122.

57. Oliveira, S.H., et al., *Neutrophil migration induced by IL-1beta depends upon LTB4 released by macrophages and upon TNF-alpha and IL-1beta released by mast cells.* Inflammation, 2008. **31**(1): p. 36-46.

58. Papayannopoulos, V., et al., *Neutrophil elastase and myeloperoxidase regulate the formation of neutrophil extracellular traps.* J Cell Biol, 2010. **191**(3): p. 677-91.

59. Brinkmann, V., et al., *Neutrophil extracellular traps kill bacteria.* Science, 2004. **303**(5663): p. 1532-5.

60. Metzler, K.D., et al., *Myeloperoxidase is required for neutrophil extracellular trap formation: implications for innate immunity.* Blood, 2011. **117**(3): p. 953-9.

61. Dohrmann, S., J.N. Cole, and V. Nizet, *Conquering Neutrophils.* PLoS Pathog, 2016. **12**(7): p. e1005682.

62. Sengupta, K., et al., *Spreading of neutrophils: from activation to migration.* Biophys J, 2006. **91**(12): p. 4638-48.

63. Zeillemaker, A.M., et al., *Neutrophil adherence to and migration across monolayers of human peritoneal mesothelial cells. The role of mesothelium in the influx of neutrophils during peritonitis.* J Lab Clin Med, 1996. **127**(3): p. 279-86.

64. Kuijpers, T.W., M. Hoogerwerf, and D. Roos, *Neutrophil migration across monolayers of resting or cytokine-activated endothelial cells. Role of intracellular calcium changes and fusion of specific granules with the plasma membrane.* J Immunol, 1992. **148**(1): p. 72-7.

65. Trevisan, G., et al., *TRPA1 receptor stimulation by hydrogen peroxide is critical to trigger hyperalgesia and inflammation in a model of acute gout.* Free Radic Biol Med, 2014. **72**: p. 200-9.

66. Klebanoff, S.J., *Myeloperoxidase: friend and foe.* J Leukoc Biol, 2005. **77**(5): p. 598-625.

67. Schultz, J. and H.W. Shmukler, *Myeloperoxidase of the Leucocyte of Normal Human Blood. Ii. Isolation, Spectrophotometry, and Amino Acid Analysis.* Biochemistry, 1964. **3**: p. 1234-8.

68. Branzk, N., et al., *Neutrophils sense microbe size and selectively release neutrophil extracellular traps in response to large pathogens.* Nat Immunol, 2014. **15**(11): p. 1017-25.

69. Urban, C.F., et al., *Neutrophil extracellular traps capture and kill Candida albicans yeast and hyphal forms.* Cell Microbiol, 2006. **8**(4): p. 668-76.

70. Stamp, L.K., et al., *Myeloperoxidase and oxidation of uric acid in gout: implications for the clinical consequences of hyperuricaemia.* Rheumatology (Oxford), 2014. **53**(11): p. 1958-65.

71. Geraghty, P., et al., *alpha1-Antitrypsin activates protein phosphatase 2A to counter lung inflammatory responses.* Am J Respir Crit Care Med, 2014. **190**(11): p. 1229-42.

72. Geraghty, P., et al., *Alpha-1-antitrypsin aerosolised augmentation abrogates neutrophil elastase-induced expression of cathepsin B and matrix metalloprotease 2 in vivo and in vitro.* Thorax, 2008. **63**(7): p. 621-6.

73. Geraghty, S., et al., *A novel, cryopreserved, viable osteochondral allograft designed to augment marrow stimulation for articular cartilage repair.* J Orthop Surg Res, 2015. **10**(1): p. 66.

74. Geraghty, P., et al., *Neutrophil elastase up-regulates cathepsin B and matrix metalloprotease-2 expression.* J Immunol, 2007. **178**(9): p. 5871-8.

75. McElvaney, N.G., *Diagnosing alpha1-antitrypsin deficiency: how to improve the current algorithm.* Eur Respir Rev, 2015. **24**(135): p. 52-7.

76. Amitani, R., et al., *Effects of human neutrophil elastase and Pseudomonas aeruginosa proteinases on human respiratory epithelium.* Am J Respir Cell Mol Biol, 1991. **4**(1): p. 26-32.

77. Chua, F. and G.J. Laurent, *Neutrophil elastase: mediator of extracellular matrix destruction and accumulation.* Proc Am Thorac Soc, 2006. **3**(5): p. 424-7.

78. Lucey, E.C., et al., *Effect of combined human neutrophil cathepsin G and elastase on induction of secretory cell metaplasia and emphysema in hamsters, with in vitro observations on elastolysis by these enzymes.* Am Rev Respir Dis, 1985. **132**(2): p. 362-6.

79. Sahoo, M., et al., *Neutrophil elastase causes tissue damage that decreases host tolerance to lung infection with burkholderia species.* PLoS Pathog, 2014. **10**(8): p. e1004327.

80. Sandhaus, R.A. and G. Turino, *Neutrophil elastase-mediated lung disease.* COPD, 2013. **10 Suppl 1**: p. 60-3.

81. Watorek, W., et al., *Neutrophil elastase and cathepsin G: structure, function, and biological control.* Adv Exp Med Biol, 1988. **240**: p. 23-31.

82. Yoo, D.G., et al., *NET formation induced by Pseudomonas aeruginosa cystic fibrosis isolates measured as release of myeloperoxidase-DNA and neutrophil elastase-DNA complexes.* Immunol Lett, 2014. **160**(2): p. 186-94.

83. Raptis, S.Z. and C.T. Pham, *Neutrophil-derived serine proteases in immune complex-mediated diseases.* Immunol Res, 2005. **32**(1-3): p. 211-5.

84. Matsuoka, T., et al., *Induction of pulmonary thromboembolism by neutrophil elastase in collagen-induced arthritis mice and effect of recombinant human soluble thrombomodulin.* Pathobiology, 2008. **75**(5): p. 295-305.

85. Rada, B., et al., *Pyocyanin-enhanced neutrophil extracellular trap formation requires the NADPH oxidase.* PLoS One, 2013. **8**(1): p. e54205.

86. Sil, P., et al., *High Throughput Measurement of Extracellular DNA Release and Quantitative NET Formation in Human Neutrophils In Vitro.* J Vis Exp, 2016(112).

87. Yoo, D.G., et al., *Release of cystic fibrosis airway inflammatory markers from Pseudomonas aeruginosa-stimulated human neutrophils involves NADPH oxidase-dependent extracellular DNA trap formation.* J Immunol, 2014. **192**(10): p. 4728-38.

88. Brinkmann, V., et al., *Neutrophil extracellular traps: how to generate and visualize them.* J Vis Exp, 2010(36).

89. Neeli, I. and M. Radic, *Opposition between PKC isoforms regulates histone deimination and neutrophil extracellular chromatin release.* Front Immunol, 2013. **4**: p. 38.

90. Neeli, I. and M. Radic, *Knotting the NETs: analyzing histone modifications in neutrophil extracellular traps.* Arthritis Res Ther, 2012. **14**(2): p. 115.

91. Kaplan, M.J. and M. Radic, *Neutrophil extracellular traps: double-edged swords of innate immunity.* J Immunol, 2012. **189**(6): p. 2689-95.

92. Radic, M. and M.J. Kaplan, *Extracellular chromatin traps interconnect cell biology, microbiology, and immunology.* Front Immunol, 2013. **4**: p. 160.

93. Remijsen, Q., et al., *Dying for a cause: NETosis, mechanisms behind an antimicrobial cell death modality.* Cell Death Differ, 2011. **18**(4): p. 581-8.

94. Baums, C.G. and M. von Kockritz-Blickwede, *Novel role of DNA in neutrophil extracellular traps.* Trends Microbiol, 2015. **23**(6): p. 330-1.

95. Hakkim, A., et al., *Activation of the Raf-MEK-ERK pathway is required for neutrophil extracellular trap formation.* Nat Chem Biol, 2011. **7**(2): p. 75-7.

96. Fuchs, T.A., et al., *Novel cell death program leads to neutrophil extracellular traps.* J Cell Biol, 2007. **176**(2): p. 231-41.

97. Kolaczkowska, E. and P. Kubes, *Neutrophil recruitment and function in health and inflammation.* Nat Rev Immunol, 2013. **13**(3): p. 159-75.

98. Urban, C.F., et al., *Neutrophil extracellular traps contain calprotectin, a cytosolic protein complex involved in host defense against Candida albicans.* PLoS Pathog, 2009. **5**(10): p. e1000639.

99. Carvalho, L.O., et al., *The Neutrophil Nucleus and Its Role in Neutrophilic Function.* J Cell Biochem, 2015.

100. Kawasaki, H., et al., *A protein with antimicrobial activity in the skin of Schlegel's green tree frog Rhacophorus schlegelii (Rhacophoridae) identified as histone H2B.* Biochem Biophys Res Commun, 2003. **312**(4): p. 1082-6.

101. Wang, Y., et al., *Human PAD4 regulates histone arginine methylation levels via demethylimination.* Science, 2004. **306**(5694): p. 279-83.

102. Rohrbach, A.S., et al., *Activation of PAD4 in NET formation.* Front Immunol, 2012. **3**: p. 360.

103. Leshner, M., et al., *PAD4 mediated histone hypercitrullination induces heterochromatin decondensation and chromatin unfolding to form neutrophil extracellular trap-like structures.* Front Immunol, 2012. **3**: p. 307.

104. Jones, J.E., et al., *Protein arginine deiminase 4 (PAD4): Current understanding and future therapeutic potential.* Curr Opin Drug Discov Devel, 2009. **12**(5): p. 616-27.

105. Wang, Y., et al., *Histone hypercitrullination mediates chromatin decondensation and neutrophil extracellular trap formation.* J Cell Biol, 2009. **184**(2): p. 205-13.

106. Yost, C.C., et al., *Neonatal NET-inhibitory factor and related peptides inhibit neutrophil extracellular trap formation.* J Clin Invest, 2016.

107. Kusunoki, Y., et al., *Peptidylarginine Deiminase Inhibitor Suppresses Neutrophil Extracellular Trap Formation and MPO-ANCA Production.* Front Immunol, 2016. **7**: p. 227.

108. Masuda, S., et al., *NETosis markers: Quest for specific, objective, and quantitative markers.* Clin Chim Acta, 2016. **459**: p. 89-93.

109. Rada, B.K., et al., *Dual role of phagocytic NADPH oxidase in bacterial killing.* Blood, 2004. **104**(9): p. 2947-53.

110. Rada, B.K., et al., *Calcium signalling is altered in myeloid cells with a deficiency in NADPH oxidase activity.* Clin Exp Immunol, 2003. **132**(1): p. 53-60.

111. Sheshachalam, A., et al., *Granule protein processing and regulated secretion in neutrophils.* Front Immunol, 2014. **5**: p. 448.

112. Mitchell, T., et al., *Primary granule exocytosis in human neutrophils is regulated by Rac-dependent actin remodeling.* Am J Physiol Cell Physiol, 2008. **295**(5): p. C1354-65.

113. Lacy, P., *Mechanisms of degranulation in neutrophils.* Allergy Asthma Clin Immunol, 2006. **2**(3): p. 98-108.

114. Byrd, A.S., et al., *An extracellular matrix-based mechanism of rapid neutrophil extracellular trap formation in response to Candida albicans.* J Immunol, 2013. **190**(8): p. 4136-48.

115. Kingsbury, S.R., P.G. Conaghan, and M.F. McDermott, *The role of the NLRP3 inflammasome in gout.* J Inflamm Res, 2011. **4**: p. 39-49.

116. Garlanda, C., C.A. Dinarello, and A. Mantovani, *The interleukin-1 family: back to the future.* Immunity, 2013. **39**(6): p. 1003-18.

117. Yao, Y., et al., *Neutrophil priming occurs in a sequential manner and can be visualized in living animals by monitoring IL-1beta promoter activation.* J Immunol, 2015. **194**(3): p. 1211-24.

118. Chen, C.J., et al., *MyD88-dependent IL-1 receptor signaling is essential for gouty inflammation stimulated by monosodium urate crystals.* J Clin Invest, 2006. **116**(8): p. 2262-71.

119. Schlesinger, N., *Anti-interleukin-1 therapy in the management of gout.* Curr Rheumatol Rep, 2014. **16**(2): p. 398.

120. Neogi, T., *Interleukin-1 antagonism in acute gout: is targeting a single cytokine the answer?* Arthritis Rheum, 2010. **62**(10): p. 2845-9.

121. Schett, G., J.M. Dayer, and B. Manger, *Interleukin-1 function and role in rheumatic disease.* Nat Rev Rheumatol, 2016. **12**(1): p. 14-24.

122. Dumusc, A. and A. So, *Interleukin-1 as a therapeutic target in gout.* Curr Opin Rheumatol, 2015. **27**(2): p. 156-63.

123. Sundy, J.S., et al., *Rilonacept for gout flare prevention in patients receiving uric acid-lowering therapy: results of RESURGE, a phase III, international safety study.* J Rheumatol, 2014. **41**(8): p. 1703-11.

124. Mitha, E., et al., *Rilonacept for gout flare prevention during initiation of uric acid-lowering therapy: results from the PRESURGE-2 international, phase 3, randomized, placebo-controlled trial.* Rheumatology (Oxford), 2013. **52**(7): p. 1285-92.

125. Schumacher, H.R., Jr., et al., *Rilonacept (interleukin-1 trap) for prevention of gout flares during initiation of uric acid-lowering therapy: results from a phase III randomized, double-blind, placebo-controlled, confirmatory efficacy study.* Arthritis Care Res (Hoboken), 2012. **64**(10): p. 1462-70.

126. Schumacher, H.R., Jr., et al., *Rilonacept (interleukin-1 trap) in the prevention of acute gout flares during initiation of urate-lowering therapy: results of a phase II randomized, double-blind, placebo-controlled trial.* Arthritis Rheum, 2012. **64**(3): p. 876-84.

127. Terkeltaub, R.A., et al., *Rilonacept in the treatment of acute gouty arthritis: a randomized, controlled clinical trial using indomethacin as the active comparator.* Arthritis Res Ther, 2013. **15**(1): p. R25.

128. Schlesinger, N., et al., *Canakinumab for acute gouty arthritis in patients with limited treatment options: results from two randomised, multicentre, active-controlled, double-blind trials and their initial extensions.* Ann Rheum Dis, 2012. **71**(11): p. 1839-48.

129. Schlesinger, N., et al., *Canakinumab reduces the risk of acute gouty arthritis flares during initiation of allopurinol treatment: results of a double-blind, randomised study.* Ann Rheum Dis, 2011. **70**(7): p. 1264-71.

130. Schlesinger, N., et al., *Canakinumab relieves symptoms of acute flares and improves health-related quality of life in patients with difficult-to-treat Gouty Arthritis by suppressing inflammation: results of a randomized, dose-ranging study.* Arthritis Res Ther, 2011. **13**(2): p. R53.

131. So, A., et al., *Canakinumab for the treatment of acute flares in difficult-to-treat gouty arthritis: Results of a multicenter, phase II, dose-ranging study.* Arthritis Rheum, 2010. **62**(10): p. 3064-76.

132. *Canakinumab for gout attacks. Too risky.* Prescrire Int, 2014. **23**(151): p. 178.

133. Brinkmann, V., et al., *Automatic quantification of in vitro NET formation.* Front Immunol, 2012. **3**: p. 413.

134. Wartha, F., et al., *Neutrophil extracellular traps: casting the NET over pathogenesis.* Curr Opin Microbiol, 2007. **10**(1): p. 52-6.

135. de Buhr, N. and M. von Kockritz-Blickwede, *How Neutrophil Extracellular Traps Become Visible.* J Immunol Res, 2016. **2016**: p. 4604713.

136. Gupta, A.K., et al., *Activated endothelial cells induce neutrophil extracellular traps and are susceptible to NETosis-mediated cell death.* FEBS Lett, 2010. **584**(14): p. 3193-7.

137. Kraaij, T., et al., *A novel method for high-throughput detection and quantification of neutrophil extracellular traps reveals ROS-independent NET release with immune complexes.* Autoimmun Rev, 2016. **15**(6): p. 577-84.

138. Ogdie, A., et al., *Imaging modalities for the classification of gout: systematic literature review and meta-analysis.* Ann Rheum Dis, 2015. **74**(10): p. 1868-74.

139. Bronkhorst, A.J., J. Aucamp, and P.J. Pretorius, *Adjustments to the preanalytical phase of quantitative cell-free DNA analysis.* Data Brief, 2016. **6**: p. 326-9.

140. Bronkhorst, A.J., et al., *Reference gene selection for in vitro cell-free DNA analysis and gene expression profiling.* Clin Biochem, 2016. **49**(7-8): p. 606-8.

141. Bronkhorst, A.J., et al., *Characterization of the cell-free DNA released by cultured cancer cells.* Biochim Biophys Acta, 2016. **1863**(1): p. 157-65.

142. Bronkhorst, A.J., J. Aucamp, and P.J. Pretorius, *Cell-free DNA: Preanalytical variables.* Clin Chim Acta, 2015. **450**: p. 243-53.

143. Gonzalez, A.S., et al., *Induction and quantification of neutrophil extracellular traps.* Methods Mol Biol, 2014. **1124**: p. 307-18.

144. Vong, L., P.M. Sherman, and M. Glogauer, *Quantification and visualization of neutrophil extracellular traps (NETs) from murine bone marrow-derived neutrophils.* Methods Mol Biol, 2013. **1031**: p. 41-50.

145. Brinkmann, V. and A. Zychlinsky, *Beneficial suicide: why neutrophils die to make NETs.* Nat Rev Microbiol, 2007. **5**(8): p. 577-82.

146. Brinkmann, V. and A. Zychlinsky, *Neutrophil extracellular traps: is immunity the second function of chromatin?* J Cell Biol, 2012. **198**(5): p. 773-83.

147. Schorn, C., et al., *Bonding the foe - NETting neutrophils immobilize the pro-inflammatory monosodium urate crystals.* Front Immunol, 2012. **3**: p. 376.

148. de Buhr, N., et al., *Streptococcus suis DNase SsnA contributes to degradation of neutrophil extracellular traps (NETs) and evasion of NET-mediated antimicrobial activity.* Microbiology, 2014. **160**(Pt 2): p. 385-95.

149. Shi, Y., J.E. Evans, and K.L. Rock, *Molecular identification of a danger signal that alerts the immune system to dying cells.* Nature, 2003. **425**(6957): p. 516-21.

150. Cekic, C. and J. Linden, *Purinergic regulation of the immune system.* Nat Rev Immunol, 2016. **16**(3): p. 177-92.

151. Junger, W.G., *Immune cell regulation by autocrine purinergic signalling.* Nat Rev Immunol, 2011. **11**(3): p. 201-12.

152. Chen, Y., et al., *Purinergic signaling: a fundamental mechanism in neutrophil activation.* Sci Signal, 2010. **3**(125): p. ra45.

153. Bao, Y., et al., *Mitochondria regulate neutrophil activation by generating ATP for autocrine purinergic signaling.* J Biol Chem, 2014. **289**(39): p. 26794-803.

154. Ibusuki, K., et al., *Human neutrophil peptides induce interleukin-8 in intestinal epithelial cells through the P2 receptor and ERK1/2 signaling pathways.* Int J Mol Med, 2015. **35**(6): p. 1603-9.

155. Uratsuji, H., et al., *P2Y6 receptor signaling pathway mediates inflammatory responses induced by monosodium urate crystals.* J Immunol, 2012. **188**(1): p. 436-44.

156. Hansen, A., et al., *The P2Y6 receptor mediates Clostridium difficile toxin-induced CXCL8/IL-8 production and intestinal epithelial barrier dysfunction.* PLoS One, 2013. **8**(11): p. e81491.

157. Nakamura, T., et al., *UDP induces intestinal epithelial migration via the P2Y6 receptor.* Br J Pharmacol, 2013. **170**(4): p. 883-92.

158. Riegel, A.K., et al., *Selective induction of endothelial P2Y6 nucleotide receptor promotes vascular inflammation.* Blood, 2011. **117**(8): p. 2548-55.

159. Meltzer, D., et al., *Synthesis and structure-activity relationship of uracil nucleotide derivatives towards the identification of human P2Y6 receptor antagonists.* Bioorg Med Chem, 2015. **23**(17): p. 5764-73.

160. Neher, J.J., et al., *Inhibition of UDP/P2Y6 purinergic signaling prevents phagocytosis of viable neurons by activated microglia in vitro and in vivo.* Glia, 2014. **62**(9): p. 1463-75.

161. Kim, S.G., et al., *Tumor necrosis factor alpha-induced apoptosis in astrocytes is prevented by the activation of P2Y6, but not P2Y4 nucleotide receptors.* Biochem Pharmacol, 2003. **65**(6): p. 923-31.

162. Grbic, D.M., et al., *Intestinal inflammation increases the expression of the P2Y6 receptor on epithelial cells and the release of CXC chemokine ligand 8 by UDP.* J Immunol, 2008. **180**(4): p. 2659-68.

163. Eltzschig, H.K., C.F. Macmanus, and S.P. Colgan, *Neutrophils as sources of extracellular nucleotides: functional consequences at the vascular interface.* Trends Cardiovasc Med, 2008. **18**(3): p. 103-7.

164. Shingu, M., K. Tatsukawa, and M. Nobunaga, *Intracellular contents of cyclic nucleotides in neutrophils and lymphocytes from patients with systemic lupus erythematosus.* Arch Dermatol Res, 1989. **281**(3): p. 203-5.

165. Smolen, J.E. and R.R. Sandborg, *Ca2(+)-induced secretion by electropermeabilized human neutrophils. The roles of Ca2+, nucleotides and protein kinase C.* Biochim Biophys Acta, 1990. **1052**(1): p. 133-42.

166. Ward, P.A., et al., *Regulatory effects of adenosine and adenine nucleotides on oxygen radical responses of neutrophils.* Lab Invest, 1988. **58**(4): p. 438-47.

167. Ko, H., et al., *Synthesis and potency of novel uracil nucleotides and derivatives as P2Y2 and P2Y6 receptor agonists.* Bioorg Med Chem, 2008. **16**(12): p. 6319-32.

168. Koizumi, S., et al., *UDP acting at P2Y6 receptors is a mediator of microglial phagocytosis.* Nature, 2007. **446**(7139): p. 1091-5.

169. Mamedova, L.K., et al., *Diisothiocyanate derivatives as potent, insurmountable antagonists of P2Y6 nucleotide receptors.* Biochem Pharmacol, 2004. **67**(9): p. 1763-70.

170. Besada, P., et al., *Structure-activity relationships of uridine 5'-diphosphate analogues at the human P2Y6 receptor.* J Med Chem, 2006. **49**(18): p. 5532-43.

171. I. Mitroulis, P.S., K. Ritis, *Targeting IL-1β in disease the expanding role of NLRP3 inflammasome.* European Journal of Internal Medicine, 2010. **21**: p. 157-163.

172. Allaeys, I., F. Marceau, and P.E. Poubelle, *NLRP3 promotes autophagy of urate crystals phagocytized by human osteoblasts.* Arthritis Res Ther, 2013. **15**(6): p. R176.

173. Gabelloni, M.L., et al., *NADPH oxidase derived reactive oxygen species are involved in human neutrophil IL-1beta secretion but not in inflammasome activation.* Eur J Immunol, 2013. **43**(12): p. 3324-35.

174. Harijith, A., D.L. Ebenezer, and V. Natarajan, *Reactive oxygen species at the crossroads of inflammasome and inflammation.* Front Physiol, 2014. **5**: p. 352.

175. Mankan, A.K., et al., *The NLRP3/ASC/Caspase-1 axis regulates IL-1beta processing in neutrophils.* Eur J Immunol, 2012. **42**(3): p. 710-5.

176. Joosten, L.A., et al., *Inflammatory arthritis in caspase 1 gene-deficient mice: contribution of proteinase 3 to caspase 1-independent production of bioactive interleukin-1beta.* Arthritis Rheum, 2009. **60**(12): p. 3651-62.

177. Joosten, L.A., et al., *Engagement of fatty acids with Toll-like receptor 2 drives interleukin-1beta production via the ASC/caspase 1 pathway in monosodium urate monohydrate crystal-induced gouty arthritis.* Arthritis Rheum, 2010. **62**(11): p. 3237-48.

178. Amaral, F.A., et al., *NLRP3 inflammasome-mediated neutrophil recruitment and hypernociception depend on leukotriene B(4) in a murine model of gout.* Arthritis Rheum, 2012. **64**(2): p. 474-84.

179. Barry L. Hainer, E.M., and R. Travis Wilkes, *Diagnosis, Treatment, and Prevention of Gout.* American Academy of Family Physicians, 2014. **90**(12): p. 831-836.

180. Yipp, B.G. and P. Kubes, *NETosis: how vital is it?* Blood, 2013. **122**(16): p. 2784-94.

181. Blackburn, M.R., *P2Y6 and vascular inflammation.* Blood, 2011. **117**(8): p. 2304-5.

182. Cox, M.A., et al., *The pyrimidinergic P2Y6 receptor mediates a novel release of proinflammatory cytokines and chemokines in monocytic cells stimulated with UDP.* Biochem Biophys Res Commun, 2005. **330**(2): p. 467-73.

183. Filippov, A.K., et al., *Dual coupling of heterologously-expressed rat P2Y6 nucleotide receptors to N-type Ca2+ and M-type K+ currents in rat sympathetic neurones.* Br J Pharmacol, 1999. **126**(4): p. 1009-17.

184. Grbic, D.M., et al., *P2Y6 receptor contributes to neutrophil recruitment to inflamed intestinal mucosa by increasing CXC chemokine ligand 8 expression in an AP-1-dependent manner in epithelial cells.* Inflamm Bowel Dis, 2012. **18**(8): p. 1456-69.

185. Haanes, K.A., et al., *New insights on pyrimidine signalling within the arterial vasculature - Different roles for P2Y2 and P2Y6 receptors in large and small coronary arteries of the mouse.* J Mol Cell Cardiol, 2016. **93**: p. 1-11.

186. Khine, A.A., et al., *Human neutrophil peptides induce interleukin-8 production through the P2Y6 signaling pathway.* Blood, 2006. **107**(7): p. 2936-42.

187. Dey, S., et al., *Effect of Two Interacting Rings in Metalloporphyrin Dimers upon Stepwise Oxidations.* Inorg Chem, 2016. **55**(7): p. 3229-38.

188. Kessenbrock, K., et al., *Netting neutrophils in autoimmune small-vessel vasculitis.* Nat Med, 2009. **15**(6): p. 623-5.

189. Leffler, J., et al., *Degradation of neutrophil extracellular traps co-varies with disease activity in patients with systemic lupus erythematosus.* Arthritis Res Ther, 2013. **15**(4): p. R84.

190. Neumann, A., et al., *The antimicrobial peptide LL-37 facilitates the formation of neutrophil extracellular traps.* Biochem J, 2014. **464**(1): p. 3-11.

191. Leon, S.A., et al., *Free DNA in the serum of cancer patients and the effect of therapy.* Cancer Res, 1977. **37**(3): p. 646-50.

192. Raptis, L. and H.A. Menard, *Quantitation and characterization of plasma DNA in normals and patients with systemic lupus erythematosus.* J Clin Invest, 1980. **66**(6): p. 1391-9.

193. Chang, C.P., et al., *Elevated cell-free serum DNA detected in patients with myocardial infarction.* Clin Chim Acta, 2003. **327**(1-2): p. 95-101.

194. Seper, A., et al., *Vibrio cholerae evades neutrophil extracellular traps by the activity of two extracellular nucleases.* PLoS Pathog, 2013. **9**(9): p. e1003614.

195. von Kockritz-Blickwede, M., O.A. Chow, and V. Nizet, *Fetal calf serum contains heat-stable nucleases that degrade neutrophil extracellular traps.* Blood, 2009. **114**(25): p. 5245-6.

196. Pilsczek, F.H., et al., *A novel mechanism of rapid nuclear neutrophil extracellular trap formation in response to Staphylococcus aureus.* J Immunol, 2010. **185**(12): p. 7413-25.

197. Kuo, C.F., et al., *Global epidemiology of gout: prevalence, incidence and risk factors.* Nat Rev Rheumatol, 2015. **11**(11): p. 649-62.

198. Abbott, K.C., et al., *New-onset gout after kidney transplantation: incidence, risk factors and implications.* Transplantation, 2005. **80**(10): p. 1383-91.

199. Abbott, R.D., et al., *Gout and coronary heart disease: the Framingham Study.* J Clin Epidemiol, 1988. **41**(3): p. 237-42.

200. Ask-Upmark, E. and L. Adner, *Coronary infarction and gout.* Acta Med Scand, 1951. **139**(1): p. 1-6.

201. Roddy, E. and M. Doherty, *Epidemiology of gout.* Arthritis Res Ther, 2010. **12**(6): p. 223.

202. So, A., *Developments in the scientific and clinical understanding of gout.* Arthritis Res Ther, 2008. **10**(5): p. 221.

203. Bauer, W. and M.M. Singh, *Management of gout.* N Engl J Med, 1957. **256**(5): p. 214-9; concl.

204. Becker, M.A., P.A. Simkin, and L.B. Sorensen, *Urate transporters: transforming the face of hyperuricemia and gout.* J Rheumatol, 2014. **41**(10): p. 1910-2.

205. So, A., *[Recent advances in the pathophysiology of hyperuricemia and gout]*. Rev Med Suisse, 2007. **3**(103): p. 720, 722-4.

206. So, A., *Epidemiology: Gout--bad for the heart as well as the joint.* Nat Rev Rheumatol, 2010. **6**(7): p. 386-7.

207. So, A., *How to regulate neutrophils in gout.* Arthritis Res Ther, 2013. **15**(5): p. 118.

208. So, A. and N. Busso, *A magic bullet for gout?* Ann Rheum Dis, 2009. **68**(10): p. 1517-9.

209. Petrilli, V. and F. Martinon, *The inflammasome, autoinflammatory diseases, and gout.* Joint Bone Spine, 2007. **74**(6): p. 571-6.

210. Grayson, P.C. and M.J. Kaplan, *At the Bench: Neutrophil extracellular traps (NETs) highlight novel aspects of innate immune system involvement in autoimmune diseases.* J Leukoc Biol, 2016. **99**(2): p. 253-64.

211. Abbracchio, M.P., et al., *International Union of Pharmacology LVIII: update on the P2Y G protein-coupled nucleotide receptors: from molecular mechanisms and pathophysiology to therapy.* Pharmacol Rev, 2006. **58**(3): p. 281-341.

212. von Kugelgen, I. and K. Hoffmann, *Pharmacology and structure of P2Y receptors.* Neuropharmacology, 2015.

213. Taylor, W.J., et al., *A modified Delphi exercise to determine the extent of consensus with OMERACT outcome domains for studies of acute and chronic gout.* Ann Rheum Dis, 2008. **67**(6): p. 888-91.

214. Grassi, F., *Purinergic control of neutrophil activation.* J Mol Cell Biol, 2010. **2**(4): p. 176-7.

215. Hidalgo, M.A., et al., *fMLP-Induced IL-8 Release Is Dependent on NADPH Oxidase in Human Neutrophils.* J Immunol Res, 2015. **2015**: p. 120348.

216. Hinnah Campwala, D.W.S., David C. Crossman and Samuel J. Fountain *P2Y6 receptor inhibition perturbs CCL2-evoked signalling.pdf.* Journal of Cell Biology, 2014.

217. Xiang, Z. and G. Burnstock, *Distribution of P2Y6 and P2Y12 receptor: their colocalization with calbindin, calretinin and nitric oxide synthase in the guinea pig enteric nervous system.* Histochem Cell Biol, 2006. **125**(4): p. 327-36.

218. Schreiber, R. and K. Kunzelmann, *Purinergic P2Y6 receptors induce Ca2+ and CFTR dependent Cl- secretion in mouse trachea.* Cell Physiol Biochem, 2005. **16**(1-3): p. 99-108.

219. Korcok, J., et al., *P2Y6 nucleotide receptors activate NF-kappaB and increase survival of osteoclasts.* J Biol Chem, 2005. **280**(17): p. 16909-15.

220. Liu, G.D., et al., *P2Y6 receptor and immunoinflammation.* Neurosci Bull, 2009. **25**(3): p. 161-4.

221. Altman, R., et al., *Development of criteria for the classification and reporting of osteoarthritis. Classification of osteoarthritis of the knee. Diagnostic and Therapeutic Criteria Committee of the American Rheumatism Association.* Arthritis Rheum, 1986. **29**(8): p. 1039-49.

222. Watford, W.T., et al., *Cytohesin binder and regulator (cybr) is not essential for T- and dendritic-cell activation and differentiation.* Mol Cell Biol, 2006. **26**(17): p. 6623-32.

223. Zhang, E., et al., *Aggrecanases in the human synovial fluid at different stages of osteoarthritis.* Clin Rheumatol, 2013. **32**(6): p. 797-803.

224. Carulli, G., et al., *Modifications in the phagocytosis of human neutrophils induced by vinblastine and cytochalasin B: the effects of lithium.* Acta Haematol, 1985. **74**(2): p. 81-5.

225. Laubinger, W., et al., *P2Y receptor specific for diadenosine tetraphosphate in lung: selective inhibition by suramin, PPADS, Ip5I, and not by MRS-2197.* Eur J Pharmacol, 2003. **468**(1): p. 9-14.

226. Charlton, S.J., et al., *PPADS and suramin as antagonists at cloned P2Y- and P2U-purinoceptors.* Br J Pharmacol, 1996. **118**(3): p. 704-10.

227. Usune, S., T. Katsuragi, and T. Furukawa, *Effects of PPADS and suramin on contractions and cytoplasmic Ca2+ changes evoked by AP4A, ATP and alpha, beta-methylene ATP in guinea-pig urinary bladder.* Br J Pharmacol, 1996. **117**(4): p. 698-702.

228. Lewis, R.S., *Store-operated calcium channels: new perspectives on mechanism and function.* Cold Spring Harb Perspect Biol, 2011. **3**(12).

229. Braganhol, E., et al., *Nucleotide receptors control IL-8/CXCL8 and MCP-1/CCL2 secretions as well as proliferation in human glioma cells.* Biochim Biophys Acta, 2015. **1852**(1): p. 120-30.

230. Kukulski, F., et al., *Extracellular ATP and P2 receptors are required for IL-8 to induce neutrophil migration.* Cytokine, 2009. **46**(2): p. 166-70.

231. Duranton, J., *Inhibition of Neutrophil Serine Proteinases by Suramin.* Journal of Biological Chemistry, 1997. **272**(15): p. 9950-9955.

232. Rost, S., et al., *P2 receptor antagonist PPADS inhibits mesangial cell proliferation in experimental mesangial proliferative glomerulonephritis.* Kidney Int, 2002. **62**(5): p. 1659-71.

233. Ralevic, V. and G. Burnstock, *Discrimination by PPADS between endothelial P2Y- and P2U-purinoceptors in the rat isolated mesenteric arterial bed.* Br J Pharmacol, 1996. **118**(2): p. 428-34.

234. Lambrecht, G., et al., *PPADS, a novel functionally selective antagonist of P2 purinoceptor-mediated responses.* Eur J Pharmacol, 1992. **217**(2-3): p. 217-9.

235. El-Tayeb, A., A. Qi, and C.E. Muller, *Synthesis and structure-activity relationships of uracil nucleotide derivatives and analogues as agonists at human P2Y2, P2Y4, and P2Y6 receptors.* J Med Chem, 2006. **49**(24): p. 7076-87.

236. Onnheim, K., et al., *A novel receptor cross-talk between the ATP receptor P2Y2 and formyl peptide receptors reactivates desensitized neutrophils to produce superoxide.* Exp Cell Res, 2014. **323**(1): p. 209-17.

237. Jacob, F., et al., *Purinergic signaling in inflammatory cells: P2 receptor expression, functional effects, and modulation of inflammatory responses.* Purinergic Signal, 2013. **9**(3): p. 285-306.

238. Nagaoka, I., et al., *Evaluation of the effect of alpha-defensin human neutrophil peptides on neutrophil apoptosis.* Int J Mol Med, 2010. **26**(6): p. 925-34.

239. Yu, W. and W.G. Hill, *Lack of specificity shown by P2Y6 receptor antibodies.* Naunyn Schmiedebergs Arch Pharmacol, 2013. **386**(10): p. 885-91.

240. Chen, J., Y. Zhao, and Y. Liu, *The role of nucleotides and purinergic signaling in apoptotic cell clearance - implications for chronic inflammatory diseases.* Front Immunol, 2014. **5**: p. 656.

241. Keshari, R.S., et al., *Cytokines induced neutrophil extracellular traps formation: implication for the inflammatory disease condition.* PLoS One, 2012. **7**(10): p. e48111.

242. Hazeldine, J., et al., *Impaired neutrophil extracellular trap formation: a novel defect in the innate immune system of aged individuals.* Aging Cell, 2014. **13**(4): p. 690-8.

243. Rada, B., et al., *NLRP3 inflammasome activation and interleukin-1beta release in macrophages require calcium but are independent of calcium-activated NADPH oxidases.* Inflamm Res, 2014. **63**(10): p. 821-30.

244. Rada, B. and T.L. Leto, *Oxidative innate immune defenses by Nox/Duox family NADPH oxidases.* Contrib Microbiol, 2008. **15**: p. 164-87.

245. Zizzo, M.G., et al., *Pharmacological characterization of uracil nucleotide-preferring P2Y receptors modulating intestinal motility: a study on mouse ileum.* Purinergic Signal, 2012. **8**(2): p. 275-85.

246. Douda, D.N., et al., *SK3 channel and mitochondrial ROS mediate NADPH oxidase-independent NETosis induced by calcium influx.* Proc Natl Acad Sci U S A, 2015. **112**(9): p. 2817-22.

247. Ide, S., et al., *Purine receptor P2Y6 mediates cellular response to gamma-ray-induced DNA damage.* J Toxicol Sci, 2014. **39**(1): p. 15-23.

248. Inoue, K., *UDP facilitates microglial phagocytosis through P2Y6 receptors.* Cell Adh Migr, 2007. **1**(3): p. 131-2.

249. Ginsburg-Shmuel, T., et al., *UDP made a highly promising stable, potent, and selective P2Y6-receptor agonist upon introduction of a boranophosphate moiety.* Bioorg Med Chem, 2012. **20**(18): p. 5483-95.

250. Warny, M., et al., *P2Y(6) nucleotide receptor mediates monocyte interleukin-8 production in response to UDP or lipopolysaccharide.* J Biol Chem, 2001. **276**(28): p. 26051-6.

251. Gupta, A.K., et al., *Efficient neutrophil extracellular trap induction requires mobilization of both intracellular and extracellular calcium pools and is modulated by cyclosporine A.* PLoS One, 2014. **9**(5): p. e97088.

252. Clemens, R.A. and C.A. Lowell, *Store-operated calcium signaling in neutrophils.* J Leukoc Biol, 2015.

253. Brazil, J.C. and C.A. Parkos, *Pathobiology of neutrophil-epithelial interactions.* Immunol Rev, 2016. **273**(1): p. 94-111.

254. Steerman, R.L., et al., *Instrinsic defect of the polymorphonuclear leucocyte resulting in impaired chemotaxis and phagocytosis.* Clin Exp Immunol, 1971. **9**(6): p. 939-46.

255. Kim, B., et al., *Uridine 5'-diphosphate induces chemokine expression in microglia and astrocytes through activation of the P2Y6 receptor.* J Immunol, 2011. **186**(6): p. 3701-9.

256. Travis, J., *Structure, function, and control of neutrophil proteinases.* Am J Med, 1988. **84**(6A): p. 37-42.

257. Smallman, L.A., S.L. Hill, and R.A. Stockley, *Reduction of ciliary beat frequency in vitro by sputum from patients with bronchiectasis: a serine proteinase effect.* Thorax, 1984. **39**(9): p. 663-7.

258. Sly, P.D., et al., *Risk factors for bronchiectasis in children with cystic fibrosis.* N Engl J Med, 2013. **368**(21): p. 1963-70.

259. Hoenderdos, K. and A. Condliffe, *The neutrophil in chronic obstructive pulmonary disease.* Am J Respir Cell Mol Biol, 2013. **48**(5): p. 531-9.

260. Neogi, T., et al., *2015 Gout classification criteria: an American College of Rheumatology/European League Against Rheumatism collaborative initiative.* Ann Rheum Dis, 2015. **74**(10): p. 1789-98.

261. Taylor, W.J., et al., *Study for Updated Gout Classification Criteria: Identification of Features to Classify Gout.* Arthritis Care Res (Hoboken), 2015. **67**(9): p. 1304-15.

262. Dalbeth, N., T.R. Merriman, and L.K. Stamp, *Gout.* Lancet, 2016.

263. Arai, Y., et al., *Uric Acid Induces NADPH Oxidase-Independent Neutrophil Extracellular Trap Formation.* Biochem Biophys Res Commun, 2013.

264. Dahl, G., *ATP release through pannexon channels.* Philos Trans R Soc Lond B Biol Sci, 2015. **370**(1672).

265. Hoyle, C.H., G.E. Knight, and G. Burnstock, *Suramin antagonizes responses to P2-purinoceptor agonists and purinergic nerve stimulation in the guinea-pig urinary bladder and taenia coli.* Br J Pharmacol, 1990. **99**(3): p. 617-21.

266. Kukulski, F., et al., *Extracellular nucleotides mediate LPS-induced neutrophil migration in vitro and in vivo.* J Leukoc Biol, 2007. **81**(5): p. 1269-75.

267. Itagaki, K., et al., *Store-operated calcium entry in human neutrophils reflects multiple contributions from independently regulated pathways.* J Immunol, 2002. **168**(8): p. 4063-9.

268. Demaurex, N. and P. Nunes, *The Role of STIM and ORAI Proteins in Phagocytic Immune Cells.* Am J Physiol Cell Physiol, 2016: p. ajpcell 00360 2015.

269. Dixit, N. and S.I. Simon, *Chemokines, selectins and intracellular calcium flux: temporal and spatial cues for leukocyte arrest.* Front Immunol, 2012. **3**: p. 188.

270. Michaelis, M., et al., *STIM1, STIM2, and Orai1 regulate store-operated calcium entry and purinergic activation of microglia.* Glia, 2015. **63**(4): p. 652-63.

271. Ide S, N.N., Tsukimoto M, Kojima S, *Purine receptor P2Y6 mediates cellular response to γ-ray-induced DNA damage.* J Toxicol Sci., 2014. **39**(1): p. 15-23.

272. Chen, Y. and W.G. Junger, *Measurement of oxidative burst in neutrophils.* Methods Mol Biol, 2012. **844**: p. 115-24.

273. Frey, R.S., M. Ushio-Fukai, and A.B. Malik, *NADPH oxidase-dependent signaling in endothelial cells: role in physiology and pathophysiology.* Antioxid Redox Signal, 2009. **11**(4): p. 791-810.

274. Calvert, J.A., et al., *Evidence for P2Y1, P2Y2, P2Y6 and atypical UTP-sensitive receptors coupled to rises in intracellular calcium in mouse cultured superior cervical ganglion neurons and glia.* Br J Pharmacol, 2004. **143**(5): p. 525-32.

275. He, J., Y. Yang, and D.Q. Peng, *Monosodium urate (MSU) crystals increase gout associated coronary heart disease (CHD) risk through the activation of NLRP3 inflammasome.* Int J Cardiol, 2012. **160**(1): p. 72-3.

276. Karmakar, M., et al., *Neutrophil P2X7 receptors mediate NLRP3 inflammasome-dependent IL-1beta secretion in response to ATP.* Nat Commun, 2016. **7**: p. 10555.

277. Martinon, F. and L.H. Glimcher, *Gout: new insights into an old disease.* J Clin Invest, 2006. **116**(8): p. 2073-5.

278. Neogi, T., *Clinical practice. Gout.* N Engl J Med, 2011. **364**(5): p. 443-52.

279. Giamarellos-Bourboulis, E.J., et al., *Crystals of monosodium urate monohydrate enhance lipopolysaccharide-induced release of interleukin 1 beta by mononuclear cells through a caspase 1-mediated process.* Ann Rheum Dis, 2009. **68**(2): p. 273-8.

280. Torres, R., et al., *Hyperalgesia, synovitis and multiple biomarkers of inflammation are suppressed by interleukin 1 inhibition in a novel animal model of gouty arthritis.* Ann Rheum Dis, 2009. **68**(10): p. 1602-8.

281. Van Emon, M.L., et al., *Supplementing metabolizable protein to ewes during late gestation: I. Effects on ewe performance and offspring performance from birth to weaning.* J Anim Sci, 2014. **92**(1): p. 339-48.

282. Dalbeth, N. and D.O. Haskard, *Mechanisms of inflammation in gout.* Rheumatology (Oxford), 2005. **44**(9): p. 1090-6.

283. Martinon, F. and J. Tschopp, *Inflammatory caspases and inflammasomes: master switches of inflammation.* Cell Death Differ, 2007. **14**(1): p. 10-22.

284. Schlesinger, N., *Canakinumab in gout.* Expert Opin Biol Ther, 2012. **12**(9): p. 1265-75.

285. Wechalekar, M.D., et al., *Intra-articular glucocorticoids for acute gout.* Cochrane Database Syst Rev, 2013. **4**: p. CD009920.

286. Meissner, F., et al., *Inflammasome activation in NADPH oxidase defective mononuclear phagocytes from patients with chronic granulomatous disease.* Blood, 2010. **116**(9): p. 1570-3.

287. van Bruggen, R., et al., *Human NLRP3 inflammasome activation is Nox1-4 independent.* Blood, 2010. **115**(26): p. 5398-400.

288. Naccache, P.H., et al., *Calcium mobilization and right-angle light scatter responses to 12-oxo-derivatives of arachidonic acid in neutrophils: evidence for the involvement of the leukotriene B4 receptor.* Biochim Biophys Acta, 1991. **1133**(1): p. 102-6.

289. Desai, J., et al., *PMA and crystal-induced neutrophil extracellular trap formation involves RIPK1-RIPK3-MLKL signaling.* Eur J Immunol, 2016. **46**(1): p. 223-9.

290. Chhana, A., G. Lee, and N. Dalbeth, *Factors influencing the crystallization of monosodium urate: a systematic literature review.* BMC Musculoskelet Disord, 2015. **16**: p. 296.

291. Chhana, A., et al., *Interactions between tenocytes and monosodium urate monohydrate crystals: implications for tendon involvement in gout.* Ann Rheum Dis, 2014. **73**(9): p. 1737-41.

292. Nakazawa, D., et al., *The responses of macrophages in interaction with neutrophils that undergo NETosis.* J Autoimmun, 2016. **67**: p. 19-28.

293. Farrera, C. and B. Fadeel, *Macrophage clearance of neutrophil extracellular traps is a silent process.* J Immunol, 2013. **191**(5): p. 2647-56.

294. Seibenhener, M.L., et al., *Sequestosome 1/p62 is a polyubiquitin chain binding protein involved in ubiquitin proteasome degradation.* Mol Cell Biol, 2004. **24**(18): p. 8055-68.

295. Chenevier-Gobeaux, C., et al., *Superoxide production and NADPH oxidase expression in human rheumatoid synovial cells: regulation by interleukin-1beta and tumour necrosis factor-alpha.* Inflamm Res, 2006. **55**(11): p. 483-90.

296. Yan, B., et al., *IL-1beta and reactive oxygen species differentially regulate neutrophil directional migration and Basal random motility in a zebrafish injury-induced inflammation model.* J Immunol, 2014. **192**(12): p. 5998-6008.

297. Singh, D. and K.K. Huston, *IL-1 inhibition with anakinra in a patient with refractory gout.* J Clin Rheumatol, 2009. **15**(7): p. 366.

298. Perretti, M. and R.J. Flower, *Modulation of IL-1-induced neutrophil migration by dexamethasone and lipocortin 1.* J Immunol, 1993. **150**(3): p. 992-9.

299. Semerad, C.L., et al., *G-CSF is an essential regulator of neutrophil trafficking from the bone marrow to the blood.* Immunity, 2002. **17**(4): p. 413-23.

300. Tanaka, K., et al., *Imaging neutrophil extracellular traps in the alveolar space and pulmonary capillaries of a murine sepsis model by multiphoton microscopy.* Am J Respir Crit Care Med, 2015. **191**(9): p. 1088-9.

301. Tanaka, K., et al., *Letter to the Editor: Intravital imaging of the association between intravascular neutrophil extracellular traps and microvascular obstruction using multiphoton microscopy.* Am J Physiol Heart Circ Physiol, 2015. **308**(8): p. H960.

302. Tanaka, K., et al., *In vivo characterization of neutrophil extracellular traps in various organs of a murine sepsis model.* PLoS One, 2014. **9**(11): p. e111888.

303. Honda, M., et al., *Intravital imaging of neutrophil recruitment in hepatic ischemia-reperfusion injury in mice.* Transplantation, 2013. **95**(4): p. 551-8.

304. Seo, J., J.S. Osorio, and J.J. Loor, *Purinergic signaling gene network expression in bovine polymorphonuclear neutrophils during the peripartal period.* J Dairy Sci, 2013. **96**(12): p. 7675-83.

305. O'Grady, S.M., *Purinergic signaling and immune cell chemotaxis. Focus on "the UDP-sugar-sensing P2Y14 receptor promotes Rho-mediated signaling and chemotaxis in human neutrophils".* Am J Physiol Cell Physiol, 2012. **303**(5): p. C486-7.

306. Frasson, A.P., et al., *Involvement of purinergic signaling on nitric oxide production by neutrophils stimulated with Trichomonas vaginalis.* Purinergic Signal, 2012. **8**(1): p. 1-9.

307. Nishimura, A., et al., *Purinergic P2Y6 receptors heterodimerize with angiotensin AT1 receptors to promote angiotensin II-induced hypertension.* Sci Signal, 2016. **9**(411): p. ra7.

308. Kelsey, R., *BPH: P2Y6 blockade might help control bladder storage symptoms.* Nat Rev Urol, 2015. **12**(7): p. 358.

309. Gutierrez, M., et al., *International Consensus for ultrasound lesions in gout: results of Delphi process and web-reliability exercise.* Rheumatology (Oxford), 2015.

310. Scanu, A., et al., *Synovial fluid proteins are required for the induction of interleukin-1beta production by monosodium urate crystals.* Scand J Rheumatol, 2016: p. 1-10.

311. Hong, W., et al., *Peroxisome proliferator-activated receptor gamma prevents the production of NOD-like receptor family, pyrin domain containing 3 inflammasome and interleukin 1beta in HK-2 renal tubular epithelial cells stimulated by monosodium urate crystals.* Mol Med Rep, 2015. **12**(4): p. 6221-6.

312. Yang, C.M., et al., *IL-1beta Induces MMP-9-Dependent Brain Astrocytic Migration via Transactivation of PDGF Receptor/NADPH Oxidase 2-Derived Reactive Oxygen Species Signals.* Mol Neurobiol, 2015. **52**(1): p. 303-17.

313. Tseng, H.C., et al., *IL-1beta promotes corneal epithelial cell migration by increasing MMP-9 expression through NF-kappaB- and AP-1-dependent pathways.* PLoS One, 2013. **8**(3): p. e57955.

314. Wang, F.M., et al., *SHP-2 promoting migration and metastasis of MCF-7 with loss of E-cadherin, dephosphorylation of FAK and secretion of MMP-9 induced by IL-1beta in vivo and in vitro.* Breast Cancer Res Treat, 2005. **89**(1): p. 5-14.

315. Banerjee, S. and M. Leptin, *Systemic response to ultraviolet radiation involves induction of leukocytic IL-1beta and inflammation in zebrafish.* J Immunol, 2014. **193**(3): p. 1408-15.

316. Dufour, A., et al., *Role of matrix metalloproteinase-9 dimers in cell migration: design of inhibitory peptides.* J Biol Chem, 2010. **285**(46): p. 35944-56.

317. Bradley, L.M., et al., *Matrix metalloprotease 9 mediates neutrophil migration into the airways in response to influenza virus-induced toll-like receptor signaling.* PLoS Pathog, 2012. **8**(4): p. e1002641.

318. Wright, H.L., R.J. Moots, and S.W. Edwards, *The multifactorial role of neutrophils in rheumatoid arthritis.* Nat Rev Rheumatol, 2014. **10**(10): p. 593-601.

319. Carmona-Rivera, C., et al., *Neutrophil extracellular traps induce endothelial dysfunction in systemic lupus erythematosus through the activation of matrix metalloproteinase-2.* Ann Rheum Dis, 2015. **74**(7): p. 1417-24.

320. Akahoshi, T., Y. Murakami, and H. Kitasato, *Recent advances in crystal-induced acute inflammation.* Current opinion in rheumatology, 2007. **19**(2): p. 146-50.